Graduate School ETD Form 9
(Revised 12/07)

PURDUE UNIVERSITY
GRADUATE SCHOOL
Thesis/Dissertation Acceptance

This is to certify that the thesis/dissertation prepared

By Manav Gupta

Entitled
Differentiation and Characterization of Cell Types Associated with Retinal Degenerative Diseases Using Human Induced Pluripotent Stem Cells.

For the degree of Master of Science

Is approved by the final examining committee:

Dr. Jason S. Meyer
Chair

Dr. Teri-Belecky Adams

Dr. Stephen Randall

To the best of my knowledge and as understood by the student in the *Research Integrity and Copyright Disclaimer (Graduate School Form 20)*, this thesis/dissertation adheres to the provisions of Purdue University's "Policy on Integrity in Research" and the use of copyrighted material.

Approved by Major Professor(s): Dr. Jason S. Meyer

Approved by: Dr. Simon Atkinson 06/25/2013
Head of the Graduate Program Date

DIFFERENTIATION AND CHARACTERIZATION OF CELL TYPES ASSOCIATED WITH RETINAL DEGENERATIVE DISEASES USING HUMAN INDUCED PLURIPOTENT STEM CELLS

A Thesis

Submitted to the Faculty

of

Purdue University

by

Manav Gupta

In Partial Fulfillment of the

Requirements for the Degree

of

Master of Science

August 2013

Purdue University

Indianapolis, Indiana

For my grandparents and parents

ACKNOWLEDGEMENTS

I would like to take this opportunity to express my gratitude to the people whose constant support and encouragement throughout my program has been essential in the preparation of my thesis and culmination of my graduate studies.

I am extremely grateful to my inspiring mentor, Dr. Jason S. Meyer for giving me the opportunity to be a part of his lab and work on an aspect of biology I love. His regular inputs and insights in lab supplemented with opportunities to learn, mentor, attend conferences, contribute to academic writings and different projects, has been critical in further augmenting my interests in the field. I also want to thank the members of my committee, Dr. Stephen Randall and Dr. Teri-Belecky Adams, for their invaluable critique and assessment of my work, and being wonderful teachers of their respectively challenging and noteworthy courses.

I wish to thank the faculty, staff, and members of the IUPUI Department of Biology for always being approachable and supportive in my endeavors throughout my program. I also want to recognize my academic peers who have helped me grow as an individual in both science and in personal life.

Finally, I want to thank my family and friends: Ashok Gupta, Usha Gupta, Rahul Gupta, Neha Ganeriwal, Vidhi Agarwal, my mates from college, and friends made along the way.

TABLE OF CONTENTS

Page

Page

LIST OF TABLES

LIST OF FIGURES

Figure Page

LIST OF ABBREVIATIONS

Age-Related Macular Degeneration	AMD
Amyotrophic Lateral Sclerosis	ALS
Bestrophin	BEST1
Complementary Deoxyribonucleic Acid	cDNA
Crossing Threshold	Ct
Deoxyribonucleic Acid	DNA
Deoxyribonucleic Acid Methyltransferase	DNMT
Dimethyl Sulphoxide	DMSO
Dulbecco's Modified Eagle Medium	DMEM
Embryonic Stem	ES
Epidermal Growth Factor	EGF
Eye Field Transcription Factors	EFTFs
Fetal Bovine Serum	FBS
Fibroblast Growth Factor	FGF
Immunocytochemistry	ICC
Induced Pluripotent Stem	iPS
Inner Cell Mass	ICM
In Vitro Fertilization	IVF
Minimal Essential Medium – Non-Essential Amino Acids	MEM-NEAA
National Institutes of Health	NIH
Neural Induction Medium	NIM
Optic Nerve Head	ONH
Paraformaldehyde	PFA
Penicillin/ Streptomycin/ Ampicillin	PSA
Phosphate Buffer Saline	PBS
Quantitative Reverse Transcription-Polymerase Chain Reaction	qRT-PCR

Retinitis Pigmentosa	RP
Retinal Differentiation Medium	RDM
Retinal Ganglion Cells	RGCs
Retinal Pigment Epithelium	RPE
Reverse Transcription-Polymerase Chain Reaction	RT-PCR
Ribonucleic Acid	RNA
Spinal Muscular Atrophy	SMA
World Health Organization	WHO

ABSTRACT

Gupta, Manav. M.S., Purdue University, August 2013. Differentiation and Characterization of Cell types Associated with Retinal Degenerative Diseases Using Human Induced Pluripotent Stem Cells. Major Professor: Jason S. Meyer

Human induced pluripotent stem (iPS) cells have the unique ability to differentiate into 200 or so somatic cell types that make up the adult human being. The use of human iPS cells to study development and disease is a highly exciting and interdependent field that holds great promise in understanding and elucidating mechanisms behind cellular differentiation with future applications in drug screening and cell replacement studies for complex and currently incurable cellular degenerative disorders. The recent advent of iPS cell technology allows for the generation of patient-specific cell lines that enable us to model the progression of a disease phenotype in a human *in vitro* model. Differentiation of iPS cells toward the affected cell type provides an unlimited source of diseased cells for examination, and to further study the developmental progression of the disease *in vitro*, also called the "disease-in-a-dish" model.

In this study, efforts were undertaken to recapitulate the differentiation of distinct retinal cell affected in two highly prevalent retinal diseases, Usher syndrome and glaucoma. Using a line of Type III Usher Syndrome patient derived iPS cells efforts were undertaken to develop such an approach as an effective *in vitro* model for studies of Usher Syndrome, the most commonly inherited disorder affecting both vision and hearing. Using existing lines of iPS cells, studies

were also aimed at differentiation and characterization of the more complex retinal cell types, retinal ganglion cells (RGCs) and astrocytes, the cell types affected in glaucoma, a severe neurodegenerative disease of the retina leading to eventual irreversible blindness.

Using a previously described protocol, the iPS cells were directed to differentiate toward a retinal fate through a step-wise process that proceeds through all of the major stages of neuroretinal development. The differentiation process was monitored for a period of 70 days for the differentiation of retinal cell types and 150 days for astrocyte development. The different stages of differentiation and the individually derived somatic cell types were characterized by the expression of developmentally associated transcription factors specific to each cell type. Further approaches were undertaken to characterize the morphological differences between RGCs and other neuroretinal cell types derived in the process.

The results of this study successfully demonstrated that Usher syndrome patient derived iPS cells differentiated to the affected photoreceptors of Usher syndrome along with other mature retinal cell types, chronologically analogous to the development of the cell types in a mature human retina. This study also established a robust method for the *in vitro* derivation of RGCs and astrocytes from human iPS cells and provided novel methodologies and evidence to characterize these individual somatic cell types.

Overall, this study provides a unique insight into the application of human pluripotent stem cell biology by establishing a novel platform for future studies of *in vitro* disease modeling of the retinal degenerative diseases: Usher syndrome and glaucoma. In downstream applications of this study, the disease relevant cell types derived from human iPS cells can be used as tools to further study disease progression, drug screening and cell replacement strategies.

CHAPTER 1 – INTRODUCTION

1.1 Nervous System and Development

The specialization of the more than 200 cell types that constitute the adult human body starts during gastrulation, an early embryonic developmental process when the embryo differentiates into the 3 germ layers – ectoderm, mesoderm, and endoderm – 14 to 16 days post-fertilization (http://stemcells.nih.gov/info/scireport/pages/appendixa.aspx). The nervous system, consisting of the brain, retina, spinal cord, and the collection of nerves and glia that together control all sensory and motor responses of the human body, is derived from the ectoderm within the first 3 weeks post-fertilization. The development of the nervous system starts when inductive signals from the mesoderm that induces the overlying layer of ectoderm to thicken and flatten out to form the first stage in nervous system development, the neural plate [1]. The neural plate can be considered to be a row of multipotent neural stem cells that eventually gives rise to all the parts of the central nervous system [2]. The ends of the neural plate gradually folds on itself creating the neural groove. This neural groove deepens further as the folds eventually close together to form the neural tube, the precursor structure now primed for the regional specification of the nervous system [1]. The anterior parts of the developing neural tube give rise to primary brain vesicles, the prosencephelon, mesencephelon, and the rhombencephelon. The remaining posterior regions give rise to the spinal cord. Molecular signals are responsible for further patterning the neural tube along the anterior-posterior and dorsal-ventral axes. The primary brain vesicles are further divided into secondary brain vesicles that give rise to different parts of the brain and the inferior regions continue to specialize into different regions of the spinal cord. Around 30-35 days of

development in humans, the prosencephelon divides into telencephalon and the diencephalon. The telencephalon forms the anterior most forebrain regions of the nervous system, the cerebral cortex, white matter, and the basal ganglia. The diencephalon, which is directly inferior to the developing cerebral cortex, differentiates into distinct regions forming the retina, thalamus, and the hypothalamus. The mesencephelon divides into the midbrain forming the tectum, the region critical in processing visual and auditory responses, and tegmentum, the region that controls motor and other reflexive pathways. The rhombencephelon is further divided into metencephelon and myelencephelon. The metencephelon forms the motor center of the brain, the cerebellum, and the pons. The myelencephelon forms the medulla oblongata, the respiratory control center of the nervous system and control center for other involuntary functions like heart beat rate, blood pressure, and other autonomic functions. The spinal cord formation is continuous with the medulla oblongata. All regions of the nervous system are essentially composed of several types of neurons that crosslink and influence each other via synaptic contact to establish an extremely intricate system of neural circuitry that along with glial cells govern the functioning of the entire nervous system.

1.2 Development of the Eye and Retina

The retina develops as a bipartite primordium from a single central field of the developing anterior neural tube [3] (Figure 1). During the first few weeks of human nervous system development, the diencephalon gives rise to a paired set of optic grooves that eventually evaginates to form the optic vesicles from a central eye field. The optic vesicles undergo further specification and coordination with the head ectoderm to differentiate into bi-layered optic cups where the inner layer eventually develops into the neural retina and the outer layer, the supportive RPE [4]. The third part of retinal development involves the specification of the optic stalk that

matures to form the optic nerve [5]. The part of the head ectoderm in close association with the developing optic cup is eventually induced to form the lens [6].

Several defining studies in identifying the ontogeny of the retina and its cell types has provided a range of molecular markers to identify individual neuroretinal cell populations and their functionalities with precision, making retina a highly accessible and amicable model for the study of nervous system development [7].

The differentiation of specific retinal cell types from the optic cup-stage progenitors is based on the activity of lineage restricted progenitors and whose fate can be divided chronologically into early and late retinogenesis [8, 9]. The earliest cell types derived in the retina are the retinal ganglion cells (RGCs), cone photoreceptors, horizontal cells, and most amacrine cells. Rod photoreceptors, bipolar interneurons and Müller glia are derived in the latter half of retinal development [10, 11]. The early stage of eye field specification has been extensively characterized for the expression of stage specific transcription factors and proteins. Early optic-vesicle structures are characterized by the expression of the eye field transcription factors (EFTFs): *PAX6, RAX, SIX3, SIX6, LHX2*, and *TBX3* distinguishing them from other lineages of neural commitment [12, 13]. Cell populations co-expressing *PAX6* and *RAX* have been identified as definitive retinal progenitor cells in early eye and later retinal specifications [14]. Genetic studies corroborate the importance of EFTFs in human eye development by showing how mutations in *PAX6, SIX3, SIX6* can result in malformations affecting the eyes [6]. Early and late stage retinal histogenesis has been similarly studied for the expression of developmentally associated factors that play a pivotal role in the understanding of the highly conserved series of events that forms the retina and its cell types. More specifically, the role of multiple basic helix-

loop-helix (bHLH) type transcription factors in combination with other homeobox and forkhead genes is crucial for the subsequent lamination of the retinal structure [15] (Figure 2).

The differentiation of retinal neurons begins around 31-35 days of human embryonic development [16]. The competence of retinal progenitors to specify a distinct neuroretinal cell type is based on the availability of both intrinsic and extrinsic cues. Dividing and proliferating multipotent retinal progenitor cells are identified by the expression of the homeobox transcription factor, *CHX10* [17]. RGCs are determined by the expression of *ATH5*, a bHLH transcription factor transiently expressed in the retinal progenitors cells, essential for the specification of RGCs [18-20]. A set of 3 POU domain transcription factors, *BRN3A, BRN3B, BRN3C*, is expressed in a restricted fashion in the RGCs in the retina, as a downstream target for ATH5 [21]. The origin of bipolar interneurons is regulated by the bHLH factors *MASH1* and *MATH3* in coordination with the homeobox gene *CHX10* [22]. Other interneurons including the amacrine cells and horizontal cells are closely associated in development with several overlapping regulatory factors. The neural bHLH transcription factors *MATH3* and *NEUROD* are required for the retinal progenitors to differentiate to amacrine cells [22] whereas the forkhead factors, *FOXN4* and *PTF1A* are critical for both amacrine and horizontal cells. Misexpression of these factors leads to greatly reduced amacrine cell numbers and a complete loss of horizontal cells [23, 24]. The expression of *PROX1* is essential for horizontal cell genesis [25]. The photoreceptors are divided into the early derived cone and the latter derived rod photoreceptors. The homeobox genes of *OTX2* and *CRX* establish the cues for photoreceptors specification [26, 27]. *NRL*, a basic leucine zipper transcription factor is selectively expressed in the rod photoreceptors through the regulation of *NR2E3 (TLL),* activating rod-specific genes [28, 29].

1.3 The Retina and its Cell Types

The retina forms the photosensitive tissue that lines the posterior surface of our eyes. The vertebrate retina harbors a repertoire of major cell types that are developmentally produced through the step-wise differentiation of multipotent retinal progenitor cells, derived in early vertebrate development from the neuroectoderm [13]. The specification of retinal cell types during development proceeds through a series of conserved events, in a highly regulated temporal and sequential manner [30]. The mature retina is a tightly layered structure consisting of different sets of neural, non-neural and glial cell types (Figure 3). The six sets of neurons that make up the neuronal tissue of the retina are part of an intricate retinal circuitry that is interconnected via synapses and responsible for the transduction of light to electrical signals required for our important sense of sight. The rod and cone photoreceptors form the outermost nerve layer of the retina and are the first ones to initiate the electrical cascade of visual function. The electric potential changes are relayed to inner layers of the retina, from the photoreceptors to the RGCs via synaptic contact with bipolar interneurons. In addition, the retina also has other types of interneurons, the amacrine cells and horizontal cells, which regulate the electrical input onto the retinal ganglion cells [31]. The ganglion cells convey the final electrical output to different brain nuclei via their axons which together form the optic nerve and leave the back of the eye in a region called the optic disc. The other cell types that make up the retina include the retinal pigment epithelium (RPE), a layer of pigmented epithelial cells on the outermost arc of the retina, responsible for the turnover of photoreceptor outer segments, and which also acts as the immune center of the eye [32]. The glial cell types found in the retina include the Müller cells that form the predominant glial cell type in the retina and aids in visual transduction and provides glial support to the retinal neurons [33]. The second kind of glial cells found in the retina are the astrocytes which are comparatively less in number and found mainly in the nerve fiber layer and the optic nerve head (ONH) of the retina in most mammalian species [34]. They form the major

glial cell type that support the non-myelinated optic nerve and are also known to secrete extracellular matrix molecules below the ONH where the optic nerve emanates out from the sclera at the mesh like structure called the laminar cibrosa [35]. The close coordination of all neural and non-neural cell types in the retina is essential for maintaining healthy visual function. Any abnormalities in its regular activity can lead to the degeneration of one or more of its specific cell types, leading to partial to complete loss of sight.

1.4 Retinal Degenerative Diseases

1.4.1 Background Information

According to World Health Organization (WHO) the total estimated number of visually impaired people as of 2012 stands at an astonishing 285 million (http://www.who.int/topics/blindness/en/). An overwhelming 165 million people worldwide are known to be afflicted with retinal diseases that cannot be prevented by corrective measures and/ or is currently completely incurable.

As described before, the retina is a thin layer of light-sensitive neural tissue at the back of the eye, made of rods and cones and other neurons that function together as part of a neural circuitry for relaying and processing visual information. Cell death of any of its several neuroretinal cell types can lead to retinal degeneration affecting visual output at different levels. Retinal degeneration can manifest itself due to genetic and age-related problems, affecting both the young and old from different races, ethnicities, and countries [36]. The limited ability for intrinsic regeneration in the mammalian retina makes it highly susceptible to irreversible damage or injury [37]. The degree and type of visual deterioration can vary from partial to complete loss of sight depending on type and stage of disease. Although different retinal neuron populations are affected in several retinal diseases, the loss of photoreceptors is often the initial and primary reason for the loss of other cell

types [37]. Glaucoma, age-related macular degeneration (AMD), and retinitis pigmentosa (RP) are among the leading causes of blindness due to cellular degeneration of specific neuroretinal cell types in the retina. The onset of retinal degeneration and loss of sight due to these diseases however can progress rapidly or perpetuate slowly in middle to late adulthood [38]. The causes for visual impairment can encompass abnormalities in different parts of the eye including the lens, choroid, ocular muscles, and vitreous body, however the therapeutic interventions currently available for cell based degeneration diseases in the retina are still quite limited compared to diagnostic advancements of the field [39]. Most of the diseases of the retina caused by the death of one or more of its neurons are currently incurable. Efforts to transplant healthy retinal cell types to replace their degenerated counterparts are considered to be the most primary approach for the prospective treatment of these diseases.

1.4.2 Retinal Diseases – Examples

The retina can be subject to several complex neuropathies affecting one or more of its cell types. Age-related diseases such as glaucoma are characterized by the progressive loss of RGCs, and AMD, by the gradual loss of photoreceptors, interneurons, and essential supporting cells, the RPE. Leading inheritable or genetic retinal disorders include RP, Stargardt's disease, Best disease, Leber's Congenital Amaurosis. These diseases progress with the early loss of photoreceptors with the subsequent loss of RGCs [40].

Glaucoma, the second largest cause of blindness in the world according to the website of WHO (http://www.who.int/bulletin/volumes/82/11/feature1104/en/) is an optic neuropathy, affecting visual function and ONH morphology due to the loss of RGC cell bodies and axons in the inner retina, nerve fiber layer and ONH respectively [41, 42]. In addition, the lamina cibrosa, openings where ganglion cell axons exit the eye, deteriorates progressively. Glaucoma is closely associated

with the rise in fluid pressure of the aqueous humor. The increase in intraocular pressure is theorized to cause RGC cell death by blocking anterograde and retrograde axonal transport at the laminar cibrosa [43, 44]. Glaucoma is divided into 2 main categories: “open angle” and “closed-angle” type glaucomas [45]. Open-angle glaucoma, the milder of the two sub-types is characterized by the slow progression of visual loss starting from the periphery and is diagnosed by an increased ratio of the optic cup area to disk. Close-angle glaucoma has a more acute onset with higher intraocular pressures due to closure of the angle between the iris and the trabecular meshwork which obstructs the flow of the aqueous humor. Close-angle glaucoma can be diagnosed by physical symptoms including dilated pupils, clouded cornea, and red eye. While there is no current cure for this disease, its progression can be slowed down if detected early. However, studies aimed at preventing the loss of RGCs and ONH architecture are more pragmatic in terms of providing a definitive solution to this devastating disease.

Age-related macular degeneration (AMD) is an age-related retinal degenerative disease caused by the loss of photoreceptors located at the macula region of the retina that affects both central and color vision. This painless form of retinopathy has distinct types of pathophysiology. The “dry” form of AMD results in the loss photoreceptors in the outermost layer of the retina. It is characterized by increased amount of yellow colored extracellular deposits called drusen, between the RPE and the choroid. The “wet” form is an exudative form of AMD caused by the neovascularization in the sub-retinal space with related macular degeneration. AMD is generally seen in elderly people; however, a childhood onset of a type of macular degeneration is known to exist in Stargardt’s disease. There are no current cures for AMD, but there are highly promising ongoing clinical trials using embryonic stem cell derived RPE cells for sub-retinal transplantation into human patients afflicted with the disease [46, 47].

Retinitis pigmentosa (RP) is the leading cause of genetically associated diseases involving retinal degeneration in juvenile and early adulthood. RP is a generic name given to all retinal dystrophies that progress primarily by affecting the rod photoreceptors first, causing night blindness or nyctalopia, and leading eventually to the loss of peripheral and central vision. A total of 45 causative genes and several mutations have been identified with different forms of RP [48, 49]. Physical manifestation of RP includes the deposition of bony-spicule shaped pigmented aggregates in the RPE, easily identifiable through the fundus examination of a diseased eye, from which the disease gets its name. A fundus examination can also reveal other signs of RP including thinning of blood vessels and the pale and waxy appearance of the optic nerve [48]. The inheritance pattern of RP shows heterogeneity as also seen with the genes involved in the disease. Mutations in RP related genes can be passed on as autosomal dominant, X-linked, and autosomal recessive. An example of an autosomal recessive mutation, and most critical the current study is the Usher Syndrome.

Usher Syndrome is the most frequent form of syndromic RP where affected patients suffer from visual and auditory abnormalities with some balance defects. The visual loss due to RP accompanies mild to severe deafness caused by degenerating neurons in the cochlea part of the inner ear. Mutations identified in atleast 10 genes are responsible for Usher syndrome [50, 51]. The severity of the progression of the symptoms in Usher syndrome divides it into 3 subtypes [52]. In type I, the disease is characterized by congenital deafness and vestibular dysfunction accompanied by the loss of night vision before the age of 10. In type II, the patient suffers from moderate to severe hearing loss at birth with reduced night vision starting in late childhood and no balance issues. Type III is characterized by the onset of sensory problems only in the late teens with normal to near-normal vestibular functions. As is the case with other retinal degenerative diseases, RP and its related disorders are currently incurable, and strategies including cell

replacement, gene therapy, and supplements with neurotrophic factors are promising avenues to study the pathophysiology of the disease, and perhaps offer new therapeutic avenues for the treatment or cure of the disease.

1.5 Human Pluripotent Stem Cells

1.5.1 Embryonic Stem Cells

Vertebrate embryogenesis is characterized by the differentiation of the totipotent zygote to all 3 germ layers including the yolk sac, the amnion, and placenta. The differentiation of all somatic and germ cells begins in late stages of the blastocyst when a subset of cells in the inner cell mass (ICM) of the blastocyst acquires pluripotent properties before gastrulation. This population of around 100 cells derived from the blastocyst stage of the embryo is the embryonic stem (ES) cells. The 2 basic properties that distinguish ES cells from any other cell type is its ability to differentiate into all adult cell types of the body in addition to the unlimited potential of self-renewal in culture [53].

ES cells were first derived from mice by the explantation and culture of the ICM of pre-implantation embryos in seminal works by Evans and Kaufman at Cambridge, and Gail Martin at University of California San Francisco [54, 55]. Mouse ES cells injected into the blastocyst of mouse embryos were competent of full development, producing chimeric mice where ES cells contributed to cell types of all three germ layers as well as the germ line. Further molecular characterization of mouse ES cells revealed interesting features when compared to its in vivo counterparts. The ICM cells were not self-renewing and globally hypopmethylated compared to the unlimited proliferation potential and hypermethylated genomes of ES cells cultured *in vitro* [56, 57].

It was not until 17 years after the discovery of mouse ES cells, in 1998, that the first human ES cell lines were successfully derived by Thomson and colleagues at the University of Wisconsin [58]. Human ES cells were derived from blastocysts of human embryos created by *in vitro* fertilization (IVF) techniques for clinical purposes. Human ES cells were characterized by a higher nucleus to cytoplasm ratio, normal karyotype, high telomerase activity, and pre-inactivated states of X chromosomes [58, 59]. Human ES cells were also extensively characterized for their molecular identifiers and properties. They expressed the pluripotency-associated genes*, OCT4, SOX2,* and *NANOG*, all of which are highly expressed during embryonic development. The ability of human ES cells to differentiate into cell types of all 3 germ layers was demonstrated by the formation of teratomas when injected subcutaneously into immunocompromised mice [58, 60, 61].

The isolation of mouse and human ES cells ushered in a new era in the field of mammalian developmental biology. The endless potential of these cells were realized in theory and then in practice for studying basic human development and in the etiology and treatment of diseases. Phenomenal concepts of disease modeling and personalized medicine emerged. Strategies for directed differentiation of ES cells to individual types of all germ layers including neurons, cardiomyocytes, hepatocytes, blood cells, airway epithelial cells, were shown and replicated by groups all over the world [62-66]. The use of host or patient derived ES cells by nuclear transfer to prevent immune rejection in autologous transplantation and promote repair was shown to be successful in a proof-of-principle study in ES-derived dopaminergic neurons in parkinsonian mice [67]. The different sources of pluripotent stem cells are summarized in (Figure 4).

1.5.2 Induced Pluripotent Stem Cells

In 2006, an alternative to ES cells was discovered when Yamanaka and colleagues at Kyoto University published their landmark study in which the simultaneous introduction of 4 developmentally associated genes, *OCT4, SOX2, KLF-4, C-MYC*, into adult mouse fibroblasts was able to revert these terminally differentiated cells to a more primitive, unspecified, and embryonic-like state [68]. The following year, the labs of both Yamanaka and Thomson successfully reprogrammed adult human skin cells to produce the first lines of ES-cell like, human induced pluripotent stem (iPS) cells [69, 70]. Human iPS cells were shown to be similar to ES cells in several defining attributes including morphology, self-renewing capacity, gene expression profile, and most importantly, its differentiation potential and ability to contribute to cells of all germ layers. Further molecular characterization of iPS cells reveals that for some selective clones they are completely indistinguishable from ES cells in terms of histone tail modifications, inactivation states of X chromosomes, and DNA methylation profiles [71].

The emergence of iPS cell colonies in culture is defined by their distinct phase bright and almost 3-dimensional morphology like appearance characterized by well-defined edges. To tell apart colonies that are partially or completely reprogrammed, scientists use the aid of molecular and epigenetic identification tools. Completely reprogrammed human iPS cells express endogenously activated proteins such as *SSEA-4*, and surface antigens *TRA-1-60* and *TRA-1-81* besides the expression of the regular cocktail of genes that were used to dedifferentiate the adult cells in the first place, *OCT4, SOX2, NANOG, LIN28, KLF-4, C-MYC*, along with their promoter de-methylation [72]. Some of the epigenetic hallmarks of iPS cells include the upregulation of de novo DNA methyltransferases *DNMT3a* and *DNMT3b*, and the role of *DNMT1* knockdown to convert the intermediately reprogrammed iPS cells into those that are fully pluripotent [73, 74]. Tests involving the formation of “all iPSC mice” are the gold standard for mouse iPS cells where

one can study the development of a normal mouse only by the iPS cells injected into tetraploid embryos, a process known as tetraploid complementation [75-78]. Due to obvious ethical issues related to generating human chimeras, the most stringent way to evaluate the developmental potential of human iPS cells is its ability to form teratomas upon subcutaneous injection into immunodeficient mice [79, 80].

The reproducible nature of iPS technology is evident by the large number of research papers that established mouse and human iPS cell lines after the first reports of its derivation was reported [80-83]. Alternate animal sources of iPS derivation have also been successful from rats [84, 85], rhesus monkeys [86], porcine [87], canines [88], indicating the evolutionary conservation of the transcriptional network governing pluripotency in different species and allowing for different animal models to be used for disease modeling. Scientists have also generated iPS cells starting with different somatic cell populations including blood cells [89], hepatocytes [90], neural cells [91], and keratinocytes [92], establishing the overall general applicability of the technology and providing alternate cell sources for reprogramming.

The overlapping clinical applications of iPS cells and ES cells are more profound for the former due to more immunocompatible cell derivatives for transplantation. The use of iPS cells finds limitless potential in normal and diseased forms of human development. The ability to be able to generate iPS cells from cells of patients provides a unique way to study disease progression compared to isogenic controls and initiate drug screening strategies on affected cell types that can be derived from the patient specific iPS cell lines. The use of disease specific iPS cell lines provides for means to recapitulate disease phenotype *in vitro*. One important criterion that currently prevents the iPS cells from being autonomously used in clinical trials and making the transition from bench to bedside is its association with potential virus like expression and random

integration of some of the genes that were initially used to reprogram the adult cells. Since 2006, however, several modifications to the protocol of reprogramming has seen the overhaul of the initially used retroviral/lentiviral approaches for the more clinically relevant transgene free protocols of introduction of the pluripotency associated factors using systems including Sendai virus [93], adenovirus [94], plasmids [95], mRNAs [96], proteins [97], and small molecules [98, 99]. Further sophisticated molecular methodologies to generate transgene free iPS cells include the doxycycline drug-inducible and floxed excisable lentiviruses [100, 101].

The overall impact of the discovery of ES and iPS cells has been potentially revolutionary. Although the use of ES and iPS cell technology has great implications in tackling several developmental concepts, a great amount of work is still needed to minimize any artifacts generated through irregular culturing techniques, non-uniform genetic backgrounds, partial reprogramming, and reprogramming factor combinations for these cells to be regularly realized in cell transplantation and curative approaches.

1.6 Induced Pluripotent Stem Cells: Disease Modeling

1.6.1 Disease Modeling in Theory

The successful generation of human iPS cells opened up new avenues of previously unanticipated possibilities to study complex degenerative disease *in vitro*. The role of iPS cells in modeling of degenerative disorders will be critical in the near future to gain further insight into identifying mechanisms and biological targets associated with disease cause and progression. The concept of disease modeling or “disease-in-a-dish” is a promising approach to screen patient derived cell types for any genetic or physiological abnormalities and identify novel therapeutic candidates which could help combat cellular stresses and disease symptoms (Figure 5). The process works

through the derivation of iPS cells from patient specific primary cells followed by the differentiation of these cells which bears the genetic memory of the affected individual to the disease relevant cell type. The establishment of a cost effective protocol to derive the diseased cell type provides an unlimited source of patient tissue that can be used to recapitulate in vivo human development and disease phenotypes. The use of patient cells as starting material holds tremendous potential for assessing disease progression when compared to cell lines derived from isogenic controls of the non-symptomatic individual. The end product of such studies, the *in vitro* derived affected somatic cell types, can be used for a wide range of medical applications including transplantation, drug targeting, molecular profiling, and personalized medicine. In theory, iPS cells can be differentiated to virtually any tissue type of the body, representing a new source of autologous tissue for cell therapy [102].

1.6.2 Disease Modeling in Practice

A significant amount of work has already been accomplished in the study of degenerative disorders of all 3 germ layers including Parkinson's, Alzheimer's, Amyotrophic Lateral Sclerosis (ALS) or Lou Gehrig's disease, Retinitis Pigmentosa, Long QT Syndrome, and Type 1 Diabetes. Several labs have successfully been able to derive iPS cells from patient specific samples of these diseases and provide criterion for differentiation to the affected cell type followed by the assessment of *in vitro* recapitulation of the expected disease phenotype. In the first demonstration of this ability of iPS cells, Park and colleagues at Harvard were successful in deriving iPS cells with their associated phenotype from different disease patients, including Huntington with its characteristic tri-nucleotide *CAG* repeats in the *HUNTINGTIN* gene, Down syndrome with the triplication of chromosome 21 (trisomy 21) seen in the karyotype analysis, Type 1 Diabetes, and Parkinson's [80]. Work done by labs in individual disease models have shown that not only can they reprogram adult cells to the embryonic-like iPS cells but also under specific culture

conditions, coax them to differentiate into the cell type associated with the disease including motor neurons in Spinal Muscular Atrophy (SMA) and ALS models, beta cells in a diabetes model, hematopoietic cell in Fanconi Anemia, and dopamine neurons in Parkinson's models [80, 103-106].

In the retina as well, important contributions have been made by different labs in the field of *in vitro* disease modeling and transplantation. Although a lot of the work has been concentrated around the use of human ES cells as starting sources, recent studies have picked up the use of iPS technology to mimic in vivo retinogenesis in disease patient samples. Gamm and colleagues at University of Wisconsin, Madison have generated iPS cells from patients with gyrate atrophy, an inherited disorder causing blindness, and used pharmacological (elevated B6 levels) and genetic strategies to correct for the genetic mutation *in vitro* [107]. The ability to model retinal degeneration was shown by Takahashi and colleagues at the RIKEN Center for Developmental Biology, when they generated iPS cells from 5 patients harboring RP specific mutations in the following genes: *RP1, RP9, PRPH2,* or *RHO*. The study was successful in recapitulating the disease phenotype by measuring the progressive loss of rhodopsin protein over time and identified markers for cellular stresses as a consequence of the genetic mutations. The same group followed this study with the derivation of RP patient specific iPS cells using a non-integrating Sendai-virus vector system to deliver the pluripotency factors for reprogramming a year later [108]. In a more recent study, Gamm and colleagues have been successful in modeling the maculopathy of BEST disease, an inherited disorder caused by a mutation in the *BESTROPHIN1* gene in the RPE, comparing the properties of iPS-RPE cells derived from the affected patient and the unaffected sibling as control [109]. The work demonstrated within this thesis is the first study to look at human iPS cells derived from fibroblasts of a Type III Usher Syndrome patient and

follow its progression towards a neuroretinal specification, more importantly, toward the affected cell type in this disease, photoreceptors.

The use of iPS cells in disease modeling promises for a highly customized approach to studying and potentially the development of treatments for several degenerative diseases. However, despite the exponential growth of the field en bloc, there is still a constant need for robust protocols to achieve and replicate lineage specific differentiation of clinical grade human iPS cells, recapitulate disease phenotype, provide functional integration of *in vitro* derived cells on transplantation, and minimize any possible immunogenic reactions in the process.

1.7 Thesis Objectives

Building on previous studies in the field and utilizing concepts of human iPS cells and directed differentiation, this work aims to provide further insight into the specification of distinct retinal cell types affected in two major retinal degenerative diseases, Usher syndrome and glaucoma. As described earlier, Usher syndrome is a genetically inherited autosomal recessive disease that is characterized by the progressive visual loss of first rod photoreceptors and later cones later in addition to auditory and vestibular dysfunction. Using iPS cells derived from a patient with Type III Usher Syndrome, experiments were designed to assess the developmental potential of this cell line towards the recapitulation of a neural and subsequently a retinal phenotype in an *in vitro* system. One of the foremost aims of this study was to establish the chronological order of retinal cell fate specification analogous to an in vivo system with a special emphasis on the feasibility of this patient specific cell line to derive the affected cell types associated with RP in Usher Syndrome, the photoreceptors. The ability of this human iPS cell line to be able to differentiate into photoreceptors and all other retinal cell types served a dual purpose. Firstly, it provides a robust model to study retinal degeneration events in Usher Syndrome by utilizing the iPS-derived

photoreceptors for further downstream applications like studying disease progression, gene correction, and potential drug targeting studies. Secondly, being able to derive all other retinal neurons and glial cell types that are not associated with Usher Syndrome, the use of this cell line and another iPS cell line that was used in the work helps to devise protocols for the derivation, characterization, and enhancement of other retinal cell types such as RGCs and astrocytes, associated with retinal degeneration in glaucoma, a severe neurodegenerative disease of the retina that affects vision. Despite their roles as functionally important cell types in the retina, the derivation of RGCs using iPS cells has been very sparsely studied in the field owing to several reasons including its unknown *in vitro* ontogenesis and difficulty of recapitulating the extensive in vivo morphologies associated with the cell type *in vitro*. In the second half of this study, efforts were made to establish a timeline for the differentiation of RGCs using human iPS cells and provide extensive methods to characterize these projection neurons further. This work also looked at the derivation of retinal astrocytes, an important glial cell population at the ONH. Since glaucoma is characterized by the remodeling of the ONH, its pathophysiology involves a direct or indirect role of these astrocytes in optic nerve degeneration. An important aspect for patient specific *in vitro* modeling of this disease in the future would require the ability of the human iPS cells to provide a good robust and plentiful supply of astrocytes along with RGCs. Based on such requirements, efforts were made to establish methods to analyze the derivation and characterization of iPS-derived astrocytes and in so doing, provide a robust differentiation protocol that could be used to derive the two affected somatic cell types in glaucoma.

CHAPTER 2 – MATERIALS AND METHODS

2.1 Cell Culture

2.1.1 Human iPS Cell Lines

The hiPS cell lines Usher 006.1.5 (Usher iPSC) or T-lymphocyte derived iPS cells (TIPS-5) were utilized for all studies. The cell lines were obtained from the lab of Dr. David Gamm at the Waisman Center at the University of Wisconsin, Madison. The Usher iPSC line was derived from the genetic reprogramming of skin fibroblasts obtained via a skin biopsy from a patient afflicted with Type III Usher Syndrome. The TIPS-5 line was established from T-lymphocytes derived from a peripheral blood draw from a healthy individual. The derivation of both iPSC lines from different somatic cells was based on methods previously established in the field [68, 69, 110].

2.1.2 Media and Media Recipes

2.1.2.1 Human iPS Cell Medium

a) mTeSR™1 Basal Medium (STEMCELL™ Technologies, Catalog #05850)

b) mTeSR™1 5X Supplement (STEMCELL™ Technologies, Catalog #05850)

The final mTeSR™1 medium was prepared under sterile conditions inside the laminar flow hood. The mTeSR™1 5X supplement was thawed overnight at 4˚C and the total of 100mL thawed 5X supplement was aseptically added to 400mL of mTeSR™1basal medium and mixing well, making a total volume of 500mL mTeSR™1 medium. Complete mTeSR™1 medium stored at 4˚C, for up to 2 weeks.

2.1.2.2 Neural Induction Medium (NIM)

For a final volume of 500 mL:

a) DMEM/F12 (+HEPES) (GIBCO™, Ref. #11330-032) ……..... 489.5mL

b) N2 Supplement (GIBCO™, Ref. #17502-048) ……. 5mL

c) MEM-NEAA (GIBCO™, Ref. #1114-050) …….. 5mL

d) Heparin …….…….. 0.5mL

The final volume of NIM was prepared under sterile conditions inside the laminar flow hood. The N2 supplement was thawed in a 37˚C waterbath before the formulation of the medium. The components were added to a 500mL, 0.2µm bottle top filter (Thermo Scientific, Catalog #0974107) attached atop a 500mL tissue culture bottle, and the medium was filter-sterilized before final usage. NIM was stored at 4˚C for up to 2 weeks.

2.1.2.3 Retinal Differentiation Medium (RDM)

For a final volume of 500 mL:

a) DMEM/F12 (+HEPES) (GIBCO™, Ref. #11330-032) ……..... 240mL

b) DMEM (1X) (GIBCO™, Ref. #12430-054) …….…… 240mL

c) B27 Supplement (GIBCO™, Ref. #17502-048) ……..... 10mL

d) MEM-NEAA (GIBCO™, Ref. #1114-050) …….……...… 5mL

e) Penicillin/ Streptomycin/ Ampicillin (PSA) ……..... 5mL

The final volume of RDM was prepared under sterile conditions inside the laminar flow hood. The B27 supplement and PSA were thawed in a 37˚C waterbath before the formulation of the medium. The components were added to a 500mL, 0.2µm bottle top filter attached atop a 500mL tissue culture bottle, and the medium was filter-sterilized before final usage. RDM was stored at 4˚C for up to 4 weeks.

2.1.2.4 Dispase

The use of the enzyme Dispase (GIBCO™, Ref. #17105-041) is recommended for passaging of human iPS cells. A final working concentration of 2mg/mL of dispase was prepared under sterile conditions inside the laminar flow chamber. 100mg of dispase was weighed and carefully added to a 50mL conical tube containing 50mL of DMEM/F12. The conical tube was mixed several times by inverting to make sure there were no floating clumps of dispase powder in the solution. The solution was warmed for 20 minutes in a 37˚C waterbath. After the dispase solution was sufficiently warm, the solution was filter sterilized using a 50mL, 0.22µm Sterifilp® filter (Millipore™). Dispase solution was stored at 4˚C for up to 2 weeks.

2.1.2.5 Matrigel

Matrigel (BD Biosciences) was used as the basement membrane matrix compound to coat 6-well plates for the growth of human iPS cells on them. Matrigel received from the vendor was thawed on ice, aliquoted, and frozen down at -80˚C. Before use, matrigel was diluted in cold DMEM/F12 according to vendor specifications and 1mL of cold matrigel was used to coat 1 well of a 6-well plate. A 50mL solution of diluted matrigel was stored at 4˚C for up to 2 weeks.

2.1.2.6 Laminin

For differentiation of human iPS cells as adherent cultures, 6-well plates were coated with laminin (Stemgent™, Catalog #08-0002), part of the extracellular matrix (ECM) family of glycoproteins. Laminin received from the vendor was stored in -80˚C. Before use, a 1mL vial of laminin was thawed overnight at 4˚C. To coat plates, laminin was diluted with DMEM (1X) in a ratio of 1:50 to achieve a final concentration of 20µg/mL. Diluted laminin was added to the center of the well and carefully spread using the back end of a P1000 micropipette tip. The laminin was uniformly spread covering majority of the well area except the edges.

2.1.3 Thawing of Cryopreserved Human iPS Cells

Media and supplements required:

1) Complete mTesr™1
2) DMEM/F12
3) Matrigel

Human iPS cells were thawed and plated onto a 6-well plate (Thermo Scientific, Nunclon treated) that was coated with matrigel and incubated for an hour at room temperature before subsequent thawing of cells. The general criterion for number of vials of cells plated/ well of a 6 well plate was based on the equivalency of number of cryovials used to freeze down cells from a single well of a 6-well plate, i.e. 1 vial of cryopreserved cells made from 1 well of a 6-well plate was used to thaw in 1 well of a 6-well plate. Before the start of the protocol and removal of the vial of cells from liquid N_2 storage, all media was well warmed in a 37˚C waterbath and the 6-well plate was prepared with matrigel. A 15ml conical tube was filled with 10mL of warm DMEM/F12. At this stage, the vial of human iPS cells was removed from the liquid N_2 tank and thawed in a 37˚C waterbath by shaking vigorously for 3-4 minutes. The contents of the cryovials were transferred into the conical tube containing the DMEM/F12 and the tube was centrifuged at 800rpm for 3 minutes. After the centrifugation was complete, the medium from the conical tube was aspirated leaving the iPS cell pellet intact. Next, the liquid matrigel was aspirated from the coated tissue culture plate. 2mL of mTeSR™1medium was slowly added to the coated well from the sides using a serological pipette. The iPS cell pellet was then resuspended in 0.5mL of mTesr™1 medium to dislodge the pellet and break down any bigger aggregates of cells and then transferred to the coated well of the 6-well plate containing 2mL of mTesr™1. The medium containing the cell aggregates was poured slowly in the middle of the well with the tip of the serological pipette perpendicular to the well. The 6-well plate was transferred to a 37˚C incubator. The cells were cultured at normal physiological conditions inside the incubator: 37˚C, with 5% CO_2, and 100%

humidity. Daily media changes with mTesr^{TM}1 were performed henceforth until the undifferentiated colonies of human iPS cells were ready to be passaged.

2.1.4 Maintenance and Passaging of Human iPS Cells

Media and supplements required:

1) Complete mTeSR™1
2) DMEM/F12
3) Dispase
4) Matrigel

Human iPS cells were maintained and expanded in an undifferentiated state using methods previously described for human pluripotent stem cells [30, 107]. iPS cells were grown on matrigel in mTeSR™1 for the maintenance of an undifferentiated state. The cells were passaged every 4-5 days when the colonies approached 70-80% confluency. They were enzymatically lifted using dispase (2mg/mL) after the differentiation colonies were first manually removed. The appearance of spontaneous differentiation in iPS colonies was identified by the loss of its prominent phase bright borders and emergence of non-uniformly shaped cell types. All culture media was well warmed and the required number of 6-well plates coated with matrigel and incubated at room temperature for 1 hour before the process. 1 well of a 6-well plated of iPS cells was expanded to 1 whole 6-well plate. Before each round of passaging, the differentiation areas were marked under the microscope and the colonies scraped out using a tip of the P1000 micropipette. The medium on the cells containing the free floating differentiated aggregates was aspirated out and 1mL of dispase was added to the well. The cells were incubated in dispase for 15-20 minutes at room temperature to allow for sufficient curling of the edges of the iPS colonies. At the end of this incubation, the dispase was aspirated and the cells were washed twice with 1mL of DMEM/F12 to remove any residual dispase on the cells. Using a 10mL serological pipette, the enzymatically loosened iPS colonies were easily dislodged by 2-3 rigorous draws with the pipette and transferred to a 15mL conical tube and allowed to settle. The matrigel on the plate was aspirated

and 2mL of mTeSR™1 medium added to the each well from the sides. The DMEM/F12 in the conical was aspirated leaving the iPS cells at the bottom. The iPS cells were then resuspended in 3mL of mTeSR™1 and a few draw and release motions were performed to break down any large aggregates of cells. To each well of a 6-well plate, 0.5mL of iPS cells in mTeSR™1 was added to the center of the well with the tip of the serological pipette perpendicular to the well. Care was taken to keep the iPS colonies at appropriate sizes as bigger colonies are more prone to differentiation and smaller colonies or single iPS cells would have less chances of survival. The 6-well plate was transferred to a 37˚C incubator and shaken to ensure the uniform distribution of the cells in the well to prevent overcrowding of proliferating colonies later on. The cells were cultured at normal physiological conditions inside the incubator: 37˚C, with 5% CO_2, and 100% humidity. The different stages in the passaging of human iPS cells are represented in (Figure 6).

2.1.5 Differentiation of Human iPS Cells

2.1.5.1 Neural Induction

Media and supplements required:

1) Complete mTeSR™1
2) NIM
3) Laminin coated plates
4) RDM

Neural differentiation and induction of human iPS cells toward an anterior neural fate was performed using methods previously described [30, 107]. A population of the enzymatically lifted iPS cell aggregates were grown in suspension in mTeSR™1 medium as embryoid bodies starting at day 0 and cultured in 3:1, 1:1, 1:3 mTeSR™1:NIM medium in the next 3 days and switched completely to the chemically defined NIM medium at day 4. After 6-7 days of growth and differentiation in suspension, the embryoid bodies were induced to attach to laminin coated 6-well plates to allow for the formation of neural cells. The neural cells were grown as adherent cultures for the next 10 days of differentiation. Within a few days of plating on laminin, the

appearance of columnar, neural tube-like cells could be observed. At day 16 of differentiation, the human iPS cell derived neural rosettes were mechanically lifted using a P1000 micropipette and grown as suspended spheres in non-adherent culture dishes in RDM. In the next 2 days, a subset of these spheres acquired a prominent golden ring-like structure around its borders indicative of the optic vesicle like appearance as in development *in vivo* [107]. These optic vesicle-like neurospheres were manually separated from other non-optic vesicle-like spheres and both populations of spheres grown in suspension in different dishes. The timeline for the neural induction of human iPS cells is explained in (Figure 7).

2.1.5.2 Retinal Differentiation of Human iPS Cells

Media and supplements required:

1) RDM

2) FGF, EGF, Heparin

3) Laminin coated coverslips

The differentiation of the human iPS cell derived optic vesicle-like or retinal neurospheres was carried out in RDM after they were manually separated from the non-optic vesicle-like or non-retinal neurospheres. The differentiation of RPE was continued as adherent cultures after day 16 until 40-50 days of differentiation in RDM. Medium changes with fresh RDM was done every 2 days depending on the amount of cells and proliferation per well of the plate. The emergence of a hexagonal morphology coupled with emergence of pigmentation was used to identify RPE. The pigmented areas were manually microdissected using a P200 micropipette and further grown as adherent RPE cultures on laminin coated coverslips. The medium was supplemented with the mitogens fibroblast growth factor 2 (FGF2) (20ng/ml) and epidermal growth factor (EGF) (20ng/ml), along with 2µg/mL of heparin to allow for the proliferation of pigmented RPE cells for 2 weeks. Differentiation of other cell types within the retina was carried out by the culture of the retinal neurospheres in suspension in RDM. For RGCs and photoreceptors, the differentiation

was carried out until different timepoints within a range of 70 days of differentiation. The suspended retinal neurospheres were fed with a strict regimen of medium changes every alternate day with RDM and conditioned RDM from the cells in a 1:1 ratio. The conditioned medium from the spheres was collected in 1.5mL eppendorf tubes and centrifuged at 2000rpm for 3 minutes before being combined with fresh RDM to be added to the cells to get rid of any cellular debris or single cells in the medium. Overgrown spheres were kept an appropriate size by regular and light trituration once a week.

2.1.5.3 Differentiation and Passaging of Astrocytes from Human iPS Cells

Media and supplements required:

1) RDM
2) EFH (20ng/mL)
3) Laminin coated plates

The population of human iPS cell derived non-retinal neurospheres was differentiated in RDM for specification towards an astrocyte cell fate. The differentiation protocol used was modified from methods previously described to derive astrocytes from human pluripotent stem cell sources [111, 112]. The non-retinal neurospheres were grown in suspension as astroshperes until 85 days of differentiation, supplemented with EGF/FGF/Heparin (EFH) (20ng/mL) from day 20. Medium changes were performed every alternate day with RDM and conditioned medium from the cells, in a 1:1 ratio, and EFH (20ng/ml) was added. The conditioned medium from the spheres was collected in 1.5mL eppendorf tubes and centrifuged at 2000rpm for 3 minutes before being combined with fresh RDM and EFH to be added to the cells to get rid of any cellular debris or single cells in the medium. At day 85, the spheres were plated down onto laminin-coated wells of 6-well dishes and allowed to proliferate in the same media conditions. Upon confluence, the mixed population of post-mitotic neurons and non-post-mitotic astroglia was enriched for astrocytes by enzymatic passaging using accutase (2mg/mL). All media was well warmed before

the process and the required number of wells of a 6-well plate was coated with laminin for 4 hours before use. Following the aspiration of media from the cells, a single wash was performed with RDM. 1mL of accutase was added to the cells and incubated at room temperature for 3-5 minutes. After 5 minutes, the accutase was inactivated by equal volume of fetal bovine serum (FBS) and the enzymatically loose cells were dislodged with a P1000 micropipette with a couple of regular draws and collected in a 15 mL conical tube. The cell solution was passed through a 70μm cell strainer (BD Falcon™, Ref. #325350) to achieve a single cell suspension. Next, the cell suspension was centrifuged at 2000rpm for 3 minutes. The supernatant was aspirated leaving the cell pellet intact. The laminin was aspirated from the 6-well plate and 1mL of RDM was added to the well from the side. The pellet of cells was resuspended in 1ml of RDM and added to the laminin-coated well. 2μl of EFH was added the well. The 6-well plate was transferred to a 37˚C incubator and shaken to ensure the uniform distribution of the cells in the well to prevent overcrowding of proliferating cells. The cells were cultured at normal physiological conditions inside the incubator: 37˚C, with 5% CO_2, and 100% humidity. The cells were passaged every 7-10 days.

For experiments measuring the doubling time and proliferation rates of astrocytes, the cells were counted using a hemacytometer (Fisher Scientific, Catalog #0267110) and plated at a density of 100,000cells/well and passaged every 7 days for 4 passages starting at day 95-100 of differentiation.

2.1.6 Freezing Human iPS Cells

Media and supplements required:

1) Complete mTeSR™1

2) FBS

3) Dimethyl Sulphoxide (DMSO)

The cryopreservation of iPS cells was performed using methods similar to the passaging of iPS cells as described above. Fresh freezing medium was prepared and well warmed before the process. As a general rule, cells from 1 well of a 6-well plate were frozen in 1 cryovial (Wheaton™, Ref. #985916). The medium used to freeze down human iPS cells consisted of 80% mTeSR™1, 10% FBS, and 10% dimethyl sulpoxide (DMSO) (Fisher Scientific, Catalog #BP231-100). Before the process, the differentiated colonies were marked and scraped out as described earlier. The cells were treated as a regular passage of iPS cells until the step of collection of the dislodged iPS cell aggregates in a 15mL conical tube. At this point, the cell suspension was centrifuged at 800rpm for 1 minute. The supernatant was discarded and the iPS cell pellet was resuspended in freezing medium. The cell suspension was added to a 2mL cryovial and placed in an isopropanol 1˚C freezing container (Nalgene™, Catalog #5100-0001) to achieve for controlled cooling rates of approximately -1˚C/minute. The freezing container was placed at -80˚C overnight. The cryovials were transferred to liquid N_2 storage, the next day.

2.2 Immunocytochemistry (ICC)

Sterile coverslips were placed into sterile 4-well or 24-well plates. The coverslips were aseptically coated with 0.1mg/mL of Poly-D-Ornithine followed by 3 washes with sterile water and kept under sterile conditions at room temperatures for overnight. Poly-D-Ornithine coated plates were ready to use for ICC experiments the next day. ICC analysis was carried out by methods described previously [30]. For ICC procedures, the polyornithine-coated coverslips were further coated with laminin and incubated for 4 hours before use. After the incubation period, neurospheres were plated onto polyornithine- and laminin-coated coverslips overnight to allow for attachment. The next day, cells were either fixed in 4% paraformaldehyde (Electron Microscopy Sciences, Catalog #15714S) or continued in culture for a few days in the required growth medium. For fixation purposes, ICC plates were brought into the fume hood and

incubated in 4% paraformaldehyde for 30 minutes at room temperature. After 30 minutes, the paraformaldehyde was aspirated and the coverslips were washed 3 times in 1X phosphate buffer saline (PBS). Cells were then permeabilized in 0.2% Triton X-100 (Fisher Scientific, Ref. #BP151-100). This was followed by a single wash with 1X PBS and a 1 hour incubation in 10% donkey serum. Next, cells were immunostained using primary antibodies listed in (Table 1), in 0.1% Triton X-100 and 5% donkey serum. Coverslips treated with primary antibodies were left in overnight at 4˚C. The following day, the primary antibody solutions were removed and the coverslips were washed 3 times with 1X PBS followed by another round of incubation with donkey serum for 10 minutes. The cells were labeled and visualized with either Alexafluor 350, 488, 584 or Cy3-conjugated secondary antibodies, and nuclei were counterstained with 4',6-diamidino-2-phenylindole (DAPI). The secondary antibodies and DAPI were diluted in 0.1% Triton X-100 and 5% donkey serum before use. Cells were incubated with the secondary antibodies for an hour at room temperature followed by 3 washes with 1X PBS. Finally, the coverslips were mounted using Aqua Poly Mount (Polysciences, Inc™, Catalog #18606) on glass slides. After allowing time for mounting, images were obtained on a Leica 5500 upright epifluorescence microscope.

2.3 Microscopy

2.3.1 Brightfield Microscopy

Images for iPS cells in its undifferentiated state and stepwise differentiation into anterior neural and retinal lineages were obtained using a Nikon Eclipse TS100 Brightfield Microscope. Late stages of differentiation into retinal cell types were easily analyzed for RPE with its characteristic hexagonal morphology and brownish yellow pigmentation with a visible apical-basal transport of proteins in the brightfield. Images for neuroretinal proliferation for other mature retinal cell types were obtained but identification of individual retinal cell types in brightfield was not possible due to lack of scientific literature for the same. Similarly, astrocytes obtained in culture at different timepoints of differentiation were identified with their characteristic stellate shaped cell bodies and extensive outward processes. The progression of differentiation of astrocytes was observed until 150 days of differentiation in culture. All brightfield images for the different experiments were taken at both 4X and 20X.

2.3.2 Fluorescence Microscopy

The analysis of characteristic protein expression at different developmental stages from pluripotency to the derivation of mature retinal cell types was performed by ICC with subsequent analysis using a Leica 5500 upright epifluorescence microscope. Three different channels identifying the labeled proteins were used to combine co-expression analysis for different ICC experiments. Further image processing and enhancement was performed using the 3-dimensional deconvolution tool on the computer. The deconvolution tool was used to bring into focus images whose 3-dimensional and complex arrangement of cells resulted in the population of cells to emit light rendering the image as a whole, out of focus. As a part of the 3-dimensional convolution tool, images were taken at different focal planes (also called as z-stacking) and corrected for

blurriness and out of focus arrangements of cells. A final image with the best possible contrast and resolution was obtained from the set of z-stacks used to deconstruct the image initially. All images for the different experiments were taken at 3 magnifications, 10X, 20X, and 40X.

2.4 Polymerase Chain Reaction (PCR)

2.4.1 Reverse Transcription-PCR (RT-PCR)

Total RNA was isolated from cells at different stages of differentiation using the RNeasy® Mini Kit (Qiagen, Catalog #746106) or the Arcturus® PicoPure® RNA isolation kit (Applied Biosystems, Catalog #12204-01). The RNA was treated with DNase I to remove any genomic DNA contamination. 1-2µg of RNA was reverse transcribed to cDNA using the iScript cDNA synthesis kit (Bio-Rad, Catalog #170-8891). The final cDNA volume was diluted in ratios of 1:10 in RNA quality water and could be stored for long term use at -80˚C. The cDNA was amplified by PCR using the GoTaq PCR master mix (Promega) and primers for specific experiments, listed in (Table 2). The cycler conditions used for RT-PCR were as follows: preheated lid at 105˚C, initial denaturation at 95˚C for 5 minutes, 30 cycles of denaturation at 95˚C for 15 seconds, annealing at 60˚C for 30 seconds, and extension at 72˚C for 1 minute, final extension at 72˚C for 5 minutes, and a final hold at 10˚C. For each run, GAPDH was used as a control and run using the same program for 20 cycles. All experiments were run for the same number of cycles unless otherwise indicated. Subsequent PCR products were run on 2% agarose gels to analyze gene patterns.

2.4.2 Quantitative RT-PCR (qRT-PCR)

For quantitative RT-PCR, RNA was isolated and cDNA synthesized as described in the previous section. cDNA was amplified using the SYBR green master mix (Applied Biosystems, Lot #4309155) and analyzed by the 7300 RT detection software (Applied Biosystems). The primers used are listed in (Table 3). A final reaction volume of 20µl was used for all experiments. The cycler conditions used for all qPCR experiments were: initial denaturation at 95˚C for 5 minutes, 40 cycles of denaturation at 95˚C for 20 seconds, annealing at 60˚C for 30 seconds, and extension at 72˚C for 1 minute, final extension at 72˚C for 5 minutes. A no template control and a ß-Actin internal control were used for all experiments. All qPCR reactions were run at 40 cycles. The change in gene expression levels was measured using the $2^{-\Delta\Delta Ct}$ method, where Ct was the crossing threshold fluorescence value. ΔCt was measured as the Ct value of the target gene minus the Ct value for ß-Actin. ΔΔCt was equal to the ΔCt value of sample minus the ΔCt value of control.

2.5 Statistical Analysis

For quantification of ICC data, cells immunolabeled with a particular marker were counted and compared to total number of cells in the view field as identified by the DNA stain DAPI. At least 2 representative fields from 2 coverslips were photographed in each of 3 separate experiments and individual cell counts were made using the ImageJ software (National Institutes of Health). The measurements of cell sizes and neurite lengths of retinal cells were done using quantification tools in the Leica 5500 upright epifluorescence microscope. Cell body areas were demarcated and measured in square microns and the lengths of RGC and photoreceptor neurites were measured in micron meters. All statistical analysis was conducted using the GraphPad PRISM version 6.0 (GraphPad Software Inc.). The statistical significance of differences was determined using the unpaired t-test. A probability value of less than 5% was considered to be significant. All experiments were conducted in triplicate unless otherwise stated. All values were expressed as means ± standard error.

CHAPTER 3 – ESTABLISHMENT OF AN *IN VITRO* SYSTEM OF USHER SYNDROME USING HUMAN IPS CELLS

3.1 Introduction

Usher syndrome is the most commonly inherited disorder affecting both vision and hearing, with or without vestibular dysfunction. It is an autosomal recessive disease which means it can affect males and females with equal frequency. A person has to inherit the altered copy of the affected gene from both parents to be diagnosed with this disease. A person inheriting only one copy of the mutated gene is an unaffected carrier for future generations. Usher syndrome patients suffer from sensorineural hearing impairment and retinal degeneration resulting in gradual to eventual loss of vision. Its symptoms include congenital, bilateral deafness and loss of vision due to retinitis pigmentosa (RP). The loss of visual function in Usher syndrome starts with the loss of night vision, progressing to the loss of photoreceptors from the periphery to the macula resulting in tunnel vision, and finally to complete blindness [113]. Hearing loss in Usher syndrome is due to degenerating nerve cells in the cochlea, the sound-transmitting structure of the inner ear. Usher syndrome can be clinically divided into 3 subtypes, Usher syndrome type I, II, and III, depending on the onset, severity, and progression of its symptoms. Usher syndrome patients also experience balance issues from birth in the type I form of the disease whereas the vestibular function is normal or near normal in types II and III. Besides the clinical differences, Usher syndrome is also characterized by its genetic heterogeneity. A total of 12 genetic loci and 10 genes have been identified to be associated with this disease [50, 51, 114]. Usher syndrome type I is divided further into the 6 subtypes: 1B, 1C, 1D, 1F, 1G, 1H depending

on mutations in the following genes, *MY07A, USH1C, CDH23, PCDH15, SANS*, and *USH1H* respectively [114, 115]. Usher syndrome type II is divided into at least 3 subtypes: 2A, 2C, 2D, affected by mutations in the genes, *USH2A, VLGR1A, WHRN* respectively, and type III has been associated with mutations in one gene *CLRN1* [115, 116]. Usher Syndrome is currently incurable, and the development of future therapeutic approaches requires further insight into disease mechanisms and progression. Current treatment strategies involve the use of educational and vocational programs to manage symptoms following early identification of the disease. Ongoing research in this disease involves the identification of more causative genes and its different variations. Identification of all genes is crucial to improved genetic counseling and quick diagnosis of the disease. Application of gene correction and pharmacological intervention strategies are also being used to slow the progression of the symptoms associated with the disease.

This study aims to provide a novel platform to further understand the genetic complications associated with Usher syndrome. More specifically, this study addresses the pathophysiology of visual degeneration in Usher syndrome patients associated with RP. RP as stated is characterized by the degeneration of photoreceptors, from the periphery to the macula, progressing from night-blindness in Usher patients to complete loss of vision. Taking advantage of the "disease-in-a-dish" concept, this study aims to characterize and establish the potential of an Usher syndrome patient specific iPS cell line to differentiate *in vitro* towards a retinal lineage progressing through all the major stages of normal retinal development. The use of iPS cell technology to model the degenerative progression of Usher syndrome provides a robust approach that employs the use of a more practical human model to study the different aspects of the disease. The eventual goal of this study is to provide a time feasible and a cost effective way to derive patient-specific affected

retinal cell types, the diseased photoreceptors, in large numbers, which could then be used for further downstream experiments to further disease development and treatment.

3.2 Results

3.2.1 Establishment of Pluripotency of Usher Syndrome iPS Cells

To establish the pluripotent and unspecialized nature of the type III Usher syndrome patient specific iPS cell line, following numerous passages *in vitro*, the Usher syndrome iPS cells were analyzed for all pluripotency associated characteristics as examined by ICC and RT-PCR analysis. ICC analysis revealed that Usher syndrome iPS cells maintained expression of pluripotency associated proteins, OCT4, SOX2, and NANOG (Figure 8: A,C,E). These 3 factors including, along with LIN28, were initially used to reprogram the skin cells of a type III Usher syndrome patient using lentivirus. ICC experiments also confirmed the expression of the endogenously activated pluripotency-related cell genes/ surface antigens such as TRA-1-60, TRA-1-81, and SSEA-4 (Figure 8: B,D,F). The onset of expression of these endogenous pluripotency genes besides the ones used for reprogramming was evidence for the completely reprogrammed nature of the Usher iPS cell line. In brightfield microscopy, the Usher syndrome iPS colonies exhibited typical pluripotent morphologies including cells that were tightly packed together with well-defined and phase bright edges (Figure 9). Larger colonies appeared to be somewhat 3-dimensional when viewed under the microscope and differences between an undifferentiated and differentiated colony were clearly visible during spontaneous differentiation events with the differentiated iPS cells easily identifiable by their non-uniform shape and lack of well-defined edges. Furthermore, RT-PCR results confirmed the expression of pluripotency-related genes, *OCT4, NANOG,* and *SOX2* and further established the undifferentiated nature of the cell line by confirming the lack of expression of markers associated with the 3 germ layers of

development, including, ALPHA-FETOPROTEIN for endoderm, BRACHYURY for mesoderm, and PAX6 for ectoderm (Figure 10).

3.2.2 Anterior Neural and Eye Field Specification from Usher Syndrome iPS Cells

The first stage in the stepwise differentiation of the Usher syndrome iPS cell line to a retinal lineage was the derivation of an anterior neuroepithelial cell fate which gives rise to the optic vesicles in vivo. As described in the methods section, iPS cells were grown as free floating embryoid bodies and transitioned into a chemically defined medium, NIM, for neural induction. The free floating embryoid bodies were plated onto laminin coated coverslips after 6-7 days of differentiation and allowed to proliferate as neural rosettes until 10 days in culture before being fixed in 4% paraformaldehyde for ICC analysis. ICC experiments revealed the loss of expression of pluripotency associated factors OCT4 and NANOG followed by the increase of transcriptional expression of factors associated with general neural induction and anterior neural development, including PAX6, SOX1, OTX2, and LHX2 (Figure 11). Furthermore, the appearance of the expression of neurodevelopmental transcription factors was associated with the formation of neural rosette like structures, reminiscent of neural tube formations *in vivo* (Figure 11). The proliferation of early neural cells as rosettes were was further confirmed as seen under brightfield microscopy (Figure 12). To further confirm the anterior nature of neural progenitor cells derived from the Usher syndrome iPS cell line, RNA samples were taken after 10 days of differentiation to be analyzed by RT-PCR analysis. RT-PCR results confirmed the accumulation of transcripts encoding numerous early neurodevelopmental transcription factors, *PAX6, SOX1, OTX2,* and *LHX2*. Also, by day 10, RT-PCR revealed expression of early eye development marked by the accumulation of transcripts encoding eye field transcription factors (EFTFs*), RAX, SIX3, SIX6,* and *NR2E1 (TLL)* (Figure 13). The committed nature of differentiation of the Usher syndrome iPS cell line was indicated by the expected decrease in the level of the pluripotency factors *OCT4*

and *NANOG*. RT-PCR of the early neural factor *PAX6* revealed a doublet, indicating the presence of the alternately spliced isoforms of the *PAX6* gene, the +5a and -5a isoforms.

3.2.3 Derivation of Retinal Progenitor Cells from Usher Syndrome iPS Cells

After establishing a primitive neural fate of the human iPS cell line, this study looked to characterize the Usher syndrome iPS line at later stages of differentiation. The free floating embryoid bodies were grown as adherent cultures in NIM until day 16 of differentiation. At this stage, the rosette containing colonies were mechanically lifted into RDM for the formation of neurospheres in suspension. Following 2 days of further induction, the suspended aggregates of cells formed two distinct sets of neurospheres when viewed in brightfield microscopy. A subset of spheres composed of an outer layer of phase bright cells, indicative of an optic vesicle like morphology whereas the other group contained spheres with a near uniform distribution of cells in each aggregate and with a more spherical looking morphology, at times with rosette internalization [107] (Figure 14). Cell aggregates possessing characteristics of both kinds of spheres were excluded from further differentiation analysis. The optic vesicle-like spheres were manually picked out and allowed to further differentiate in suspension in RDM. Following 20 total days of differentiation, these manually picked retinal neurospheres were analyzed for their RNA and protein expression patterns. ICC revealed that a subset of cells exhibited numerous characteristics of retinal development, including the presence of key transcription factors including the definitive retinal progenitor marker CHX10, and other early retina associated transcription factors SIX6, LHX2 and PAX6 (Figure 15). RT-PCR analysis further confirmed the presence of the retinal progenitor transcriptional markers including the critical retinal progenitor gene *RAX*, and other genes*, CHX10, LHX2, OTX2,* and *PAX6* (Figure 16). The development of retinal progenitor cells after 20 days of iPS cell differentiation was analogous to the origin of optic vesicles in normal human development.

3.2.4 Mature Neural Specification from Usher Syndrome iPS Cells

After 30 days of differentiation, the development of more mature neuronal characteristics was assessed in culture. Neural, non-retinal cells mechanically lifted at day 16 were grown as spheres in suspension in RDM until day 28 before being plated onto laminin coated polyornithine coverslips and fixed in 4% paraformaldehyde for ICC analysis. ICC results confirmed that a subset of cells co-expressed both the master neuroectoderm nuclear marker PAX6 and the cytoskeletal marker for newly committed neurons, ß-III TUBULIN (Figure 17: A). Emergences of tubulin expression after 30 days of differentiation were good indication of regular maturation of neuronal cell types from the iPS cells. Further evidence of neural characteristics was observed by the co-expression of another set of early and mature neuronal specific factors, OTX2 and the microtubule associated protein MAP2 respectively. MAP2 proteins are associated with the mature neuronal cytoskeleton in the dendrites and the cell body. ICC analysis confirmed the expression of OTX2 and MAP2 in a subset of neural progenitor cells indicating a mixed population of progenitor and mature neurons (Figure 17: B). The evidence of neural morphologies in brightfield microscopy revealed the formation of rosettes in the neurospheres after almost 30 days of differentiation. These spheres once plated and given time to proliferate produced neuronal colonies with individually identifiable cells with its characteristic axon like processes (Figure 18).

3.2.5 Differentiation of Mature Retinal Cell Types

3.2.5.1 Retinal Pigment Epithelium (RPE)

The ability of the Usher iPS cell line to differentiate into mature retinal cell types was established at later time points in the retinal differentiation protocol. Consistent with vertebrate retinogenesis, the RPE was the first retinal cell type to be observed in culture. Early anterior neural rosettes after 16 days of differentiation were grown in RDM as adherent cultures until day 40-50 when the first definitive characteristics of RPE like cells were observed. Colonies of cells organized themselves in distinct patches of hexagonal shaped epithelial-like cells with a characteristic pigmentation pattern that was easily identifiable in brightfield microscopy. The levels of pigmentation increased over a period of next 10 days of differentiation and were maintained at even higher levels at later time points in culture (Figure 19: A,B). For protein analysis of these RPE-like cells, the pigmented areas were carefully microdissected and allowed to proliferate on laminin coated coverslips in the presence of RDM and mitogens, EGF and FGF, along with heparin. Following a week of treatment with mitogens, the cells were then grown as typical monolayers in the absence of the growth factors for an additional 1 week. After 60 days of differentiation, the cells were fixed in 4% paraformaldehyde and analyzed for their protein expression profiles. Immunostaining revealed co-expression of the RPE associated gene OTX2 along with the RPE-associated tight junction protein ZO-1 (Figure 20: A-C). The cells also contained more mature RPE-related apical proteins such as EZRIN and basolateral proteins such as BESTROPHIN (Figure 20: D-F). ICC analysis further revealed a clear cobblestone RPE-like morphology for these cells derived from human iPS cells. To identify the level of transcriptional expression of RPE-related genes, the microdissected pigmented RPE-like cells were analyzed by RT-PCR. RT-PCR experiments further confirmed the transcriptional expression of RPE associated genes including the RPE progenitor marker *MITF*, and mature markers including RPE secreted factors like *PEDF*,

important visual cycle proteins, *RPE65, CRALBP*, and transcript levels of other RPE genes confirmed by ICC, *OTX2, ZO-1, EZRIN,* and *BESTROPHIN* (Figure 21).

3.2.5.2 Neural Retina

The derivation of RPE was followed by the specification of the neural retina from the iPS cells at even later time points of differentiation. The study aimed to establish the potential of the Usher syndrome patient-specific iPS cell line to differentiate into mature retinal cell types including the most important for this study, photoreceptors. Usher syndrome iPS cell derived retinal progenitor cells were grown as retinal neurospheres for a period of 70 days in RDM growth medium. The neurospheres were kept at an appropriate size by regular and light trituration of overgrown spheres and cultured in fresh RDM every alternate day. After 70 days of differentiation, the retinal neurospheres were treated accordingly for analysis of their gene and protein expression characteristics. RT-PCR analysis revealed presence of *CHX10* and *CRX* transcripts, further highlighting the progenitor stage of these retinal cell types (Figure 22). RGCs and cone photoreceptors are among the very first neuroretinal cell types to be derived in retinal development [15]. The emergence of RGCs was studied using ICC analysis after 70 days of differentiation. ICC results revealed a population of cells positive for the RGC specific transcription factor in the retina BRN3 that identifies all 3 isoforms of the gene, BRN3A, BRN3B, and BRN3C. Directed differentiation of RGCs was confirmed by translational co-expression of BRN3 and another RGC-specific protein in the retina, ISLET1 (Figure 23). Populations expressing BRN3 and ISLET1 alone might be indicative of possibly different types and early stage RGCs found in the retina. Immunostaining also revealed a subset of cells expressing the cone and rod photoreceptor-specific precursor transcription factor CRX indicative of the acquisition of a mature retinal phenotype. Among the total population of cells, a group of CRX positive cells also expressed the mature phototransduction protein for cone and rod

photoreceptors specification, RECOVERIN indicating the stepwise conversion from an immature to mature photoreceptor cell fate (Figure 24). Population of cells expressing CRX and RECOVERIN are further evidence of the different stages of development and maturation of the photoreceptors from the human iPS cells.

3.3 Discussion and Future Studies

One of the major limitations when it comes to studying disease progression in a patient is the limited accessibility to patient tissue material among other technical and ethical problems. The advent of iPS cell technology circumvents such problems by establishing patient cells in a laboratory dish which harbor the genetic mutations that caused or facilitated disease onset and development [80]. The use of patient specific iPS cells provides an unlimited supply of diseased cells to address issues like genetic contributions to the disease and provides means for gene correction and pharmacological strategies to potentially cure it.

This study aims to achieve similar goals for the most commonly inherited deaf-blindness disorder, Usher Syndrome. The study provides the first evidence of neural and retinal differentiation of iPS cells derived from an Usher syndrome patient. The differentiation of mature retinal cell types was chronologically analogous to normal development in the human retina. The results demonstrate the proof-of-principle study that affected cell types can be generated from Usher syndrome patient specific iPS cells. This study provides a novel platform for future *in vitro* disease modeling of this disorder, which could lead to further insights into its neurogenetic abnormalities. Current studies in Usher syndrome are trying to identify all genetic contributors and variations that lead to combined symptoms of hearing and vision loss. An *in vitro* system like the one described in this study provides a feasible time frame in which we can derive the affected photoreceptors bearing the DNA signature of the disease. Qualitative analysis of iPS

differentiation to mature retinal cell types indicates a robust potential of the Usher iPS cell line to yield a neural retina phenotype in good quantity.

In this study, the pluripotency of the Usher iPS cells is established using molecular and morphological characteristics as described in previous studies [70, 82]. The maintenance of pluripotency is indicated by the endogenous onset of expression of surface molecules including TRA-1-61, TRA-1-81, and SSEA-4. The genetically reprogrammed ES cell like and unbiased nature of the Usher iPS cell line is important for the recapitulation of time wise directed differentiation *in vitro*. The study establishes a step wise differentiation of the Usher syndrome iPS cell line from onset of early anterior neural characteristics to the future retinal specification at optic vesicle stage after 18 days of differentiation [107]. The maturation of neural and retinal phenotype progresses in accordance with the *in vivo* vertebrate development. Emergence of mature retinal cell types was identified by expressions of characteristic transcription factors and proteins associated with each somatic cell type. An efficient output of the disease cell type was achieved within an attainable and time period of 70 days.

Overall, this study established a novel platform to further delve into the origins of the disease and for future studies of *in vitro* disease modeling, as these cells can be utilized as a tool for the study of disease progression, with applications for future cell replacement and drug screening studies. Establishment of a source of photoreceptors from disease patients provides the potential for gene correction and cellular therapy in personalized medicine strategies. Efforts to use iPS cell derived diseased cells for gene replacement and drug screening strategies have already been initiated in other neurodegenerative disorders including Amyotrophic Lateral Sclerosis (ALS) and cardiac disorders like the Long QT Syndrome [117, 118]. The use of such a system is highly beneficial to

understand the neurogenetic complexities of the Usher syndrome and subsequently devise experiments to produce treatments for this currently incurable disorder.

In future studies, it will be warranted to quantify the yield of retinal progenitors and mature retinal cells from this cell line and compare the numbers to the cells derived from iPS cells taken from an isogenic carrier control and/ or a completely healthy individual. The derivation of retinal characteristics among these cell lines would provide for an interesting criterion to assess the significance of the diseased state. This study defines the onset of differentiation of photoreceptors but mimicking the disease phenotype and identifying old and new mutations associated with the disease are future directions this study envisages. Prolonged differentiation of the photoreceptors would be an ideal place to start for a comparative analysis in disease development and progression as indicated by Takahashi and colleagues in modeling the retinal disease of RP [49]. The short terms goals of this study is to provide a novel *in vitro* system to model the visual loss progression in Usher syndrome whereas long term applications include utilizing the diseased cell types for gene correction, cell replacement, and drug screening experiments to provide an overall data set of consensus information and potential treatment alternatives in personalized medicine for this disease.

CHAPTER 4 – DIFFERENTIATION AND CHARACTERIZATION OF AFFECTED CELL TYPES IN GLAUCOMA USING HUMAN IPS CELLS

4.1 Introduction

Glaucoma is the leading cause of age-related optic neuropathy in humans. It is characterized by the abnormal rise in intraocular pressure leading to the loss of RGC cell bodies and degeneration of its axons leading to complete remodeling of the ONH, especially at the level of the laminar cibrosa through which the optic nerve leaves the eye. As stated earlier, glaucoma is clinically divided into 2 main subtypes. The milder "open-angle glaucoma" is characterized by an increased ratio of optic cup to disk with a slow progressive loss of vision. The second subtype is the "closed-angle glaucoma", which has a more acute onset with higher intraocular pressures with diagnosable physical symptoms including dilated pupils, a clouded cornea, and red eye. However, a crucial element in the pathophysiology of all forms of glaucoma is the loss of RGCs, the output projection neurons of the retina that make connections with different regions of the brain for processing of visual information. Another cell type recently associated with glaucoma is the retinal astrocytes, the dominant glial support of the otherwise non-myelinated RGC axons. Retinal astrocytes are not present at the somas of ganglion cells, and even in areas of retina in which they are numerous, they are sharply confined to the layer of ganglion cell axons. Astrocytes at the ONH are responsible for providing cellular support to RGCs and synthesizing extracellular molecules. It is suggested that retinal astrocytes with its vasculature are migratory and enter the developing retina from the brain at the optic nerve head (ONH) [119]. They have been associated with glaucomatous neurodegeneration, although the direct or indirect role for

these cells in disease is still under investigation. A majority of ongoing studies in the field of glaucoma research have strived to identify better ways to diagnose and subsequently characterize and manage the disease. There is a marked lack of studies aimed at another aspect of disease intervention, cell therapy. It is very well known that the reason underlying visual loss in glaucoma is the degeneration of RGCs and roles of astrocytes in ONH remodeling. Since not all cases of glaucoma are related to established genetic causes of this disease, more work needs to be done to identify ways to recapitulate disease progression and establish ways to derive its affected cell types in the laboratory.

This study is aimed at achieving the directed differentiation and characterization of the somatic cell types associated with glaucoma using human induced pluripotent stem cells. Directed differentiation of several somatic cell types from human iPS cells have been successfully achieved with great implications for disease modeling and cell replacement strategies. RGCs have proven to be a complex cell type to be derived in the laboratory dish owing to different reasons including lack of reliable markers and complex morphologies. In humans, RGCs can be divided into several types depending on their molecular and morphological characteristics including the human specific Midget RGCs (P cells), Parasol RGCs (M cells), Bistratified RGCs (K cells), and photosensitive RGCs [120, 121]. Astrocytes in general have been difficult to derive from human pluripotent cells. This study aims to provide ways to derive and characterize these cell types using human iPS cells in an achievable and pragmatic time frame. Cell therapy may be a potential way to restore vision in glaucoma and one of the first steps of attaining that goal would be to devise *in vitro* protocols to produce, characterize, and enhance the yield of the clinically relevant cell types associated with this disease. With no current cure for this disease, its progression can be slowed down if detected early. However, studies aimed at preventing the loss of RGCs and ONH

architecture are more clinically relevant in terms of providing a definitive solution to this devastating disease that affects millions all around the world.

4.2 Results

4.2.1 Differentiation of RGC Neurons from Human iPS Cells

Using lines of human iPS cells including the Usher iPS cell line and the TIPS-5 iPS cell line, and building upon the preliminary data for the differentiation of RGCs from human iPS cells, this study further characterized both molecularly and physically, the yield and specification of RGCs attained after as early as 40 days of differentiation, an expected timepoint for *in vitro* RGCs specification from human iPS cells, according to recent literature and the timeline of retinogenesis [122]. The optic vesicle-like neurospheres manually separated after 18 days of differentiation and grown as retinal progenitor cells in suspension until day 40, with a specific regimen of medium changes every alternate day with 1:1 RDM: Conditioned RDM and a regular light trituration of overgrown spheres to keep at an appropriate size. At day 39, the spheres were plated onto laminin coated polyornithine coverslips for ICC analysis. BRN3 was used as the "master transcription factors" for identification of RGCs given its highly specific expression in the retina in early and mature RGCs. After 40 days of differentiation, ICC analysis revealed a subset of BRN3 positive cells that co-expressed the pro-neural cytoskeletal marker, ß-III TUBULIN, identifying the dendrites, cell body, and axons of BRN3 positive cells (Figure 25: A). The neuronal nature of the RGCs was further characterized by ICC analysis of the RGC specific BRN3 transcription factors and the neuronal axon marker, TAU. After 40 days of differentiation a subset of neurospheres co-expressed the BRN3 and TAU proteins providing for the efficient identification of RGC neurons (Figure 25: B). Analysis at higher magnifications revealed an elongated axonal morphology for the RGCs as would be expected since these cell types

eventually form the optic nerve making its way to the different areas of the brain. This qualitative identification of RGC neurons formed the basis for further morphological quantification of RGC axons in future experiments.

4.2.2 Further Characterization of RGCs

In an effort to further characterize the sub-population of retinal progenitor cell-derived RGCs, ICC analysis was used to identify expression patterns of other RGC specific transcription factors. The RGCs derived in culture were further specified by utilizing the expression and co-expression of markers associated with early and late ontogeny of RGCs *in vivo*. Retinal progenitor spheres were plated onto laminin coated polyornithine coverslips after 39 days in culture and fixed the subsequent day in 4% paraformaldehyde for ICC analysis. After 40 days of differentiation, a subset of retinal progenitor cells were double positive for the RGCs specific proteins BRN3 and ISLET1 (Figure 26: A). Although ISLET1 has been recently shown to also be expressed in some progenitor cells in the retina, the co-expression with BRN3 proteins is a definitive indication of the successful derivation of RGCs in culture. The study also looked at the expression of PAX6, a marker for neural/retinal progenitor cells, and is restricted in the retina to mature ganglion cells and interneurons such as amacrine cells. ICC analysis revealed that almost all BRN3 expressing cells co-expressed PAX6 with populations of cells that expressed either only BRN3 or PAX6, indicative of the retinal progenitor nature of cells including the onset of RGCs markers, given that it is the first neuroretinal cell type to be derived in development (Figure 26: B).

4.2.3 Molecular and Morphological Quantification of RGCs

After establishing a qualitative setup to identify the derivation of RGCs from human iPS cells, this study looked to quantify the yield of RGCs and take advantage of some morphological differences between RGCs and other neuroretinal cell types to further characterize this cell type.

It has been known that RGCs exist in different morphological forms in the human retina. These can be divided on the basis of dendritic forms, extent of cell body and dendritic sizes, and stratification levels of RGCs in the IPL [123]. Pioneering work by Cajal described in his 1892 book, *The Structure of the Retina*, described the Golgi staining of these ganglion cells as a way to identify the different subtypes. Since then around 18 different types of RGCs have been identified in the human retina with the parasol, midget, and bistratified RGCs being specific only in the primate retina. Other types have also been seen to be present in other vertebrates like the cat. Another physical feature that distinguishes RGCs from other retinal cell types is its ability to project to long distances in areas of the brain on account of its larger diameter and longer axons [123]. Axonal lengths associated with RGCs are quite significantly longer compared to other interneurons and photoreceptor segments.

4.2.3.1 Quantification of Yield of RGCs

Firstly, the study quantified the yield of RGCs among a mixed population of neuroretinal cell types by counting individual cells in the co-expression pattern of RGC specific proteins from experiments described previously. Retinal progenitor cells were analyzed by ICC after 40 days of differentiation. As stated, at least 2 representative fields from different coverslips in a set of 3 replicable experiments was photographed and counted. The publicly available image processing software, Image J, developed at the National Institutes of Health was used for image analysis and quantifying cell counts. Cell counts were taken for the subset of progenitor cells positive for BRN3 and ISLET1 co-expression and the yield of RGCs calculated (Figure 27). Individual expressions of BRN3 and ISLET1 were counted in addition to the cells expressing both. This data was quantified over a value of all nuclear labeled DAPI positive cells in the area. Approximately 18.17% (S.E. of 3.97%) of the cells were positive for the expression of BRN3, specific to the RGCs, whereas around 22.58% (S.E. of 3.09%) of the cells expressed ISLET1, a broad

transcription factor expressed by the RGCs and retinal progenitors. However, a more definitive statistic for the number of RGCs derived was that around 12.77% of the total population of cells that expressed both BRN3 and ISLET1. This quantification of co-expression provides further evidence for the efficient derivation of RGCs from human iPS cells. A similar count for BRN3 positive cells was also observed for ICC experiments with BRN3 and PAX6.

4.2.3.2 Quantification of Cell Sizes of RGCs

Taking advantage of the larger cell bodies of RGCs compared to other retinal neurons, this study measured the area of RGCs and compared it to other retinal neurons derived in the process. To measure difference in cell body sizes the study again used the master transcription factor BRN3 as a basis for identifying the population of RGCs. BRN3 was used in combination with the neural cytoskeletal marker ß-III TUBULIN to highlight the cell bodies, axons and dendrites of the BRN3 positive and BRN3 negative cells in a population of retinal progenitor cells. ICC analysis revealed 2 populations of retinal progenitor cells, one proportion of the cells that were double positive for BRN3 and ß-III TUBULIN indicative of RGC neurons and another proportion that was negative for BRN3 but positive for ß-III TUBULIN indicative of non-RGC retinal neurons (Figure 28: A, B). The DAPI dye was used for identification of nuclei. Using the quantification tools on the Leica 5500 upright epifluorescence microscope, the areas occupied by the cell bodies were measured for 4 different sets of experiments and the values quantified using the unpaired student's t-test (Figure 28). An average of at least 15 BRN3 positive and 20 BRN3 negative cells were measured for each experiment The comparatively analysis revealed a statistically significant ($p < 0.005$) difference between the two population where the RGCs had a mean cell body size of 102.18 square microns (S.E. of 9.35) where was the non-RGC population had a very consistent mean cell size value of 67.17 square microns (S.E. of 0.88).

4.2.3.3 Comparison of RGCs and Photoreceptor Neurite Lengths

To identify differences in neurite lengths between RGCs and other retinal cell types such as photoreceptors, this study established an important criterion for the classification of RGC by measuring the lengths of axons of the derived RGCs vs neurite lengths of photoreceptors differentiated from the same human iPS cell line. RGCs were triple-labeled for BRN3, MAP2, and axon-specific protein TAU (Figure 29: A). Photoreceptors were derived in culture after 70 days of differentiation and their neurites were identified by the expression of the photoreceptor-specific, calcium binding protein, RECOVERIN (Figure 29: B). The lengths were measured in microns and the data quantified using the unpaired student's t-test, for 3 different sets of experiments (Figure 29). An average of 15 RGCs axons and 30 photoreceptor segments were measured for each experiment. The difference in lengths were highly significant ($p < 0.001$) with the RGC axons measuring at a mean length of 95.31 microns (S.E. of 6.28) and the photoreceptor neurite lengths at 29.18 microns (S.E. of 3.67).

4.2.4 RT-PCR and qPCR Analysis of RGCs

The expression of RGC-related genes was further determined by PCR analysis and quantification. Transcription factors associated with *in vivo* RGC development including the basic helix-loop-helix *ATOH7 (MATH5)* is known to be highly specific for the early derivation of RGCs and known to regulate critical downstream targets of RGC differentiation, including BRN3B [18, 20]. THY1.2 is a cell surface glycoprotein that is used to identify RGC populations in later retinal histogenesis [124]. These two genes are highly specific to RGCs in the retina. RT-PCR analysis of cDNA synthesized from RNA isolated after 40 days of differentiation of human iPS cells revealed increased levels of RGC transcripts, *BRN3, ATOH7, THY1.2,* and *PAX6* (Figure 30). PAX6 identified a broad stage of retinal progenitors including a possible restriction to RGC cell fate as was confirmed in ICC analysis. Further, the expression levels of *BRN3* and *PAX6* were

quantified over a time course from day 0 to day 40 of differentiation to identify the gradual increase in RGC specification from human iPS cells (Figure 30).

4.2.5 Differentiation of Astrocytes from Human iPS Cells

Using our line of human iPS cells, this study next looked to derive a second important cell type associated in the ONH changes during glaucoma, retinal astrocytes. The differentiation of astrocytes from iPS cells was monitored over prolonged periods of time in culture and novel methods were established to enrich for the glial cell types. The first evidence of astrocytes in culture was observed after 60 days of differentiation. Non-retinal neurospheres at day 18 were separated manually and cultured separately in suspension with doses of RDM and 20ng/mL of EFG/FGF/Heparin (EFH) every alternate day until day 60 when they were subsequently plated down onto laminin-coated polyornithine coverslips for analysis by immunostaining. A subset of cells dramatically expressed the cytoskeletal intermediate filament protein, glial fibrillary acidic protein (GFAP) highly present in astrocytes confirming the appropriate differentiation to an astrocytic fate. After 60 days of differentiation, a significantly high number of cells were observed expressing GFAP and higher magnification analysis revealed the characteristic stellate type morphology of astrocytes with outward extending processes (Figure 31). In efforts to further characterize the differentiation and retinal specification of astrocytes, this study analyzed the development of astrocytes at later time points of differentiation. Brightfield microscopy revealed the progressive and stepwise increase in number and maturation of a subset of these astrocytes (Figure 32: A-C). Starting with a population of astrospheres around day 70, subsequent plating and growth of these spheres after 10 days revealed mixed populations of cells comprising of astrocytes and neuronal cells. *In vitro* passaging using accutase helped enrich for the mitotically active astrocytes within the mixed population of neuronal cells. After a couple of passages, there was a significant increase in the number of astrocyte-like cells compared to neurons. Cells with

anatomical features similar to both protoplasmic and fibrous astrocytes, with long, unbranched and short, branched processes were observed at later timepoints of differentiation.

4.2.6 Anterior Specification of Astrocytes

To determine the anterior nature of the astrocytes derived in culture, the study used immunostaining strategies to identify the presence of markers associated with anterior neural development and the absence of those associated with a more posterior nervous system phenotype. OTX2, a marker used to identify derivatives of the anterior neuroepithelium was used to characterize the anterior nature of the astrocytes. HOXB4, a transcription factor associated with posterior/ spinal cord development served as a measure for lack of posterior nervous system origin of the glial cells being derived in the study. The presence of astrocytes was confirmed by the translational expression of GFAP (Figure 33: A). ICC analysis revealed that after 125 days of differentiation, a high subset of astrocytes expressed the OTX2 protein but were almost completely negative for HOXB4, indicating the anterior nature of the astrocytes derived in culture (Figure 33: B,C). The importance of anterior specification of the astrocytes stems from the important concept that all retinal astrocytes are derived in early forebrain regions of the developing neural tube and eventually migrate through the optic nerve to take their position as astroglia in the retina. A complete lack of HOXB4 is indicative of such a pattern of derivation from the human iPS cells.

4.2.7 Increase in GFAP Expression at Later Time Points of Differentiation

Next, the study established the qualitative increase in GFAP and OTX2 expression in astrocytes with a comparative analysis at different time points on course of differentiation. Astrocytes were analyzed after approximately 100 days of differentiation by ICC (Figure 34: A). Similar ICC analysis was done after 150 days of differentiation. By 120 days, the astrocyte cultures were

passaged up to 3 times using accutase providing an enriched population of astrocytes in culture. Cells until then were maintained in RDM and 20ng/uL of EGF/FGF/ Heparin (EFH). To measure GFAP expression at 150 days of differentiation, astrospheres were plated onto laminin coated polyornithine 4-well plates and cultured without the growth factors but in the presence of 10% FBS during the last month to provide further nutrient enrichment for better survival and maturation of this cell type. Indeed, ICC analysis revealed enhanced expression of GFAP over the time course of differentiation from 100 days to 150 days and more OTX2 positive cells compared to Day 125 (Figure 34: B,C). However, the qualitative increase in GFAP seemed to be attributed to the eventual loss of the mitotically active nature and further experiments were devised to study astrocyte doubling time and senescence as an important feature of further characterization of this *in vitro* derived cell type.

4.2.8 Measurement of Astrocyte Proliferation/ Doubling Rate

To measure proliferation statistics of astrocytes, a strategy was devised to maintain and passage astrocyte cultures at consistent time intervals for a predetermined period of time. To achieve this end, experiments were conducted simultaneously with both the human iPS cell lines in use for the experiments in this entire study, Usher iPS and TIPS-5 lines. Proliferating cultures of plated astrocytes were passaged every week for a total period of 4 weeks from day 100 to day 130 of differentiation. The passaging of astrocytes was accomplished with accutase as explained and cells were grown in RDM and 20ng/mL EFH. Beginning at each passage and for each subsequent passage, a total of 100,000 cells each were plated onto 2 wells of a 6-well plate and expanded in EFH for 1 week. At the end of each week, viable cell counts were taken from both wells with the aid of trypan blue solution and the average of the 2 numbers were determined to be the acceptable cell count for that passage. Similarly, counts were taken for rest of the time points for both cell lines and proliferation/ day and doubling times calculated (Figure 35). For the TIPS-5 iPS cell

line, there was a progressive decrease of proliferation and increase in doubling time of astrocytes measured. Astrocyte proliferation decreased from 120.57% at passage 1 to 101.42%, 79.28%, and 48.85% for the next 3 passages. Doubling time increased from 1.48 days for passage 1 to 1.72, 2.13, and 3.17 days for the next 3 passages respectively. For the Usher syndrome iPS cell line, a similar trend was observed however, the proliferation was not as pronounced as the TIPS-5 iPS cell line. Proliferation rates decreased from 19.29% at passage 1 to 18.86%, 14.86%, and 14.57% for the next 3 passages respectively. Similarly, the increase in doubling time measured 5.96 days at passage 1 to 6.03, 6.86, and 6.93 for the next 3 passages respectively. The presence of neuronal-like or proliferating neural progenitor cells was nullified by the almost lack of expression of PAX6 in these cultures after 125 days of differentiation.

4.3 Discussion and Future Studies

New avenues of disease research are under investigation after the discovery of human iPS cells by Yamanaka and colleagues in 2007. These cells are essentially embryonic-like in terms of their potency and can be coaxed to differentiate to potentially any cell type in the human body. The importance of directed differentiation of somatic cell types from ES/ iPS cells is critical for cell replacement strategies in degenerative diseases. Once an efficient protocol to do so has been established, work needs to be done to characterize, enhance, and purify such cell populations to be tested in preclinical and eventually clinically models of diseases.

This works cites efforts to establish methods to derive and characterize the affected cell types in the most prevalent retinal degenerative disease, glaucoma. Tackling differentiation of 2 somatic cell types associated with the disease individually, this study is successful in using techniques including ICC and PCR, to characterize the derived somatic cells types by the expression of developmentally associated transcription factors specific to each cell type. Further approaches

were undertaken to characterize the morphological differences between RGCs and other neuroretinal cell types derived in the process. This study provides methods to identify RGC neurons in culture and discusses novel ways and valuable data for the quantification of morphological properties of RGCs including its bigger cell bodies and longer axons which can be used as identifying properties compared to other retinal neurons including the photoreceptors and interneurons. The amount of RGCs identified by the translational co-expression of BRN3 and ISLET1 (12.77%) is a promising number and gives a basis to be used for further enhancing the yield of RGCs by intrinsic or extrinsic manipulation of the cell system. Further RGCs characterization is established by RT-PCR and qPCR experiments identifying RGC specific genes *ATOH7* and *THY1.2* and documenting the stepwise increase in *BRN3* expression starting from a pluripotent iPS cell source through the neural and retina progenitor stages to the eventual derivation of RGCs. Experiments with similar goals have been attempted but require better optimization for definitive and replicable results. The study overall provides a robust way to generate RGCs in culture from human iPS cells. Human iPS cells were also shown to be successful in deriving astrocyte like cells identified by their physical and molecular characteristics. This work also demonstrates the ability to maintain and expand human iPS cells derived astrocytes *in vitro* and provides further characterization by measuring the doubling rates of these cell types. A timeline for the specification of the non-retinal neurospheres in suspension to growth as astrocytes as adherent cultures is shown in this study. *In vitro* passaging of astrocytes with accutase reveals an enrichment of astrocytes and decrease in progenitor and post-mitotic neuronal cells. The anterior origin of these astrocytes is anticipated by determining the anterior nature of these cells as characterized by the expression of OTX2 and lack of the posterior markers, HOXB4. This work also provides evidence for the qualitative increase in GFAP expression within astrocyte populations as an indication of more survival and maturation at later time points up to 150 days of differentiation.

Overall, this work has shown methods to efficiently derive and characterize RGCs and astrocytes although much work still needs to be done. In future studies, the yield of RGCs could be increased by exogenous addition of growth factors known to be associated with RGCs specification or use overexpression of RGCs specific genes to improve its production. Electrophysiological studies of iPS-RGCs would be an elegant way to establish their functional properties. Prolonged differentiation of iPS cultures could be planned to further study the onset of more RGC related proteins and track changes in proteins used in this study. Astrocytes would need more molecular characterization with markers like S100ß, PAX2, and VIMENTIN. Identification of retina specific astrocytes as found dispersed in the nerve fiber layer and the optic nerve regions would be the next steps in further understanding this glial cell type. A major future application of this study is to use information from this work and apply the same to iPS cells derived from cells of glaucoma patients. One would then be able to successfully compare a diseased phenotype with a control to better understand the complications *in vitro*. Another area to explore will be to initiate a co-culture system of RGCs and retinal astrocytes where the dynamics of interactions between the 2 somatic cell types could provide significant insights as to how these cell types are affected and behave in glaucoma.

CHAPTER 5 – DISCUSSION

The last decade has seen a capacious amount of increase in works related to stem cells and their application in different human organ systems. Different aspects of human biology have been under continuous study using the incredible potential of stem cells. The two breakthrough landmarks in the field spaced 9 years apart, human ES cells in 1998 and human iPS cells in 2007, have dramatically changed the landscape of studying human biology and finding cures for currently untreatable cell degenerative diseases. The discovery of iPS cells, more so, has been welcomed in the scientific community, as it does away with any ethical dilemmas of working with human embryos and at the same time bearing resemblances in function and appearance to the currently clinically acceptable human ES cells. The use of iPS cells in disease research is based on the goals of finding genetic and environmental cues of disease ontogeny and development, generating clinical grade cells that are transplantation competent, and identifying novel mechanisms and drugs that could intervene or completely halt disease progression.

The research presented in this work, overall, demonstrates the promising ability of human iPS cells to be used as a model system for the study of retinal development and degenerative diseases. In this study, human iPS cells were successfully used to establish a developmentally analogous time line for the derivation of retinal cells, in addition to the differentiation of mature retinal neurons that are specifically affected in complex types of blinding diseases. From the first known studies identifying primate ES cell-derived RPE cells in 2002 [125], the generation of retinal cells from human pluripotent stem cell sources including ES cells and iPS cells, today, has been achieved by several labs with different efficiencies [30, 126-129]. This study provides in an

achievable time frame identification of the onset of specific retinal cell types and shows novel ways and strategies to characterize them.

Using human iPS cells to study neurodegenerative diseases is a very popular research domain but is still restricted to the laboratory culture dish. The methods of generation of iPS cells make it less conducive to use in a human patient setting, although new virus/ integration free methods to derive iPS cells have been successfully reported [96, 99, 130]. Using human iPS cells to model retinal degenerative disease has only been a very recent endeavor, with the first reports for RP being published only in 2011 [49]. There have been proof-of-principle studies demonstrating the use of patient specific iPS cells to model diseases including gyrate atrophy and Best disease [107, 109] and many more efforts are required to unravel the complexities associated with the highly prevalent retinal diseases like RP, AMD, and glaucoma. The use of iPS cells in culture can be used to either study disease progression and phenotype if using patient specific cells or be used to provide a novel source for functioning somatic cell types affected in the disease if working with wild type cell lines that can be transplanted into patients to reverse or slow down the progression of the disease. In this study, the above two concepts are simultaneously applied to someday develop tools to study blinding disorders including, Usher syndrome and glaucoma.

The first half this work demonstrates the potency of the iPS cell line derived from skin fibroblasts of a patient with type III Usher syndrome, to differentiate in accordance to previously established studies, towards an anterior neuroepithelium and progressing through all major stages of retinal development. The differentiation of the Usher iPS cell line was assessed though the initial eye field specification, optic-vesicle definitive retinal progenitor stage, and finally to the final derivation of mature retinal cell types [107]. The patient specific cell line was characterized from its pluripotent stage termed as day 0 until 70 days of differentiation, during which the different

developmental checkpoints were analyzed by utilizing the expression of stage specific transcription factors and proteins. As described in chapter 3, establishing the pluripotency of the cell line is the most critical point, when working with stem cells. The completely undifferentiated state of the Usher syndrome iPS cell line was shown by its specific brightfield morphologies and molecular expression profiles. The anterior region of the developing neural tube gives rise to the future areas of brain and eyes which was shown by the expression of anterior neural and eye field specific-factors including, *PAX6, OTX2, SIX6, RAX, LHX2*. The separation of neurospheres in suspension for retinal differentiation was based on a method described previously [107]. The iPS-retinal progenitor cells were characterized as neurons and subsequently cultured for greater lengths of time for generation or retinal cell types. After 40 days, the first signs of the outer pigmented layer of the retina, RPE, emerged. These were distinctly recognized by their cobblestone morphology and onset and gradual increase in brown-black pigmentation in brightfield. The expression of RPE related proteins including EZRIN and BESTROPHIN, identifying its apical-basal property respectively, and RPE65, CRALBP was shown in ICC and RT-PCR experiments further confirmed its specification. The generation of more neuroretinal cell types from a subset of retinal progenitor cells was shown, including RGCs and photoreceptors, after 70 days of differentiation. Using ICC analysis, a general trend was observed in the progression from an immature to a mature state of photoreceptors as identified by expression patterns of CRX and RECVOERIN. RGCs were also present as subsets in differentiated cells, identified definitely by the widely established RGCs marker, BRN3, a POU domain transcription factor. The BRN3 antibody used was capable of identifying all three forms of the protein including BRN3A, BRN3B, and BRN3C. Further specification was achieved by a subset of BRN3 positive cells expressing another transcription factor specific to RGCs and progenitors in the retina, ISLET1. In totality, the patient specific cell line was shown to be competent for

recapitulating retinal development *in vitro* and successful in deriving, in good amounts, photoreceptors as early as after 70 days of differentiation.

The second half of this study concentrated on establishing a timeline for optimizing a protocol for the derivation of RGCs and astrocytes, affected cell types in glaucoma, from non-glaucoma patient iPS cells. Two iPS cell lines mentioned in the methods section were used interchangeably in this part of the work. The use of the Usher iPS cell line was justified because there is no known reason to believe it would affect the derivation of RGCs in culture. The results of this work further confirmed this theory. Based on the findings of a recent paper in the field that showed that RGCs can be detected at earlier timepoints, after 40 days of differentiation [122], this study confirmed the generation of RGCs from iPS cells at the same time point by identifying populations of cells expressing the RGC specific BRN3 and the neural cytoskeletal marker, ß-III TUBULIN. Tubulin positive neurites were observed to be specific and emanating from the BRN3/ DAPI double positive nuclei. Since BRN3 identifies a large subset of RGCs but not all of them [21, 131], the study further characterized the RGCs populations by immunostaining for restricted markers for RGCs in the retina, PAX6 and ISLET1. PAX6 is developmentally restricted to RGCs during later time points and is known to promote differentiation of retinal progenitor cells to non-photoreceptor neurons [132]. ICC revealed different populations of cells including a population that was only BRN3 positive, one that co-expressed BRN3 and ISLET1/ PAX6, another which was only positive for ISLET1 or PAX6, and the remaining cells that only stained for DAPI. Cell populations expressing BRN3 individually or in combination were definitive for RGCs specification, given its derivation through a retinal progenitor stage of cells. PAX6 is a broad neural progenitor marker and restriction to RGCs neurons is expected at later stages in *in vitro* culture. The expression of PAX6 together with BRN3 in the same cells, along with cells expressing these markers individually can be early signs of RGCs maturation and

PAX6 restriction. The study quantified the number of cells that doubly expressed BRN3 and ISLET1/PAX6. Approximately 12.77% of the total cells co-expressed BRN3 and ISLET1. Total cells positive for only BRN3 or ISLET1 was around 18.17% (S.E. of 3.97%) and 22.58% (S.E. of 3.09%) respectively. These numbers are good indications to derive basic conclusions on where to start and what to expect when trying to increase or improve the yield in future studies. Similar studies looking at derivation of RGCs as cell replacement resources have been published with mouse ES cells reported to generate approximately 14.30% BRN3B positive cells after 50 days of differentiation [133]. Another study with mouse iPS cells generated around 10% BRN3B positive cells, after overexpression of the RGC specific MATH5 in addition to external factors including DKK1 and Noggin [134]. Still another study was only able to generate approximately 2% of RGC-like cells from mouse ES cells treated with FGF2 and SHH [135]. This study established a serum-free method to derive RGCs with better productive efficiencies without the addition of any exogenous factors and at an attainable time frame. Next, this work showed novel ways to characterize the RGCs derived from iPS cells. Morphological traits including bigger cell bodies and thicker and longer axons for conduction of the electrical impulse are features that distinguish RGCs from other cell types in the retina. The study used molecular approaches to firstly identify these dissimilarities and then quantify the differences. The differences in cell sizes were compared for BRN3/ ß-III TUBULIN double positive neurons with ß-III TUBULIN positive neurons that were BRN3 negative. All cell populations were derived from iPS-retinal progenitor cells. BRN3 positive nuclei of cells were surrounded by the ß-III TUBLIN staining identifying the cell body, dendrites, and axon. Cell body areas were demarcated using tools in the microscope and values of areas covered calculated. The differences in cell sizes between the two corresponding populations were clearly significant with a p value of 0.0047 and a mean cell body size of 102.18 square microns (S.E. of 9.35) for BRN3 positive neurons versus 61.17 square microns (S.E. of 0.88) for the BRN3 negative neurons. BRN3 negative neurons were consistently

measured to be of the same sizes. Using similar tools, RGC axons were identified by BRN3 positive TAU positive cells. The lengths of these cells were measured in microns and compared to neurite lengths of photoreceptors derived from the same cell line. The differences in neurite lengths between these 2 neuroretinal cell types, 95.31 microns (S.E. of 6.28) for RGCs and 29.18 microns (S.E. of 3.67) for photoreceptors demonstrates the ability of human iPS cells to generate RGCs with morphological traits similar to their *in vivo* counterparts ($p = 0.0008$). The second cell type in glaucoma that affects the ONH is the retinal astrocytes. In this study the derivation of astrocytes based on their brightfield morphologies and GFAP expression was achieved using the lines of iPS cells. A protocol to passage and purify these cell types was demonstrated using accutase that enriched for the non-post-mitotic astrocytes gradually from among a population of mixed astrocytes and neuronal cells. Astrocytes with different morphologies characteristics were observed at longer time points in culture, after approximately 110 days. Both protoplasmic: long cell bodies with unbranched processes, and fibrous type: short stellate shaped bodies with branched processes, type astrocytes were observed in brightfield. A gradual increase in GFAP and OTX2 expression was observed until 150 days of differentiation indicating more maturation and specification of astrocyte cells. The anterior nature of these astrocytes was established after a few passages with accutase by the positive expression of OTX2 after 125 days and lack of markers for posterior origins in the developing nervous system, HOXB4. The field of cells yielded a high number of OTX2 positive cells from the plated astrospheres, indicating the highly anterior nature of these cells. The non-post-mitotic nature of astrocytes was characterized by measuring the proliferation rate of astrocytes in a controlled protocol as described in chapter 4. The results revealed a gradual decrease in proliferation and increase in doubling time from day 100 up to day 130. The doubling rate for astrocytes derived from TIPS-5 iPS cell line increased by a factor of approximately 1.29 days for the 4 passages. For the Usher iPS cell line, the doubling rate increased similarly by 1.05 days. The proliferation rates of cells was however quite

higher for the former cell line. This can indicate a property of cell line to cell line variation. The lack of progenitor cells in these cultures was confirmed by the very low levels of PAX6.

Overall, this study provides novel insights into the use of human iPS cells in retinal disease research. It established a proof-of-principle study that affected cell types can be generated from patients suffering from Usher syndrome and such a system can be used to further study the neurogenetic abnormalities of this disease. Human iPS cells can also be used to generate RGCs and astrocytes with reasonable efficiency, both of which are cell types that degenerate in glaucoma. The study provided novel evidence of molecular and physical characterization of RGCs, and established the anterior nature of the astrocytes derived from iPS cells. The differentiation of RGCs and astrocytes from non-glaucoma patient derived iPS cells lays the groundwork for future disease modeling of this disorder by the direct applications of this study to glaucoma patient derived iPS cells and paves the way for future work in cell replacement and drug screening applications in glaucoma research.

.

REFERENCES

REFERENCES

1. Purves, D., Augustine, G., and Fitzpatrick, D., *Initial Formation of the Nervous System: Gastrulation and Neurulation.* Neuroscience2001, Sunderlan (MA): Sinauer Associates.
2. Weinstein, D.C. and A. Hemmati-Brivanlou, *Neural Induction.* Annual Review of Cell and Developmental Biology, 1999. **15**(1): p. 411-433.
3. Li, H., et al., *A single morphogenetic field gives rise to two retina primordia under the influence of the prechordal plate.* Development, 1997. **124**(3): p. 603-615.
4. Fuhrmann, S., *Chapter Three - Eye Morphogenesis and Patterning of the Optic Vesicle*, in *Current Topics in Developmental Biology*, L.C. Ross and A.R. Thomas, Editors. 2010, Academic Press. p. 61-84.
5. Lamb, T.D., Collin, S.P., and Pugh, E.N., *Evolution of the vertebrate eye: opsins, photoreceptors, retina and eye cup.* Nature Reviews Neuroscience, 2007. **8**(12): p. 960-976.
6. Wawersik, S. and Maas R.L., *Vertebrate eye development as modeled in Drosophila.* Human Molecular Genetics, 2000. **9**(6): p. 917-925.
7. Gamm, D.M. and Meyer, J.S., *Directed differentiation of human induced pluripotent stem cells: a retina perspective.* Regenerative Medicine, 2010. **5**(3): p. 315-317.
8. Harris, W.A., *Cellular diversification in the vertebrate retina.* Current Opinion in Genetics & Development, 1997. **7**(5): p. 651-658.
9. Cepko, C.L., et al., *Cell fate determination in the vertebrate retina.* Proceedings of the National Academy of Sciences, 1996. **93**(2): p. 589-595.
10. Sidman, R.L., *Histogenesis of the mouse retina.Studies with [3H] thymidine.* , 1961, New York: Acadmeic Press.
11. Rapaport, D.H., et al., *Timing and topography of cell genesis in the rat retina.* The Journal of Comparative Neurology, 2004. **474**(2): p. 304-324.
12. Zuber, M.E., et al., *Specification of the vertebrate eye by a network of eye field transcription factors.* Development, 2003. **130**(21): p. 5155-5167.
13. Bailey, T.J., et al., *Regulation of vertebrate eye development by Rx genes.* The International Journal of Developmental Biology, 2004. **48**: p. 761-770.
14. Ikeda, H., et al., *Generation of Rx+/Pax6+ neural retinal precursors from embryonic stem cells.* Proceedings of the National Academy of Sciences of the United States of America, 2005. **102**(32): p. 11331-11336.
15. Ohsawa, R. and Kageyama, R., *Regulation of retinal cell fate specification by multiple transcription factors.* Brain Research, 2008. **1192**(0): p. 90-98.
16. Graw, J., *Chapter Ten - Eye Development*, in *Current Topics in Developmental Biology*, K. Peter, Editor 2010, Academic Press. p. 343-386.
17. Liu, I.S.C., et al., *Developmental expression of a novel murine homeobox gene (Chx10): Evidence for roles in determination of the neuroretina and inner nuclear layer.* Neuron, 1994. **13**(2): p. 377-393.
18. Brown, N.L., et al., *Math5 is required for retinal ganglion cell and optic nerve formation.* Development, 2001. **128**(13): p. 2497-2508.

19. Brzezinski Iv, J.A., Prasov, L., and Glaser, T., *Math5 defines the ganglion cell competence state in a subpopulation of retinal progenitor cells exiting the cell cycle.* Developmental Biology, 2012. **365**(2): p. 395-413.
20. Wang, S.W., et al., *Requirement of math5 in the development of retinal ganglion cells.* Genes & Development, 2001. **15**(1): p. 24-29.
21. Xiang, M., et al., *The Brn-3 family of POU-domain factors: primary structure, binding specificity, and expression in subsets of retinal ganglion cells and somatosensory neurons.* The Journal of Neuroscience, 1995. **15**(7): p. 4762-4785.
22. Hatakeyama, J., et al., *Roles of homeobox and bHLH genes in specification of a retinal cell type.* Development, 2001. **128**(8): p. 1313-1322.
23. Fujitani, Y., et al., *Ptf1a determines horizontal and amacrine cell fates during mouse retinal development.* Development, 2006. **133**(22): p. 4439-4450.
24. Li, S., et al., *Foxn4 Controls the Genesis of Amacrine and Horizontal Cells by Retinal Progenitors.* Neuron, 2004. **43**(6): p. 795-807.
25. Dyer, M.A., et al., *Prox1 function controls progenitor cell proliferation and horizontal cell genesis in the mammalian retina.* Nature Genetics, 2003. **34**(1): p. 53-58.
26. Chen, S., et al., *Crx, a Novel Otx-like Paired-Homeodomain Protein, Binds to and Transactivates Photoreceptor Cell-Specific Genes.* Neuron, 1997. **19**(5): p. 1017-1030.
27. Furukawa, T., Morrow, E.M., and Cepko, C.L., *Crx, a Novel otx-like Homeobox Gene, Shows Photoreceptor-Specific Expression and Regulates Photoreceptor Differentiation.* Cell, 1997. **91**(4): p. 531-541.
28. Cheng, H., et al., *Photoreceptor-specific nuclear receptor NR2E3 functions as a transcriptional activator in rod photoreceptors.* Human Molecular Genetics, 2004. **13**(15): p. 1563-1575.
29. Mears, A.J., et al., *Nrl is required for rod photoreceptor development.* Nature Genetics, 2001. **29**(4): p. 447-452.
30. Meyer, J.S., et al., *Modeling early retinal development with human embryonic and induced pluripotent stem cells.* Proceedings of the National Academy of Sciences, 2009. **106**(39): p. 16698-16703.
31. Lamba, D.A., Karl, M.O., and Reh, T.A., *Strategies for retinal repair: cell replacement and regeneration*, in *Progress in Brain Research*, E.M.H.I.H.J.W.A.B.B.G.J.B. Joost Verhaagen and F.S. Dick, Editors. 2009, Elsevier. p. 23-31.
32. Ong, J.M. and Da Cruz, L., *A review and update on the current status of stem cell therapy and the retina.* British Medical Bulletin, 2012. **102**(1): p. 133-146.
33. Roesch, K., et al., *The transcriptome of retinal Müller glial cells.* The Journal of Comparative Neurology, 2008. **509**(2): p. 225-238.
34. Newman, E., *Glia of the retina*, in *Retina*, S. Ryan, Editor 2001, Mosby: St. Louis. p. 89-103.
35. Hernandez, M.R., *The optic nerve head in glaucoma: role of astrocytes in tissue remodeling.* Progress in Retinal and Eye Research, 2000. **19**(3): p. 297-321.
36. Tibbetts, M.D., et al., *Stem cell therapy for retinal disease.* Current Opinion in Ophthalmology, 2012. **23**(3): p. 226-34.
37. West, E.L., et al., *Cell transplantation strategies for retinal repair*, in *Progress in Brain Research*, E.M.H.I.H.J.W.A.B.B.G.J.B. Joost Verhaagen and F.S. Dick, Editors. 2009, Elsevier. p. 3-21.
38. Meyer, J.S., Katz, M.L., and Kirk, M.D., *Stem Cells for Retinal Degenerative Disorders.* Annals of the New York Academy of Sciences, 2005. **1049**(1): p. 135-145.
39. Jin, Z.B., et al., *Induced pluripotent stem cells for retinal degenerative diseases: a new perspective on the challenges.* Journal of Genetics, 2009. **88**(4): p. 417-424.

40. Siqueria, R.C., *Stem cell therapy for retinal diseases: update.* Stem Cell Research & Therapy, 2011. **2**(6): p. 50.
41. Giles, C.L. and S. A.R., *Intracranial hypertension and tetracycline therapy.* American Jounral of Ophthalmology, 1971. **72**(5): p. 981-982.
42. Minckler, D.S., *Histology of optic nerve damage in ocular hypertension and early glaucoma.* . Survey of Ophthalmology, 1989. **33**: p. 401-411.
43. Anderson, D.R. and Hendrickson, A., *Effect of Intraocular Pressure on Rapid Axoplasmic Transport in Monkey Optic Nerve.* Investigative Ophthalmology & Visual Science, 1974. **13**(10): p. 771-783.
44. Quigley, H., Guy, J., Anderson, D.R., *Blockade of rapid axonal transport: Effect of intraocular pressure elevation in primate optic nerve.* Archives of Ophthalmology, 1979. **97**(3): p. 525-531.
45. Casson, R.J., et al., *Definition of glaucoma: clinical and experimental concepts.* Clinical & Experimental Ophthalmology, 2012. **40**(4): p. 341-349.
46. Schwartz, S.D., et al., *Embryonic stem cell trials for macular degeneration: a preliminary report.* The Lancet, 2012. **379**(9817): p. 713-720.
47. Lu, B., et al., *Long-Term Safety and Function of RPE from Human Embryonic Stem Cells in Preclinical Models of Macular Degeneration.* STEM CELLS, 2009. **27**(9): p. 2126-2135.
48. Hamel, C., *Retinitis pigmentosa.* Orphanet Journal of Rare Diseases, 2006. **1**: p. 40.
49. Jin, Z.B., et al., *Modeling Retinal Degeneration Using Patient-Specific Induced Pluripotent Stem Cells.* PLoS ONE, 2011. **6**(2): p. e17084.
50. Roux, A.F., *[Molecular updates on Usher syndrome].* Journal for Ophthalmology, 2005. **28**(1): p. 93-97.
51. Reiners, J., et al., *Molecular basis of human Usher syndrome: Deciphering the meshes of the Usher protein network provides insights into the pathomechanisms of the Usher disease.* Experimental Eye Research, 2006. **83**(1): p. 97-119.
52. Smith, R., et al., *Clinical diagnosis of the Usher syndromes. Usher Syndrome Consortium.* American Jounral of Medical Genetics, 1994. **50**(1): p. 32-38.
53. Fairchild, P.J., *The challenge of immunogenicity in the quest for induced pluripotency.* Nature Reviews Immunology, 2010. **10**(12): p. 868-875.
54. Evans, M.J. and Kaufman, M.H., *Establishment in culture of pluripotential cells from mouse embryos.* Nature, 1981. **292**(5819): p. 154-156.
55. Martin, G.R., *Isolation of a pluripotent cell line from early mouse embryos cultured in medium conditioned by teratocarcinoma stem cells.* Proceedings of the National Academy of Sciences, 1981. **78**(12): p. 7634-7638.
56. Santos, F., et al., *Dynamic Reprogramming of DNA Methylation in the Early Mouse Embryo.* Developmental Biology, 2002. **241**(1): p. 172-182.
57. Meissner, A., et al., *Genome-scale DNA methylation maps of pluripotent and differentiated cells.* Nature, 2008. **454**(7205): p. 766-770.
58. Thomson, J.A., et al., *Embryonic Stem Cell Lines Derived from Human Blastocysts.* Science, 1998. **282**(5391): p. 1145-1147.
59. Nichols, J. and Smith, A., *Naive and Primed Pluripotent States.* Cell Stem Cell, 2009. **4**(6): p. 487-492.
60. Reubinoff, B.E., et al., *Embryonic stem cell lines from human blastocysts: somatic differentiation in vitro.* Nature Biotechnology, 2000. **18**(4): p. 399-404.
61. Gertow, D.K., et al., *Organized Development from Human Embryonic Stem Cells after Injection into Immunodeficient Mice* Stem Cells and Development, 2004. **13**(4): p. 421-435.

62. Reubinoff, B.E., et al., *Neural progenitors from human embryonic stem cells.* Nature Biotechnology, 2001. **19**(12): p. 1134-1140.
63. Mummery, C., et al., *Cardiomyocyte differentiation of mouse and human embryonic stem cells.* Journal of Anatomy, 2002. **200**(3): p. 233-242.
64. Rambhatla, L., et al., *Generation of Hepatocyte-Like Cells From Human Embryonic Stem Cells.* Cell Transplantation, 2003. **12**(1): p. 1-11.
65. Kaufman, D.S., et al., *Hematopoietic colony-forming cells derived from human embryonic stem cells.* Proceedings of the National Academy of Sciences, 2001. **98**(19): p. 10716-10721.
66. Coraux, C., et al., *Embryonic Stem Cells Generate Airway Epithelial Tissue.* American Journal of Respiratory Cell and Molecular Biology, 2005. **32**(2): p. 87-92.
67. Tabar, V., et al., *Therapeutic cloning in individual parkinsonian mice.* Nature Medicine, 2008. **14**(4): p. 379-381.
68. Takahashi, K. and Yamanaka, S. *Induction of Pluripotent Stem Cells from Mouse Embryonic and Adult Fibroblast Cultures by Defined Factors.* Cell, 2006. **126**(4): p. 663-676.
69. Yu, J., et al., *Induced Pluripotent Stem Cell Lines Derived from Human Somatic Cells.* Science, 2007. **318**(5858): p. 1917-1920.
70. Takahashi, K., et al., *Induction of Pluripotent Stem Cells from Adult Human Fibroblasts by Defined Factors.* Cell, 2007. **131**(5): p. 861-872.
71. Hanna, J.H., Saha, K., and Jaenisch, R., *Pluripotency and Cellular Reprogramming: Facts, Hypotheses, Unresolved Issues.* Cell, 2010. **143**(4): p. 508-525.
72. Chan, E.M., et al., *Live cell imaging distinguishes bona fide human iPS cells from partially reprogrammed cells.* Nature Biotechnology, 2009. **27**(11): p. 1033-1037.
73. Mikkelsen, T.S., et al., *Dissecting direct reprogramming through integrative genomic analysis.* Nature, 2008. **454**(7200): p. 49-55.
74. Okita, K. and Yamanaka, S., *Induced pluripotent stem cells: opportunities and challenges.* Philosophical Transactions of the Royal Society B: Biological Sciences, 2011. **366**(1575): p. 2198-2207.
75. Boland, M.J., et al., *Adult mice generated from induced pluripotent stem cells.* Nature, 2009. **461**(7260): p. 91-94.
76. Kang, L., et al., *iPS Cells Can Support Full-Term Development of Tetraploid Blastocyst-Complemented Embryos.* Cell Stem Cell, 2009. **5**(2): p. 135-138.
77. Zhao, X.-y., et al., *iPS cells produce viable mice through tetraploid complementation.* Nature, 2009. **461**(7260): p. 86-90.
78. Stadtfeld, M., et al., *Aberrant silencing of imprinted genes on chromosome 12qF1 in mouse induced pluripotent stem cells.* Nature, 2010. **465**(7295): p. 175-181.
79. Lensch, M.W., et al., *Teratoma Formation Assays with Human Embryonic Stem Cells: A Rationale for One Type of Human-Animal Chimera.* Cell Stem Cell, 2007. **1**(3): p. 253-258.
80. Park, I.-H., et al., *Disease-Specific Induced Pluripotent Stem Cells.* Cell, 2008. **134**(5): p. 877-886.
81. Maherali, N., et al., *Directly Reprogrammed Fibroblasts Show Global Epigenetic Remodeling and Widespread Tissue Contribution.* Cell Stem Cell, 2007. **1**(1): p. 55-70.
82. Wernig, M., et al., *In vitro reprogramming of fibroblasts into a pluripotent ES-cell-like state.* Nature, 2007. **448**(7151): p. 318-324.
83. Lowry, W.E., et al., *Generation of human induced pluripotent stem cells from dermal fibroblasts.* Proceedings of the National Academy of Sciences, 2008. **105**(8): p. 2883-2888.

84. Liao, J., et al., *Generation of Induced Pluripotent Stem Cell Lines from Adult Rat Cells.* Cell Stem Cell, 2009. **4**(1): p. 11-15.
85. Li, W., et al., *Generation of Rat and Human Induced Pluripotent Stem Cells by Combining Genetic Reprogramming and Chemical Inhibitors.* Cell Stem Cell, 2009. **4**(1): p. 16-19.
86. Liu, H., et al., *Generation of Induced Pluripotent Stem Cells from Adult Rhesus Monkey Fibroblasts.* Cell Stem Cell, 2008. **3**(6): p. 587-590.
87. Esteban, M.A., et al., *Generation of Induced Pluripotent Stem Cell Lines from Tibetan Miniature Pig.* Journal of Biological Chemistry, 2009. **284**(26): p. 17634-17640.
88. Shimada, H., et al., *Generation of canine induced pluripotent stem cells by retroviral transduction and chemical inhibitors.* Molecular Reproduction and Development, 2010. **77**(1): p. 2-2.
89. Loh, Y.-H., et al., *Generation of induced pluripotent stem cells from human blood.* Blood, 2009. **113**(22): p. 5476-5479.
90. Liu, H., et al., *Generation of endoderm-derived human induced pluripotent stem cells from primary hepatocytes.* Hepatology, 2010. **51**(5): p. 1810-1819.
91. Eminli, S., et al., *Reprogramming of Neural Progenitor Cells into Induced Pluripotent Stem Cells in the Absence of Exogenous Sox2 Expression.* STEM CELLS, 2008. **26**(10): p. 2467-2474.
92. Aasen, T., et al., *Efficient and rapid generation of induced pluripotent stem cells from human keratinocytes.* Nature Biotechnology, 2008. **26**(11): p. 1276-1284.
93. Fusaki, N., et al., *Efficient induction of transgene-free human pluripotent stem cells using a vector based on Sendai virus, an RNA virus that does not integrate into the host genome.* Proceedings of the Japan Academy, Series B, 2009. **85**(8): p. 348-362.
94. Stadtfeld, M., et al., *Induced Pluripotent Stem Cells Generated Without Viral Integration.* Science, 2008. **322**(5903): p. 945-949.
95. Okita, K., et al., *A more efficient method to generate integration-free human iPS cells.* Nature Methods, 2011. **8**(5): p. 409-412.
96. Warren, L., et al., *Highly Efficient Reprogramming to Pluripotency and Directed Differentiation of Human Cells with Synthetic Modified mRNA.* Cell Stem Cell, 2010. **7**(5): p. 618-630.
97. Kim, D., et al., *Generation of Human Induced Pluripotent Stem Cells by Direct Delivery of Reprogramming Proteins.* Cell Stem Cell, 2009. **4**(6): p. 472-476.
98. Huangfu, D., et al., *Induction of pluripotent stem cells by defined factors is greatly improved by small-molecule compounds.* Nature Biotechnology, 2008. **26**(7): p. 795-797.
99. Shi, Y., et al., *Induction of Pluripotent Stem Cells from Mouse Embryonic Fibroblasts by Oct4 and Klf4 with Small-Molecule Compounds.* Cell Stem Cell, 2008. **3**(5): p. 568-574.
100. Hockemeyer, D., et al., *A Drug-Inducible System for Direct Reprogramming of Human Somatic Cells to Pluripotency.* Cell Stem Cell, 2008. **3**(3): p. 346-353.
101. Sommer, C.A., et al., *Excision of Reprogramming Transgenes Improves the Differentiation Potential of iPS Cells Generated with a Single Excisable Vector.* STEM CELLS, 2010. **28**(1): p. 64-74.
102. Sareen, D. and C.N. Svendsen, *Stem cell biologists sure play a mean pinball.* Nature Biotechnology, 2010. **28**(4): p. 333-335.
103. Ebert, A.D., et al., *Induced pluripotent stem cells from a spinal muscular atrophy patient.* Nature, 2009. **457**(7227): p. 277-280.
104. Dimos, J.T., et al., *Induced Pluripotent Stem Cells Generated from Patients with ALS Can Be Differentiated into Motor Neurons.* Science, 2008. **321**(5893): p. 1218-1221.

105. Soldner, F., et al., *Parkinson's Disease Patient-Derived Induced Pluripotent Stem Cells Free of Viral Reprogramming Factors.* Cell, 2009. **136**(5): p. 964-977.
106. Raya, A., et al., *Disease-corrected haematopoietic progenitors from Fanconi anaemia induced pluripotent stem cells.* Nature, 2009. **460**(7251): p. 53-59.
107. Meyer, J.S., et al., *Optic Vesicle-like Structures Derived from Human Pluripotent Stem Cells Facilitate a Customized Approach to Retinal Disease Treatment.* STEM CELLS, 2011. **29**(8): p. 1206-1218.
108. Jin, Z.B., et al., *Integration-Free Induced Pluripotent Stem Cells Derived from Retinitis Pigmentosa Patient for Disease Modeling.* Stem Cells Translational Medicine, 2012. **1**(6): p. 503-509.
109. Singh, R., et al., *iPS cell modeling of Best disease: insights into the pathophysiology of an inherited macular degeneration.* Human Molecular Genetics, 2013. **22**(3): p. 593-607.
110. Brown, M.E., et al., *Derivation of induced pluripotent stem cells from human peripheral blood T lymphocytes.* PLoS ONE, 2010. **5**(6).
111. Krencik, R., et al., *Specification of transplantable astroglial subtypes from human pluripotent stem cells.* Nature Biotechnology, 2011. **29**(6): p. 528-534.
112. Krencik, R. and Zhang, S.C., *Directed differentiation of functional astroglial subtypes from human pluripotent stem cells.* Nature Protocols, 2011. **6**(11): p. 1710-1717.
113. Wang, D.Y., et al., *Gene mutations in retinitis pigmentosa and their clinical implications.* Clinica Chimica Acta, 2005. **351**(1–2): p. 5-16.
114. Ahmed, Z.M., et al., *USH1H, a novel locus for type I Usher syndrome, maps to chromosome 15q22-23.* Clinical Genetics, 2009. **75**(1): p. 86-91.
115. Millán, J., et al., *An update on the genetics of usher syndrome.* Journal for Ophthalmology, 2011.
116. Saihan, Z., et al., *Update on Usher Syndrome.* Current Opinion in Neurology, 2009. **22**(1): p. 19-27.
117. Egawa, N., et al., *Drug Screening for ALS Using Patient-Specific Induced Pluripotent Stem Cells.* Science Translational Medicine, 2012. **4**(145): p. 145ra104.
118. Liang, P., et al., *Drug Screening Using a Library of Human Induced Pluripotent Stem Cell–Derived Cardiomyocytes Reveals Disease-Specific Patterns of Cardiotoxicity.* Circulation, 2013. **127**(16): p. 1677-1691.
119. Stone, J. and Dreher, Z., *Relationship Between Astrocytes, Ganglion Cells and Vasculature of the Retina.* The Journal of Comparative Neurology, 1987. **255**: p. 35-49.
120. Rodieck, R.W., Binmoeller, K.F., and Dineen, J., *Parasol and midget ganglion cells of the human retina.* The Journal of Comparative Neurology, 1985. **233**(1): p. 115-132.
121. Dacey, D.M. and Petersen, M.R., *Dendritic field size and morphology of midget and parasol ganglion cells of the human retina.* Proceedings of the National Academy of Sciences, 1992. **89**(20): p. 9666-9670.
122. Phillips, M.J., et al., *Blood-Derived Human iPS Cells Generate Optic Vesicle–Like Structures with the Capacity to Form Retinal Laminae and Develop Synapses.* Investigative Ophthalmology & Visual Science, 2012. **53**(4): p. 2007-2019.
123. Kolb, H., *Morphology and Circuitry of Ganglion Cells*, in *Webvision: The Organization of the Retina and Visual System* H. Kolb, et al., Editors. 2001: Salt Lake City (UT): University of Utah Health Sciences Center.
124. Beale, R. and Osborne, N.N., *Localization of the Thy-1 antigen to the surfaces of rat retinal ganglion cells.* Neurochemistry International, 1982. **4**(6): p. 587-595.
125. Kawasaki, H., et al., *Generation of dopaminergic neurons and pigmented epithelia from primate ES cells by stromal cell-derived inducing activity.* Proceedings of the National Academy of Sciences, 2002. **99**(3): p. 1580-1585.

126. Lamba, D.A., et al., *Generation, Purification and Transplantation of Photoreceptors Derived from Human Induced Pluripotent Stem Cells.* PLoS ONE, 2010. **5**(1): p. e8763.
127. Lamba, D.A., et al., *Efficient generation of retinal progenitor cells from human embryonic stem cells.* Proceedings of the National Academy of Sciences, 2006. **103**(34): p. 12769-12774.
128. Osakada, F., et al., *Toward the generation of rod and cone photoreceptors from mouse, monkey and human embryonic stem cells.* Nature Biotechnology, 2008. **26**(2): p. 215-224.
129. Osakada, F., et al., *In vitro differentiation of retinal cells from human pluripotent stem cells by small-molecule induction.* Journal of Cell Science, 2009. **122**(17): p. 3169-3179.
130. Anokye-Danso, F., et al., *Highly Efficient miRNA-Mediated Reprogramming of Mouse and Human Somatic Cells to Pluripotency.* Cell Stem Cell, 2011. **8**(4): p. 376-388.
131. Xiang, M., et al., *Brn-3b: a POU domain gene expressed in a subset of retinal ganglion cells.* Neuron, 1993. **11**(4): p. 689-701.
132. Canto-Soler, M.V., et al., *Transcription factors CTCF and Pax6 are segregated to different cell types during retinal cell differentiation.* Developmental Dynamics, 2008. **237**(3): p. 758-767.
133. Parameswaran, S., et al., *Induced Pluripotent Stem Cells Generate Both Retinal Ganglion Cells and Photoreceptors: Therapeutic Implications in Degenerative Changes in Glaucoma and Age-Related Macular Degeneration.* STEM CELLS, 2010. **28**(4): p. 695-703.
134. Chen, M., et al., *Generation of Retinal Ganglion–like Cells from Reprogrammed Mouse Fibroblasts.* Investigative Ophthalmology & Visual Science, 2010. **51**(11): p. 5970-5978.
135. Jagatha, B., et al., *In vitro differentiation of retinal ganglion-like cells from embryonic stem cell derived neural progenitors.* Biochemical and Biophysical Research Communications, 2009. **380**(2): p. 230-235.

TABLES

Table 1: List of Primary Antibodies Used for Immunocytochemistry Analysis

Antibody	Type	Source	Dilution
Bestrophin	Mouse monoclonal	Chemicon	1:100
ß-III Tubulin	Rabbit polyclonal	Covance	1:1000
Brn3	Goat polyclonal	Santa Cruz	1:200
Chx10	Sheep polyclonal	Exalpha Biologicals	1:200
Crx	Mouse monoclonal	Abnova	1:100
Ezrin	Rabbit polyclonal	Cell Signaling Technology	1:100
GFAP	Mouse monoclonal	Chemicon	1:5000
Hoxb4	Rat polyclonal	MRC NIMR	1:50
Islet1	Mouse monoclonal	Columbia University	1:200
Lhx2	Goat polyclonal	Santa Cruz	1:1000
MAP-2	Rabbit polyclonal	Santa Cruz	1:200
Nanog	Goat polyclonal	R&D Biosystems	1:20
Oct4	Rabbit polyclonal	Stemgent	1:100
Otx2	Goat polyclonal	R&D Biosystems	1:1000
Pax6	Mouse polyclonal	Stemgent	1:100
Recoverin	Rabbit polyclonal	Chemicon	1:1000
Six6	Rabbit polyclonal	Sigma Life Science	1:200
Sox1	Goat polyclonal	R&D Biosystems	1:1000
Sox2	Rabbit polyclonal	R&D Biosystems	1:100
SSEA-4	Mouse monoclonal	Stemgent	1:100
Tau	Mouse monoclonal	Santa Cruz	1:50
Tra-1-60	Mouse monoclonal	Stemgent	1:100
Tra-1-81	Mouse monoclonal	Stemgent	1:100
ZO-1	Rabbit polyclonal	Invitrogen	1:100

Table 2: List of Primers Used for RT-PCR Analysis

Gene	Forward (5' – 3')	Reverse (5' – 3')	Band Size (bp)
α-fetoprotein	AGA ACC TGT CAC AAG CTG TG	GAC AGC AAG CTG AGG ATG TC	676
Atoh7	GAG CGC GCG TTG CAC	GGG TCT CGT ACT TGG ACA GC	210
Best1	GCA AGC AGG CGT TTA GCA TGC C	CTG GGA GAC GAT GTC CAC GGC T	92
Brachyury	ACC CAG TTC ATA GCG GTG AC	CAA TTG TCA TGG GAT TGC AG	392
Brn3	GCA AGC AGG CGT TTA GCA TGC C	CTG GGA GAC GAT GTC CAC GGC T	344
Chx10	ATT CAA CGA AGC CCA CTA CCC AGA	ATC CTT GGC TGA CTT GAG GAT GGA	229
Cralbp	TTC AAG GGC TTT ACC ATG CAG CAG	AGT ACC ATG GCT GGT GGA TGA AGT	130
Crx	TAT TCT GTC AAC GCC TTG GCC CTA	TGC ATT TAG CCC TCC GGT TCT TGA	253
Ezrin	ACC ACC ATG GAT GCA GAG CTG GA	ACA CTT CCC GGA GGC CGA TAG T	101
Gapdh	ACC ACA GTC CAT GCC ATC AC	TCC ACC ACC CTG TTG CTG TA	450
Lhx2	CAA GAT CTC GGA CCG CTA CT	CCG TGG TCA GCA TCT TGT TA	284
Mitf	TTC ACG AGC GTC CTG TAT GCA GAT	TTG CAA AGC AGG ATC CAT CAA GCC	106
Nanog	CAA AGG CAA ACA ACC CAC TT	TCT GCT GGA GGC TGA GGT AT	158
Nr2e1	ATG GCA AAT TCT GTG GCG CTG AAG	GCG CTG ATT TCC CAA GTG CAT TCT	352
Oct4	CGA GCA ATT TGC CAA GCT CCT GAA	TTC GGG CAC TGC AGG AAC AAA TTC	324
Otx2	CAA CAG CAG AAT GGA GGT CA	CTG GGT GGA AAG AGA GAA GCT G	429, 190 (qPCR)
Pax6	CGG AGT GAA TCA GCT CGG TG	CCG CTT ATA CTG GGC TAT TTT GC	301 (+5a), 259 (-5a)
Pedf	AGA TCT CAG CTG CAA GAT TGC CCA	ATG AAT GAA CTC GGA GGT GAG GCT	127
Rax	GAA TCT CGA AAT CTC AGC CC	CTT CAC TAA TTT GCT CAG GAC	279
RPE65	GCC CTC CTG CAC AAG TTT GAC TTT	AGT TGG TCT CTG TGC AAG CGT AGT	92
Six3	CGA GCA GAA GAC GCA TTG CTT CAA	CGG CCT TGG CTA TCA TAC ATC ACA	395
Six6	ATT TGG GAC GGC GAA CAG AAG ACA	ATC CTG GAT GGG CAA CTC AGA TGT	384

Sox1	CAA TGC GGG GAG GAG AAG TC	CTC TGG ACC AAA CTG TGG CG	464
Sox2	CCC CCG GCG GCA ATA GCA	TCG GCG CCG GGG AGA TAC AT	448
Thy 1.2	TAG TCG ACC AGA GCC TTC GT	GCC CTC ACA CTT GAC CAG TT	311
ZO-1	AGA CCG TGC TGA CTT CTG GAG ATT	ACT TTG TTT GAA CAG GCT GAG CGG	101

Table 3: List of Primers Used for qRT-PCR Analysis

Gene	Forward (5' – 3')	Reverse (5' – 3')	Band Size (bp)
ß-Actin	GCG AGA AGA TGA CCC AGA TC	CCA GTG GTA CGG CCA GAG G	103
Brn3	AGC GCT CTC ACT TAC CCT TAC ACA	AAA TGG TGC ATC GGT CAT GCT TCC	94
Pax6	AGT GAA TCA GCT CGG TGG TGT CTT	TGC AGA ATT CGG GAA ATG TCG CAC	120

FIGURES

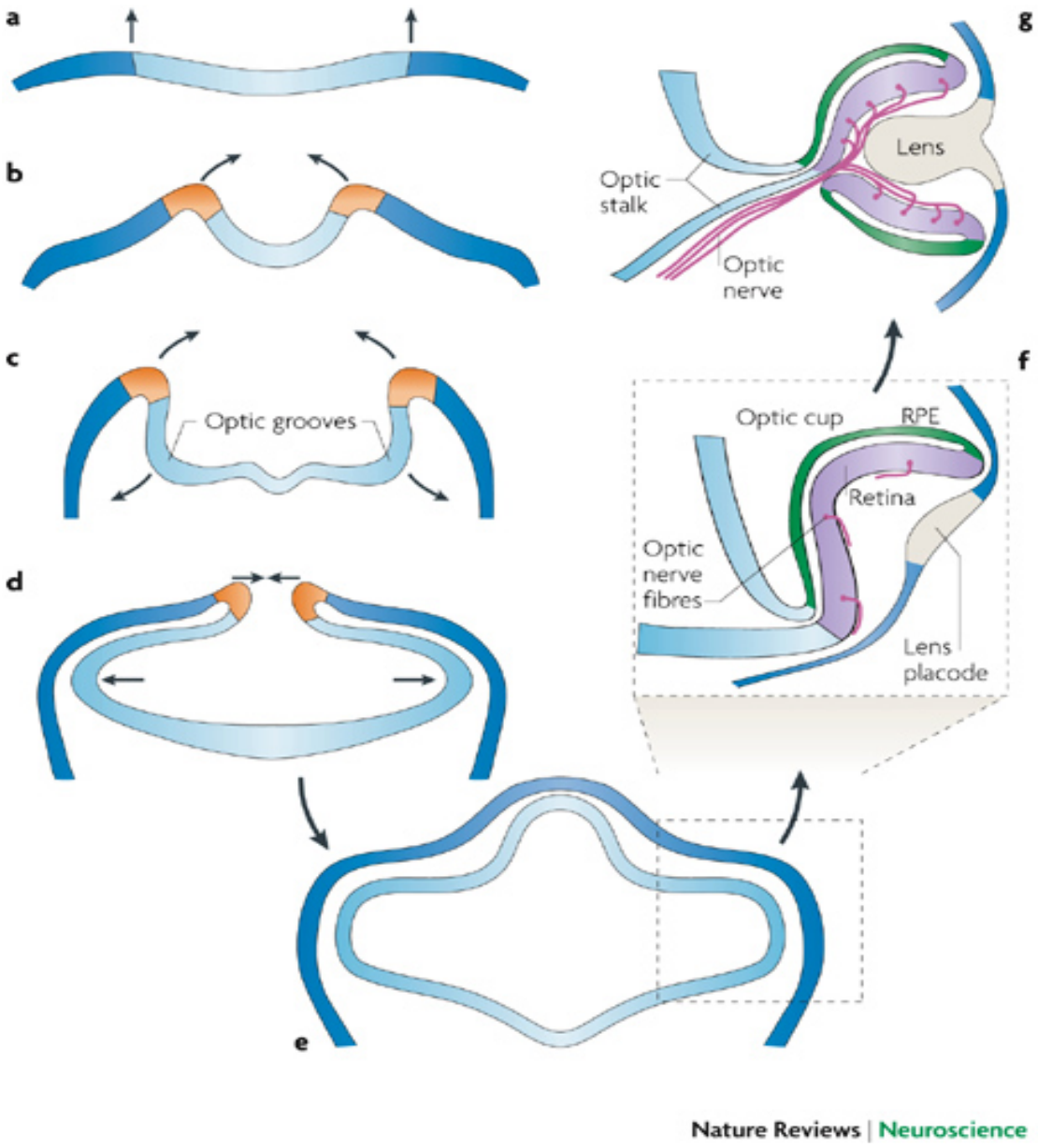

Figure 1: Development of the retina. (a) The formation of the eye is initiated in the regions of the neural plate. (b) The neural plate proceeds to fold upwards and inwards. (c) The optic grooves evaginate. (d) The two distinct optic vesicles now bulge further towards the surface ectoderm. (e) The optic vesicle coordinates with the head ectoderm to form the lens placode. (f) The optic vesicle now invaginates to form the optic cup and the specialized layers of retina and RPE. (g) The axons of RGCs are enclosed together at the close of the choroid fissure to form the optic nerve. (Adapted with permission from *Nature Reviews Neuroscience*, [5])

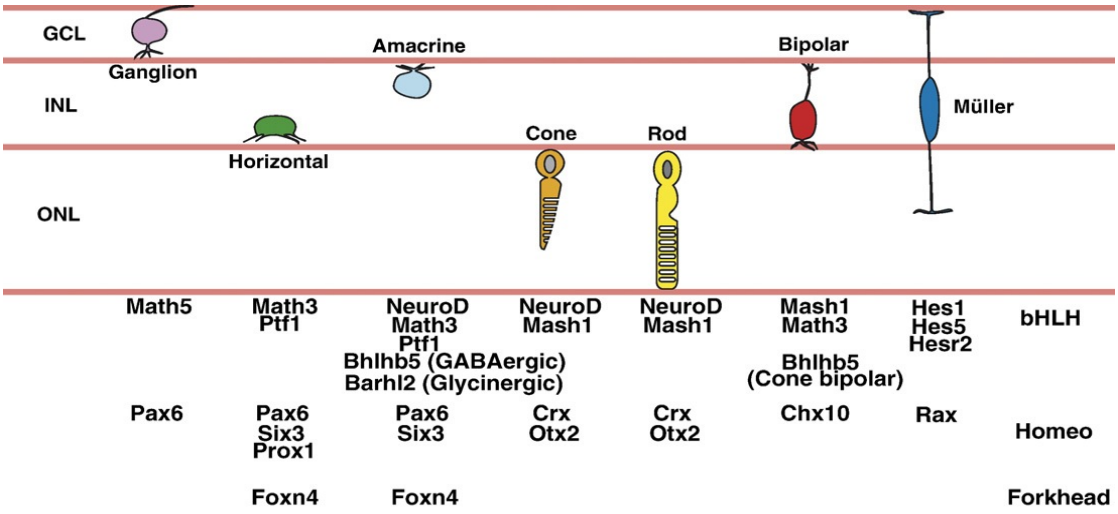

Figure 2: Role of multiple transcription factors in the retina. The different types and combinations of transcription factors associated with the specification and differentiation of retinal cell types during development. (Adapted with permission from *Brain Research*, [15])

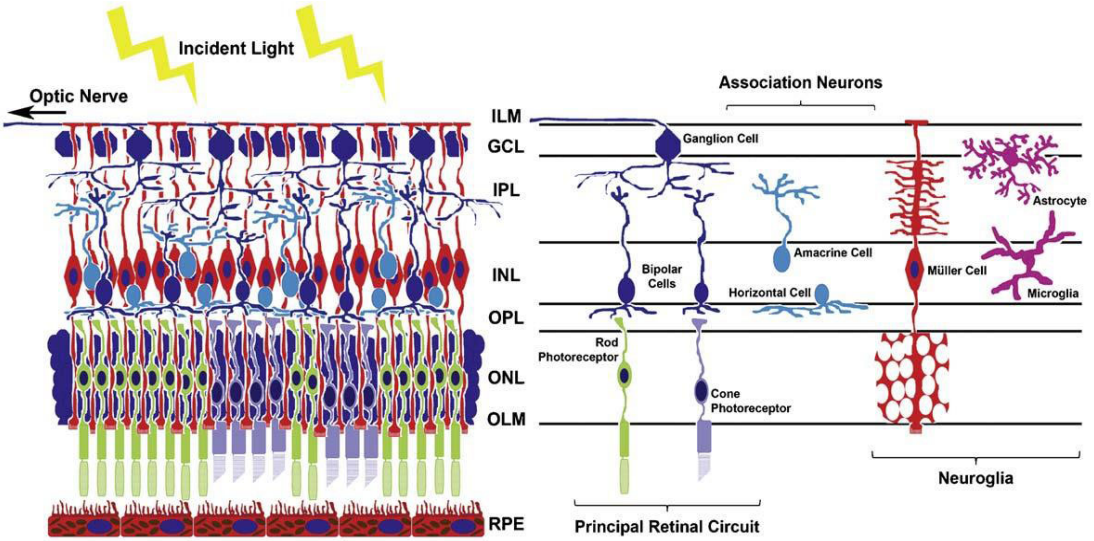

Figure 3: The Retina. The highly defined and layered structure of the retina comprises of 5 sets of interconnected neurons and the outermost RPE. Light incident on the ventral part of the eye traverses through all layers to be processed by the photoreceptors first and then travel back towards to the RGCs and to the brain via the optic nerve. (Adapted with permission from *Elsevier* Books, [37])

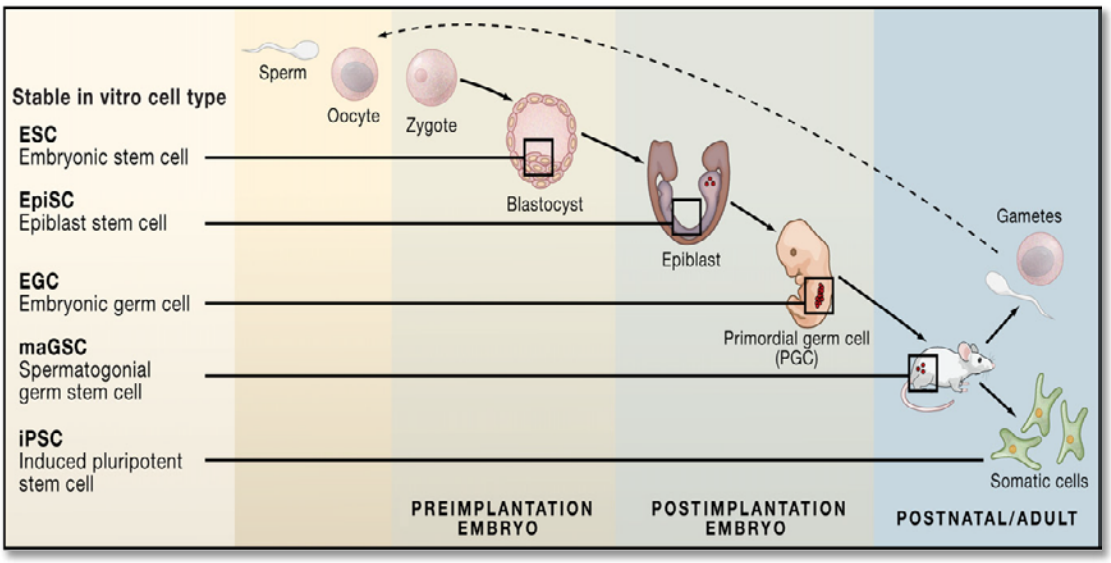

Figure 4: Different source of pluripotent stem cells. Sources of pluripotent stem cells during chronological stages of development. iPS cells are sources of pluripotent stem cells achieved by inducing mature somatic cells to an embryonic-like state via genetic reprogramming. (Adapted with permission from *Cell*, [71])

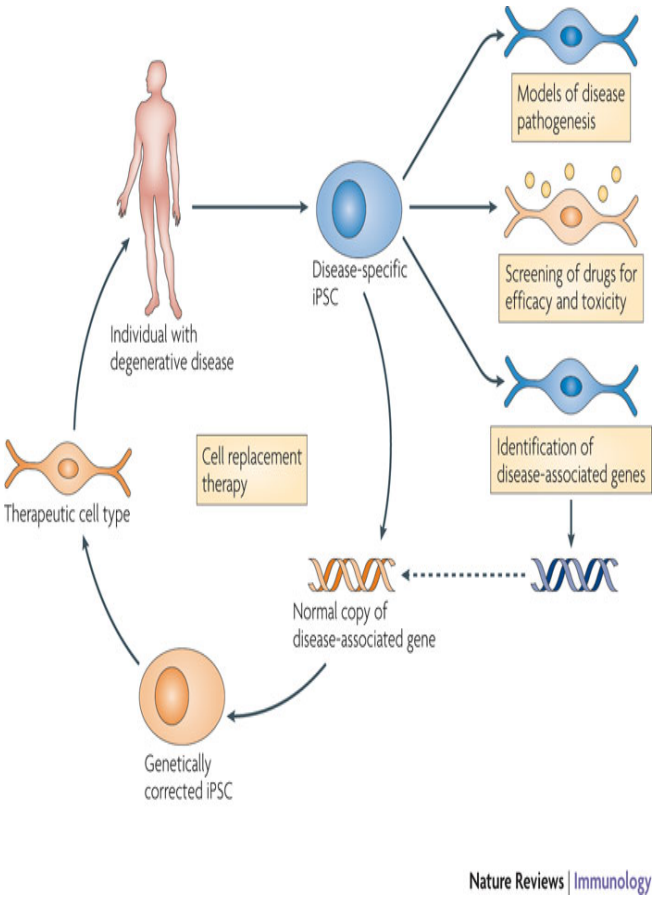

Figure 5: Disease Modeling Using Human iPS Cells. A schematic of how patient derived iPS cells can be used to model cellular degenerative diseases. Starting with somatic cells, e.g. skin, blood, of patients, these cells can be induced to become patient specific iPS cells that are isogenic in character. Disease specific iPS cells can then be directed to differentiate towards the affected cell type *in vitro*. Affected cell types derived can be analyzed for disease phenotype and progression, testing drug candidates, or transplantation after gene correction. (Adapted with permission from Nature *Reviews Immunology*, [53])

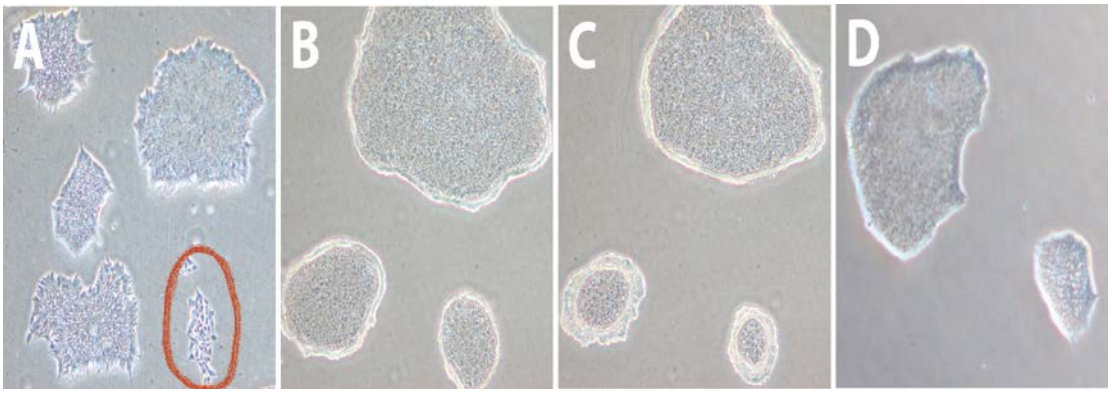

Figure 6: Maintenance and passaging of human iPS cells. Passaging of human iPS cells starts by identifying, marking (A), and scraping out any spontaneously differentiated colonies. The colonies are made then incubated in dispase for 15-20 minutes to allow for loosening of colonies (B,C) and then mechanically dislodged, triturated, and replated in fresh mTeSR^{TM}1 medium (D).

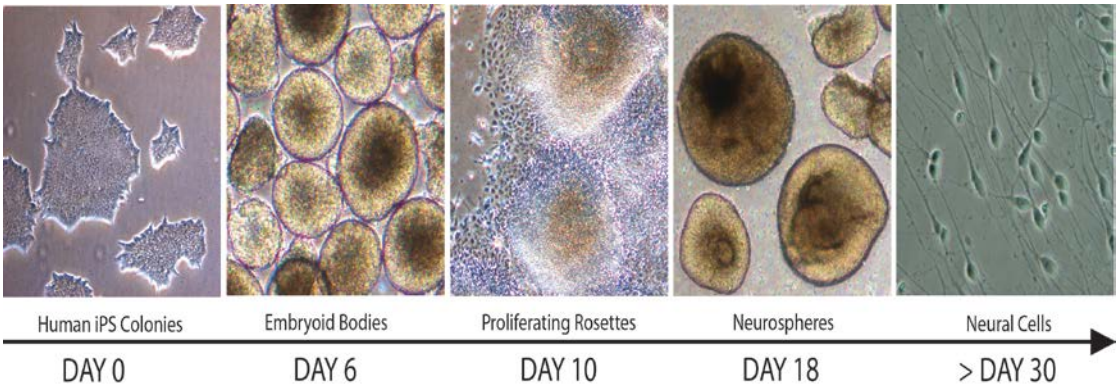

Figure 7: Timeline for neural induction of human iPS cells. Human iPS cells were differentiated according to the timeline shown. iPS cells were differentiated as embryoid bodies and eased into NIM during the first 6 days. Embryoid bodies were then plated and grown as adherent clusters until day 16 in NIM. At day 16, the clusters were lifted and allowed to form spheres for the next 2 days in RDM. The spheres were differentiated for later time points in suspension. Starting day 30, high number of neural cells was observed in culture.

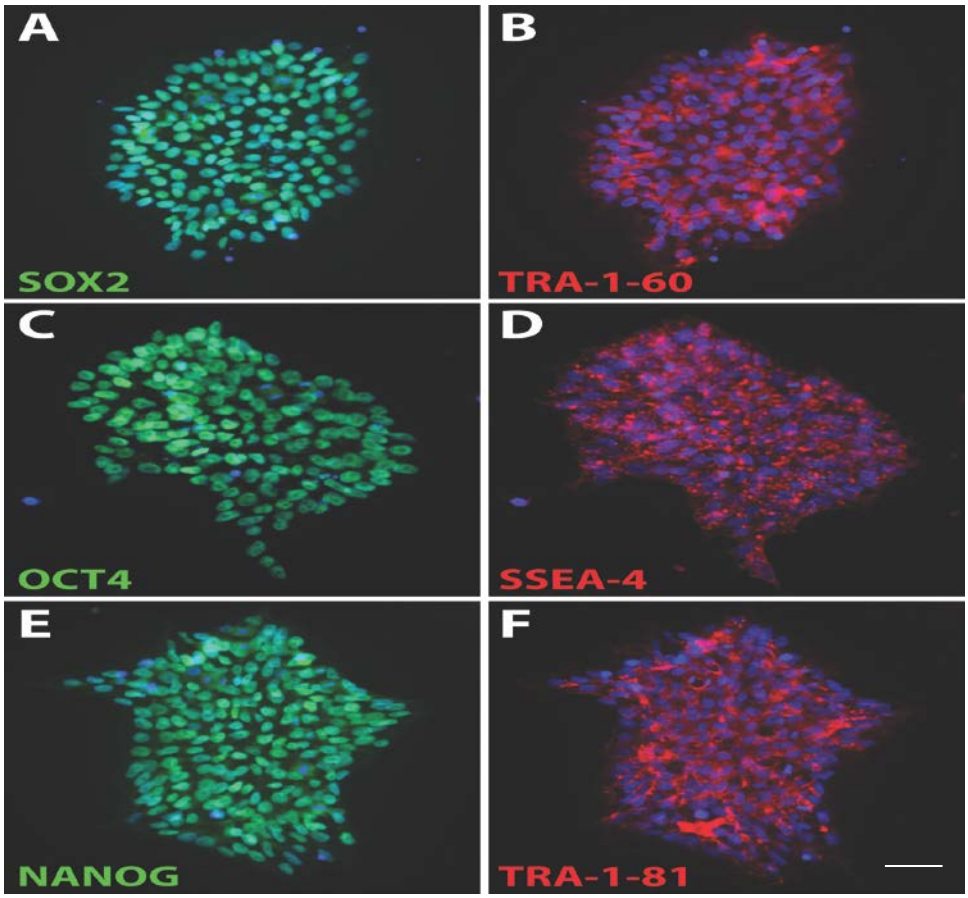

Figure 8: ICC Analysis of Pluripotency of Usher iPS Cells. Following numerous passages, Usher Syndrome iPS cells maintained the expression of all pluripotency-related characteristics examined by immunocytochemistry (A-F), including the transcription factors SOX2, OCT4, and NANOG (A, C, E). Furthermore, these cells expressed pluripotency-related cell surface antigens such as TRA-1-60 (B), SSEA-4 (D), and TRA-1-81 (F). (Scale bars, 15 μm in panels A-F).

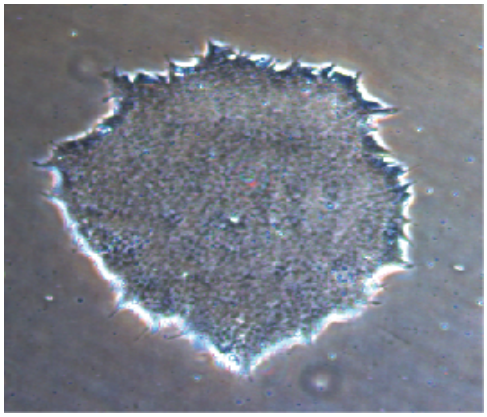

Figure 9: Brightfield stage of pluripotency. Colonies of Usher iPS cells exhibited typical pluripotent morphologies with tightly packed cells with a clearly defined and phase bright edges to each colony.

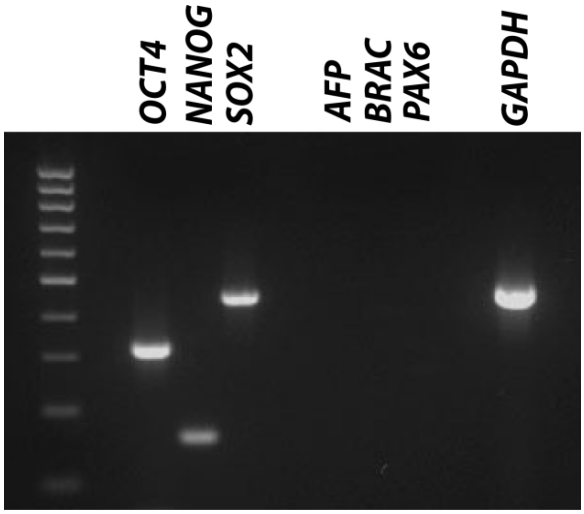

Figure 10: Transcript Analysis of Factors Associated with Pluripotency. RT-PCR analysis confirmed the expression of pluripotency-related genes, *OCT4*, *NANOG,* and *SOX2*, as well as the lack of expression of markers of differentiation, *AFP* (endoderm), *BRAC* (mesoderm), and *PAX6* (ectoderm).

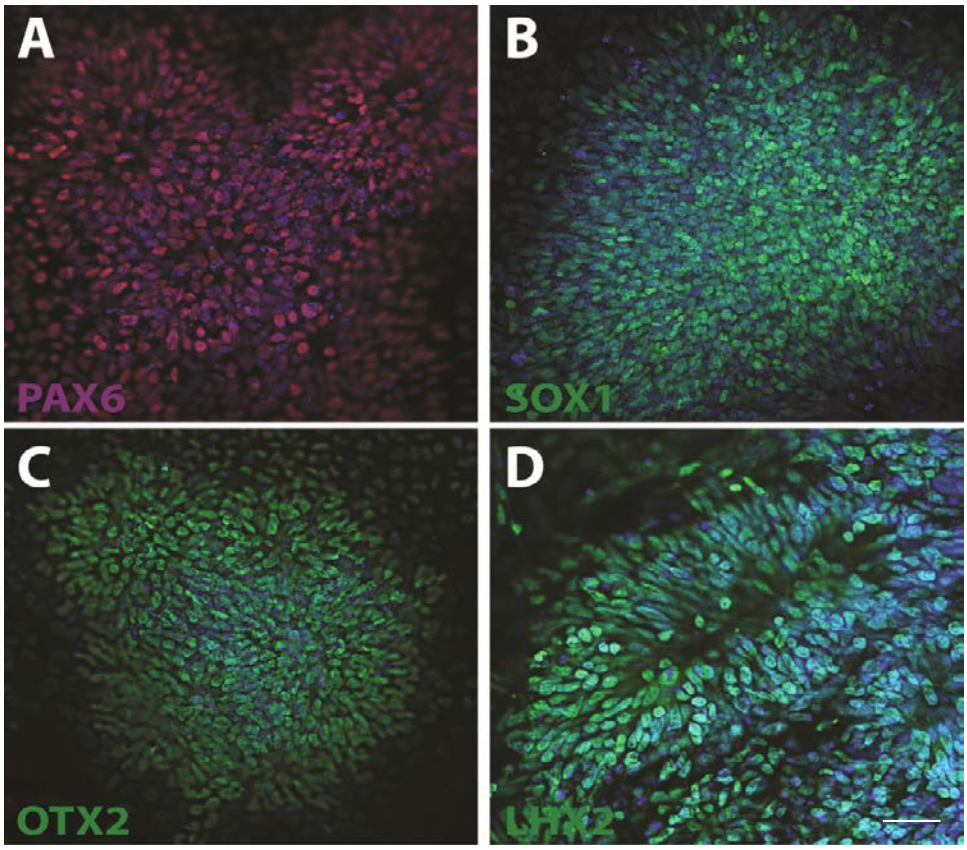

Figure 11: **ICC Analysis of Primitive Neural Induction of Usher iPS Cells.** After 10 days of differentiation, immunocytochemistry results demonstrated near uniform expression of early neural developmental transcription factors including PAX6 (A), SOX1 (B), OTX2 (C), and LHX2 (D). (Scale bars, 15 μm in panels A-D).

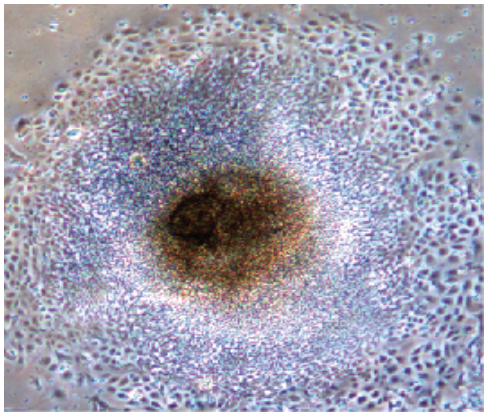

Figure 12: Brightfield stage of neural induction. At day 10, neural progenitor cells were characterized as outwardly proliferating cells from plated embryoid bodies.

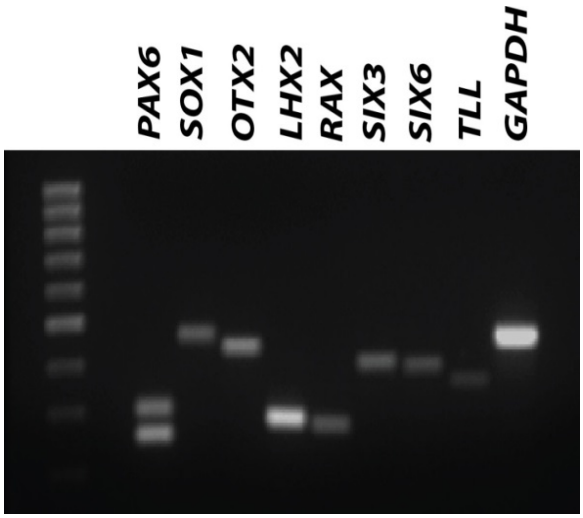

Figure 13: Transcript Analysis of Primitive Neural Induction of Usher iPS Cells. RT-PCR analysis confirmed the expression of numerous early neurodevelopmental transcription factors, *PAX6, SOX1, OTX2, LHX2,* including the expression of factors for eye field specification including, *RAX, SIX3, SIX6, and TLL.*

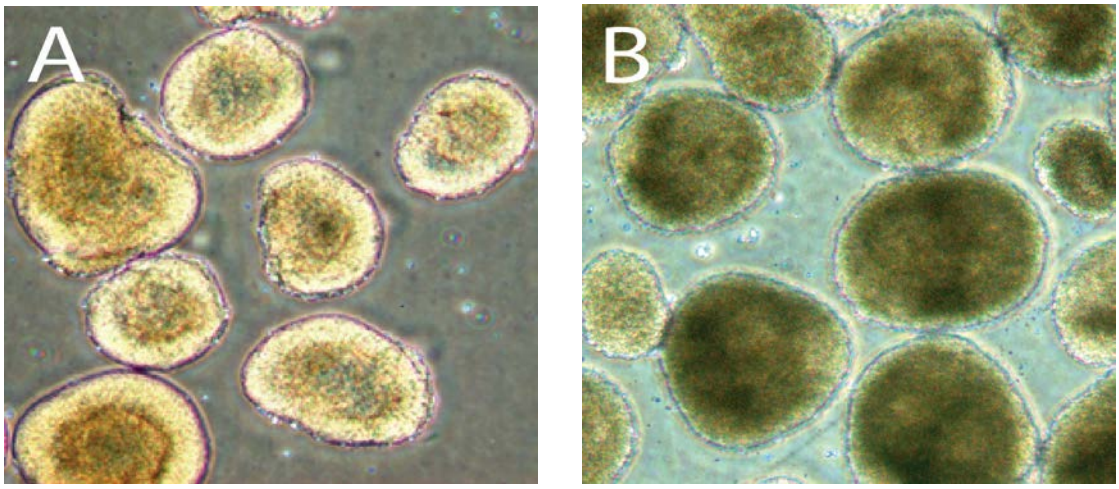

Figure 14: Identification of retinal and non-retinal neurospheres. At day 18, two distinct populations of spheres were identified. One population of spheres expressed a uniform phase bright ring around its periphery and had an optic vesicle-like appearance (A) whereas the other population had a uniformly darker appearance with internalized rosettes (B).

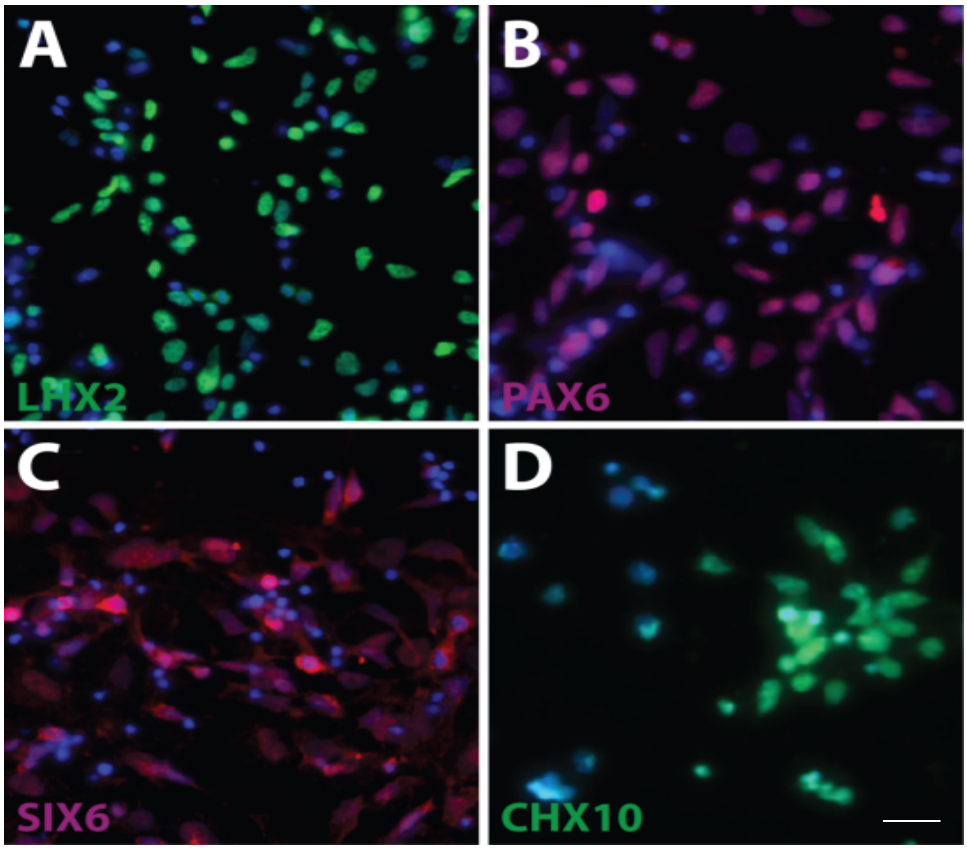

Figure 15: ICC Analysis of Retinal Progenitor Cells Derived from Usher iPS Cells. (A-D) Following 20 days of differentiation, a subset of cells exhibited numerous characteristics of retinal progenitor cells, including the expression of key transcription factors including LHX2, PAX6, SIX6, and CHX10. (Scale bars, 15 μm in panels A-D).

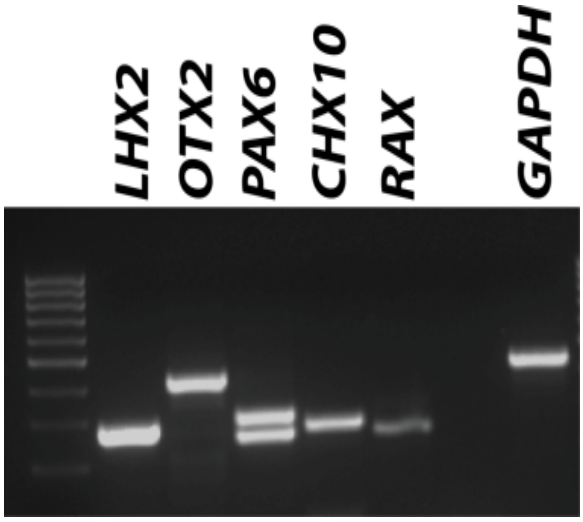

Figure 16: Transcript Analysis of Retinal Progenitor Cells Derived from Usher iPS Cells. Gene expression analysis further confirmed the expression of key transcription factors associated with retinal progenitor cells including, RAX, CHX10, PAX6, LHX2, and OTX2.

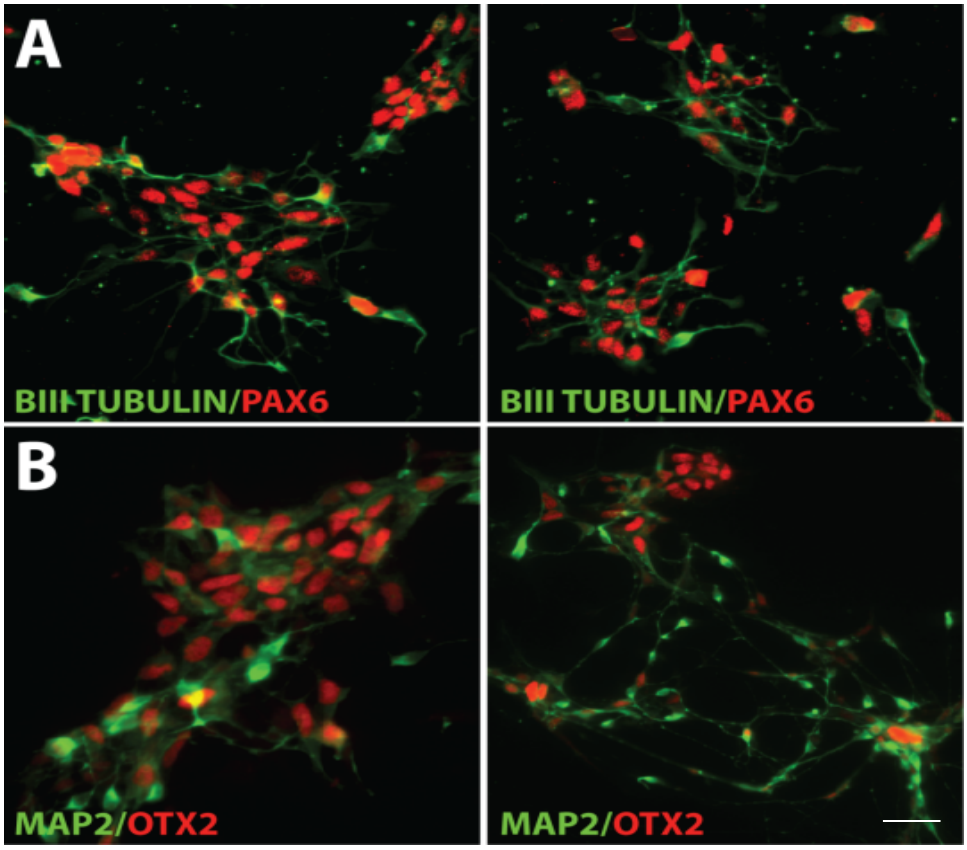

Figure 17: **ICC Analysis of Neuronal Specification from Usher iPS Cells.** (A, B) After 30 days of differentiation, cells exhibited numerous characteristics of neurons, including the expression of transcription factors PAX6 and OTX2, as well as the cytoskeletal proteins ß-III TUBULIN and MAP2. (Scale bars, 15 µm in panels A and B).

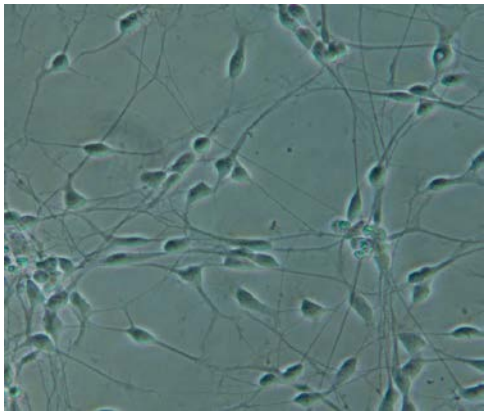

Figure 18: Brightfield example of *in vitro* derived neuronal cells. Under brightfield microscopy, numerous neuronal morphologies were observed including well defined and emanating axonal like processes from *in vitro* derived neuronal cell bodies.

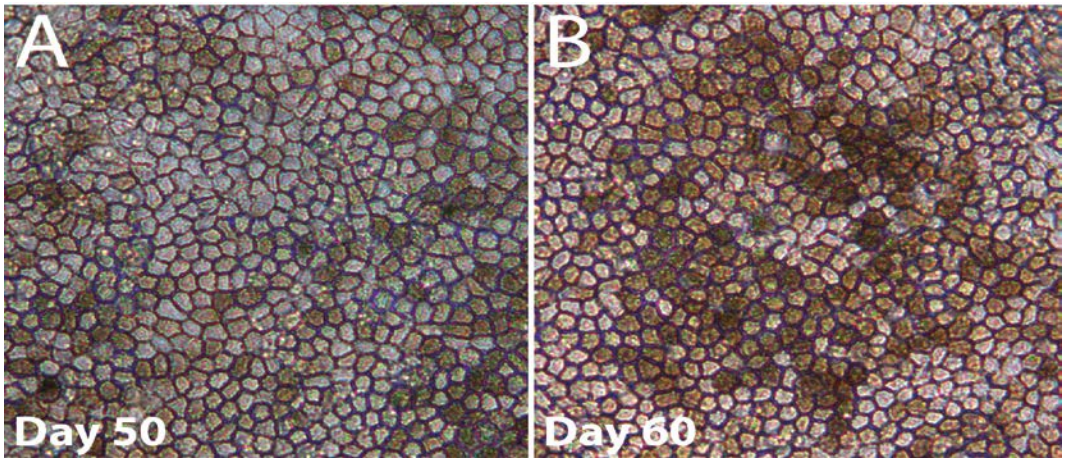

Figure 19: Identification of RPE Differentiation by increase in pigmentation. The successful generation of RPE cells from Usher iPS cells was identified after 40-50 days of differentiation. RPE exhibited typical cobblestone morphologies with characteristic pigmentation that increased in intensity with increasing timepoints in culture (A, B).

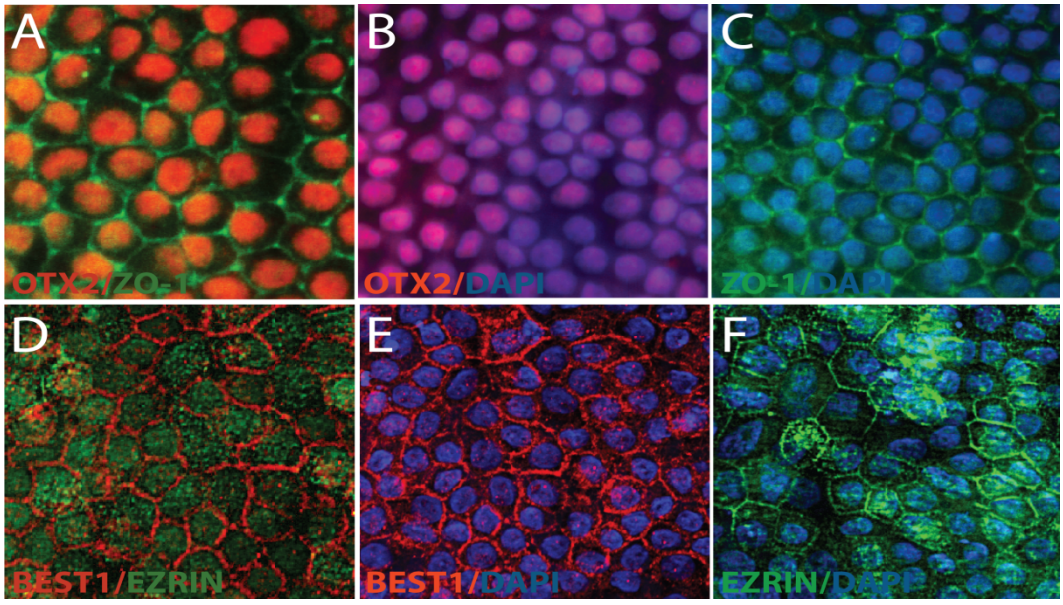

Figure 20: ICC analysis of RPE Differentiation from Usher iPS Cells. After 60 days, RPE was characterized by immunocytochemistry. RPE cells co-expressed the tight junction protein ZO-1 and OTX2 (A-C), and stained positive for other RPE specific proteins including the apical-basal proteins, EZRIN and BEST1 respectively (D-F).

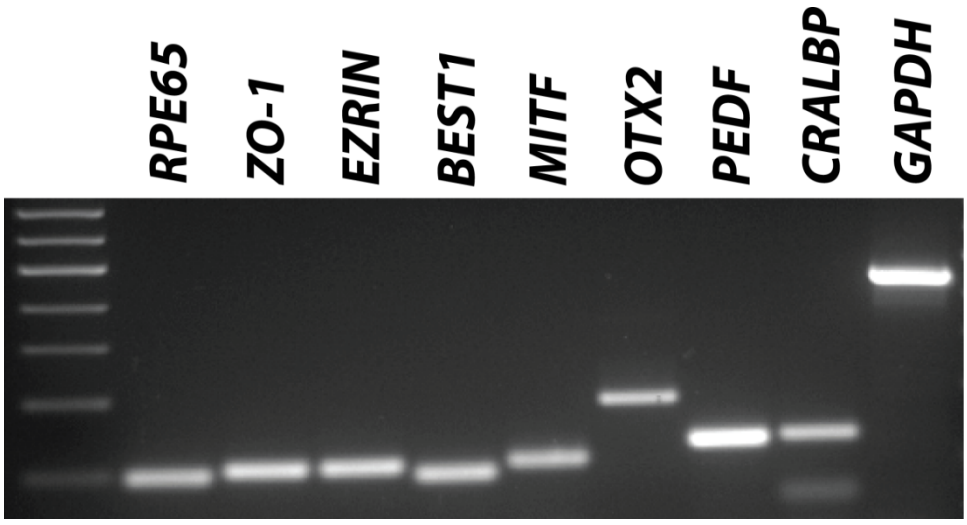

Figure 21: Transcript analysis of RPE Differentiation from Usher iPS Cells. Gene expression profiling of iPS derived RPE cells further confirmed the expression of RPE specific factors including *MITF, RPE65, PEDF,* and *CRALBP.*

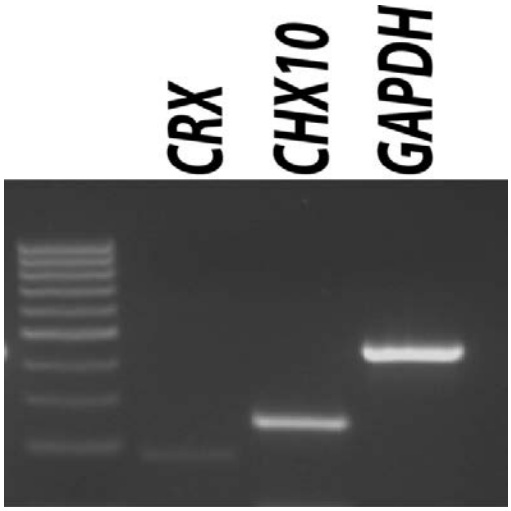

Figure 22: Transcript Analysis of Retinal Progenitor Cells at Day 70. Gene expression results after 70 days of differentiation revealed the expression of markers associated with retinal progenitor cells including the broad marker *CHX10,* and *CRX*, a transcription factor characteristic of photoreceptor precursors.

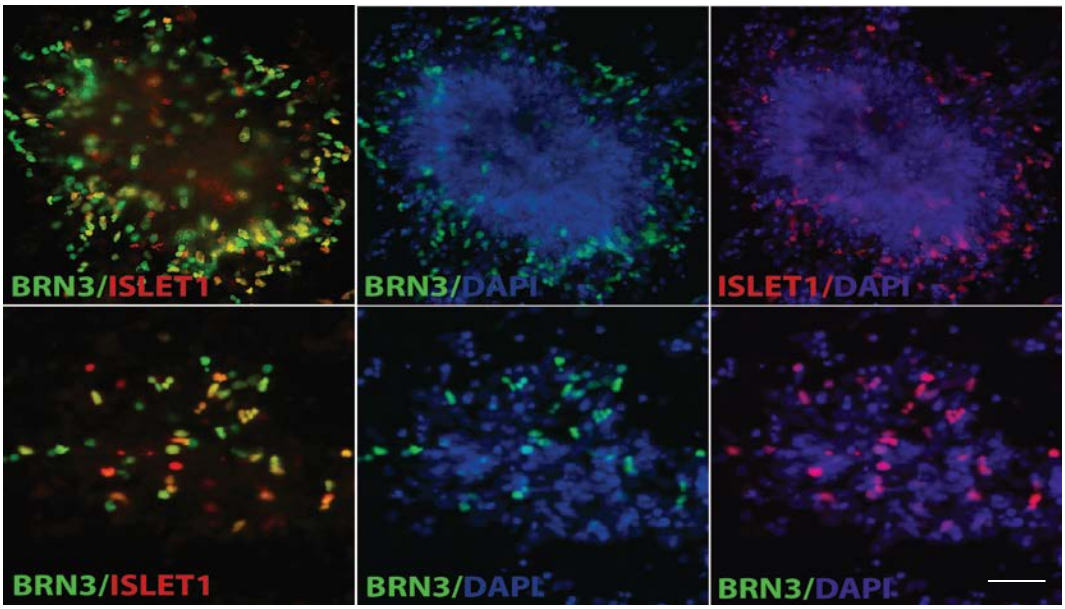

Figure 23: **Differentiation of RGCs at day 70.** The generation of RGCs from Usher iPS cells was analyzed by immunostaining after 70 days of differentiation. Subsets of retinal progenitor cells adopted characteristics of retinal ganglion cells, including the expression of the transcription factors BRN3 and ISLET1. (Scale bars, 15 µm).

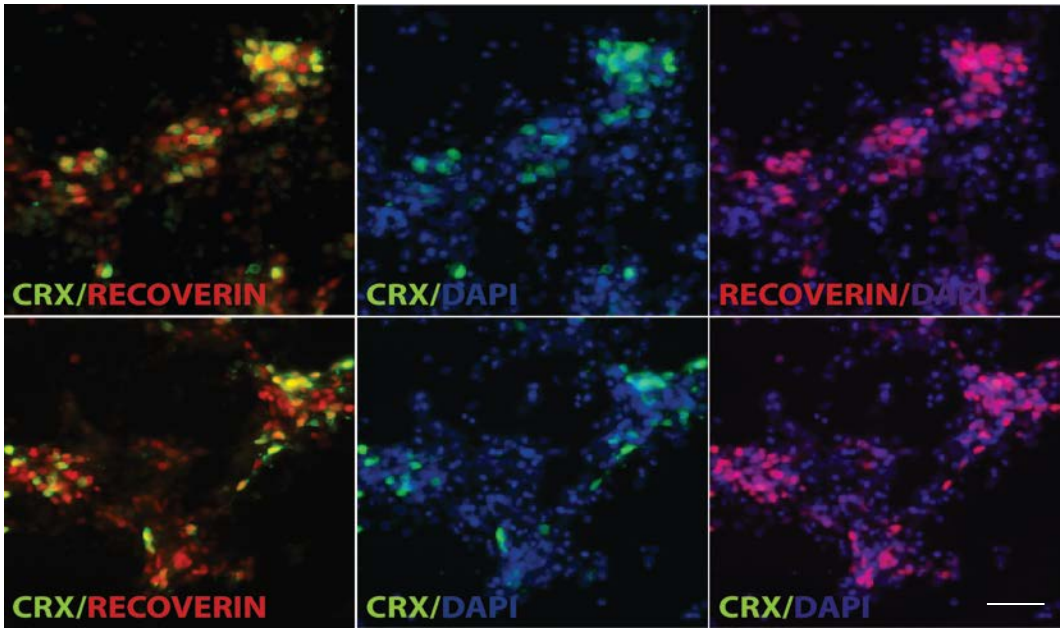

Figure 24: Differentiation of photoreceptors at day 70. ICC analysis of *in vitro* Usher iPS derived photoreceptors revealed expression of CRX and RECOVERIN, indicating a progressive increase from a more immature to a more mature photoreceptor cell type. (Scale bars, 15 µm).

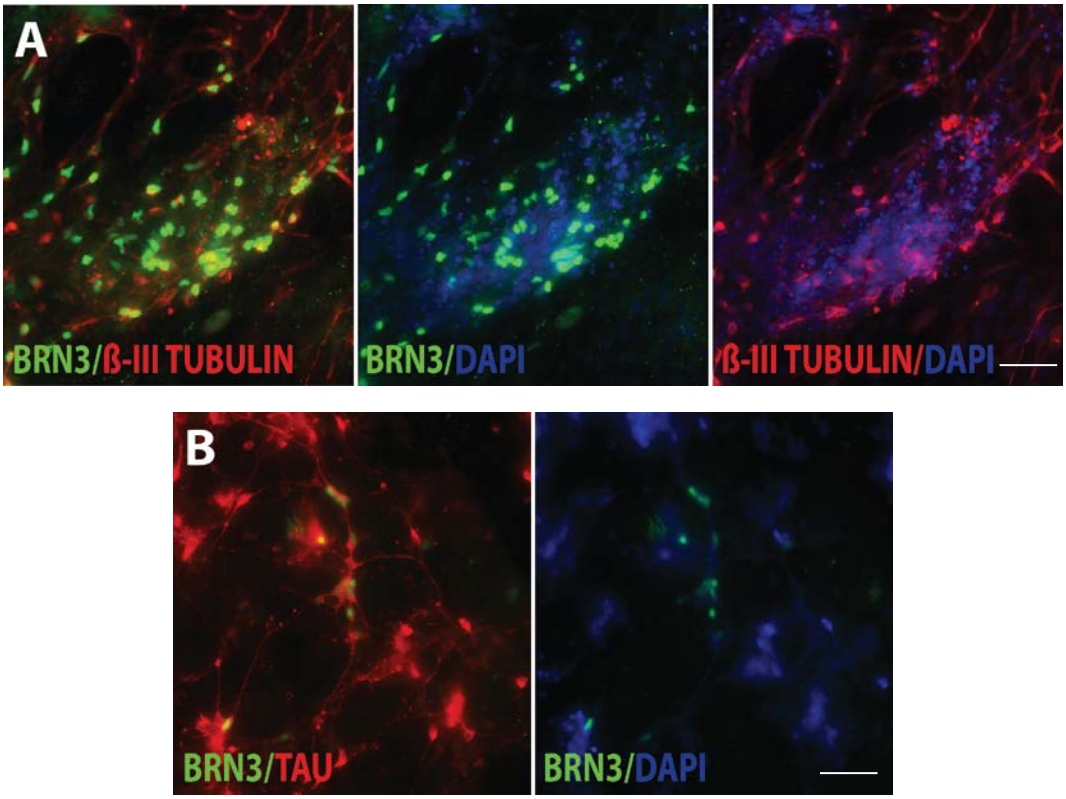

Figure 25: Identification of RGC neurons at day 40. RGCs were derived after 40 days of differentiation and identified by the expression of the RGC specific transcription factor BRN3. The neural nature of RGCs were further characterized by co-expression of BRN3 with the neural cytoskeletal marker ß-III TUBULIN (A) and with the axon specific marker, TAU (B). (Scale bars 11 µm in panel A, 15 µm in panel B)

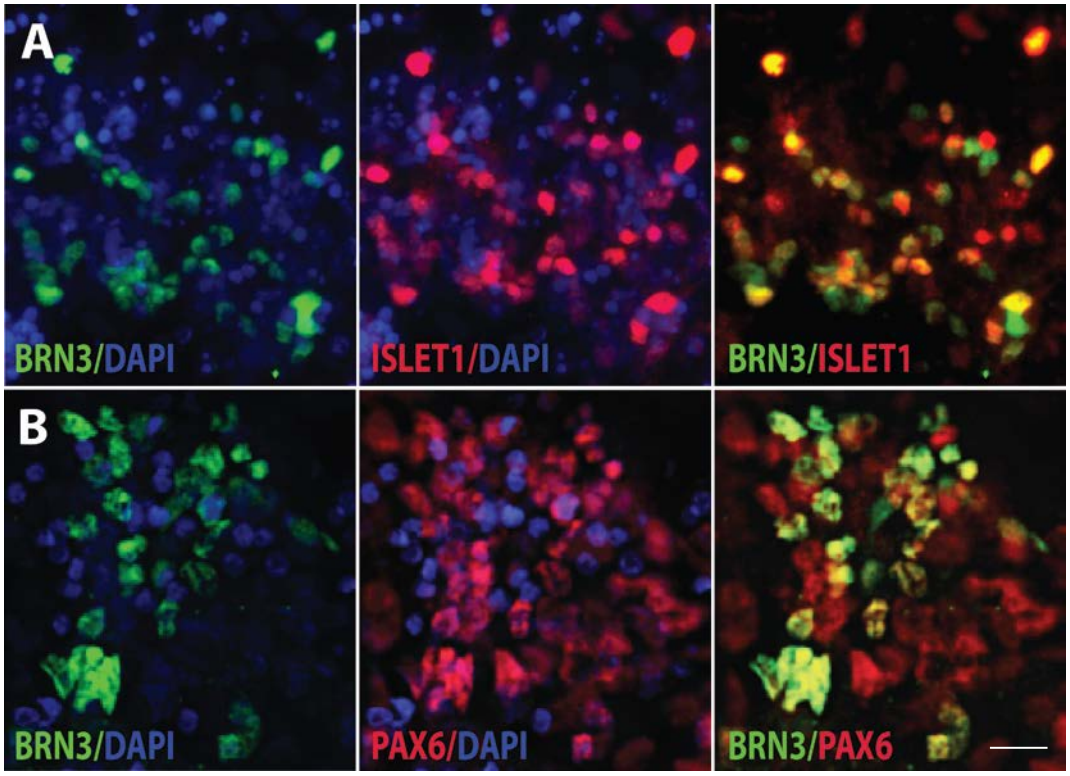

Figure 26: Further molecular characterization of RGCs. The differentiation of RGCs was further characterized by immunocytochemistry after 40 days of differentiation. (A) A subset of retinal progenitor cells co-expressed RGC specific factors BRN3 and ISLET1. (B) A population of cells was also double positive for BRN3 and PAX6, a neurodevelopmental marker known to be restricted to RGCs in the retina during later ontogenesis. (Scale bars 6.25 μm in panel A, 3.40 μm in panel B)

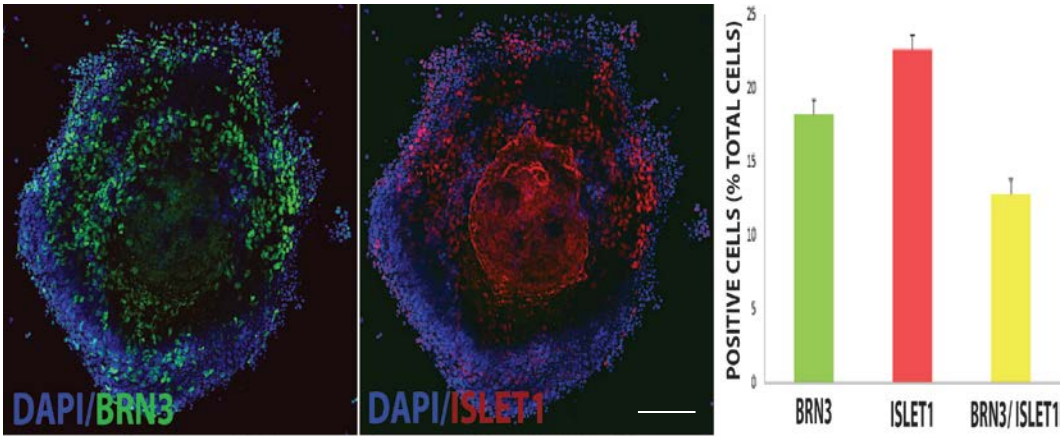

Figure 27: Quantification of yield of RGCs. After 40 days of differentiation the amount of human iPS-derived RGCs was quantified by counting the number of cells positive for the RGC specific markers, BRN3 and ISLET1. Approximately 18.17% (S.E. of 3.97%) of the cells were positive for the expression of BRN3 and 22.58% (S.E. of 3.09%) of the cells expressed ISLET1. A total of 12.77% of the total population of cells expressed both BRN3 and ISLET1. (Scale bar, 19 μm)

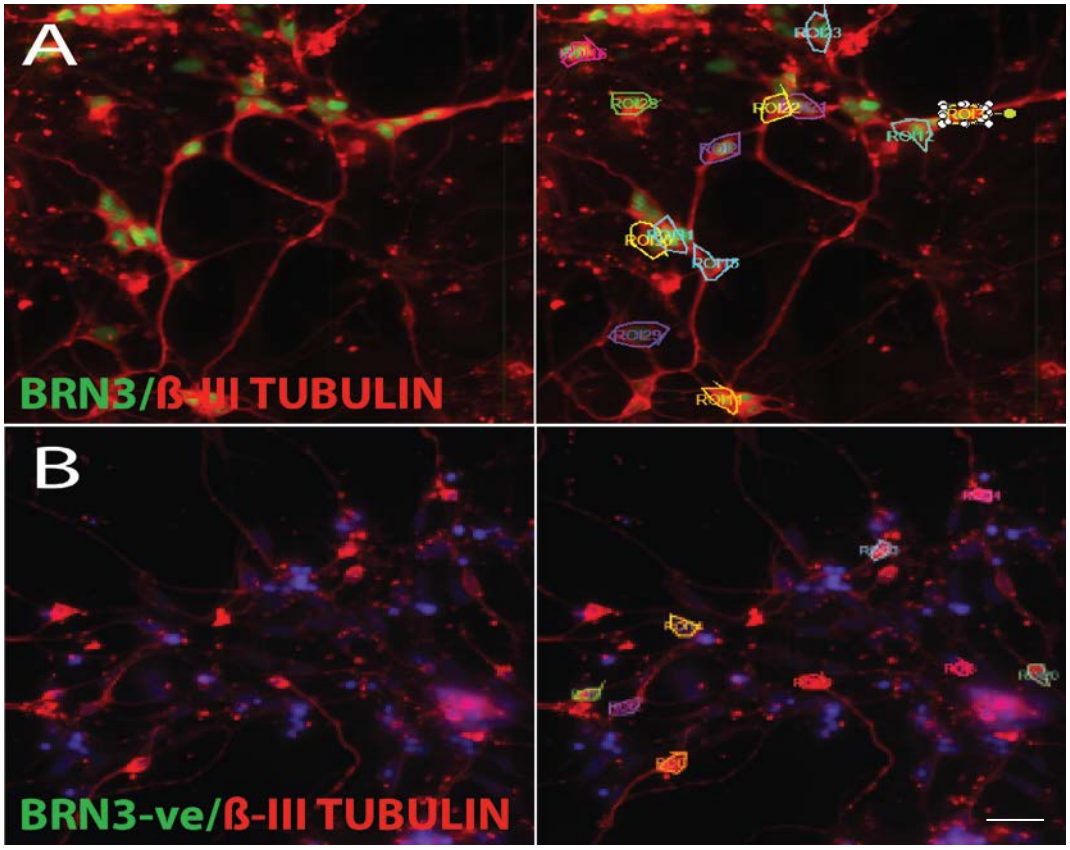

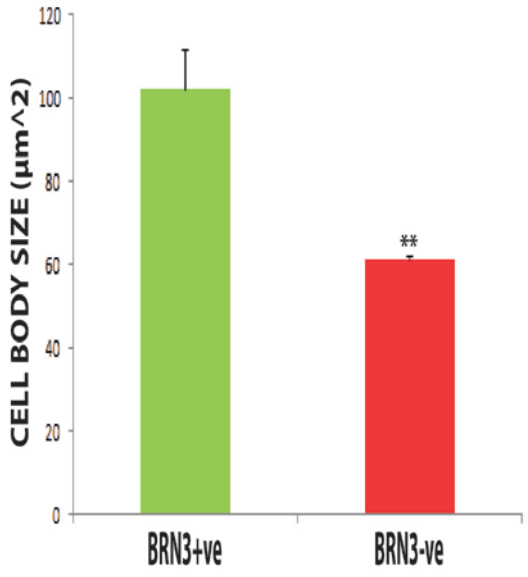

Figure 28: Quantification of cell sizes of RGCs. Cell body areas of cells expressing ß-III TUBULIN with (A) or without (B) BRN3 derived from the same set of retinal progenitor cells was analyzed. RGCs identified by the positive expression of BRN3 had a significantly greater mean cell soma area of 102.18 μm^2 (S.E. of 9.35) compared to 67.17 μm^2 (S.E. of 0.88) for that of other neuronal cell types derived in the process. ($n=4$, $p<0.05$). (Scale bars, 15 µm in panels A and B)

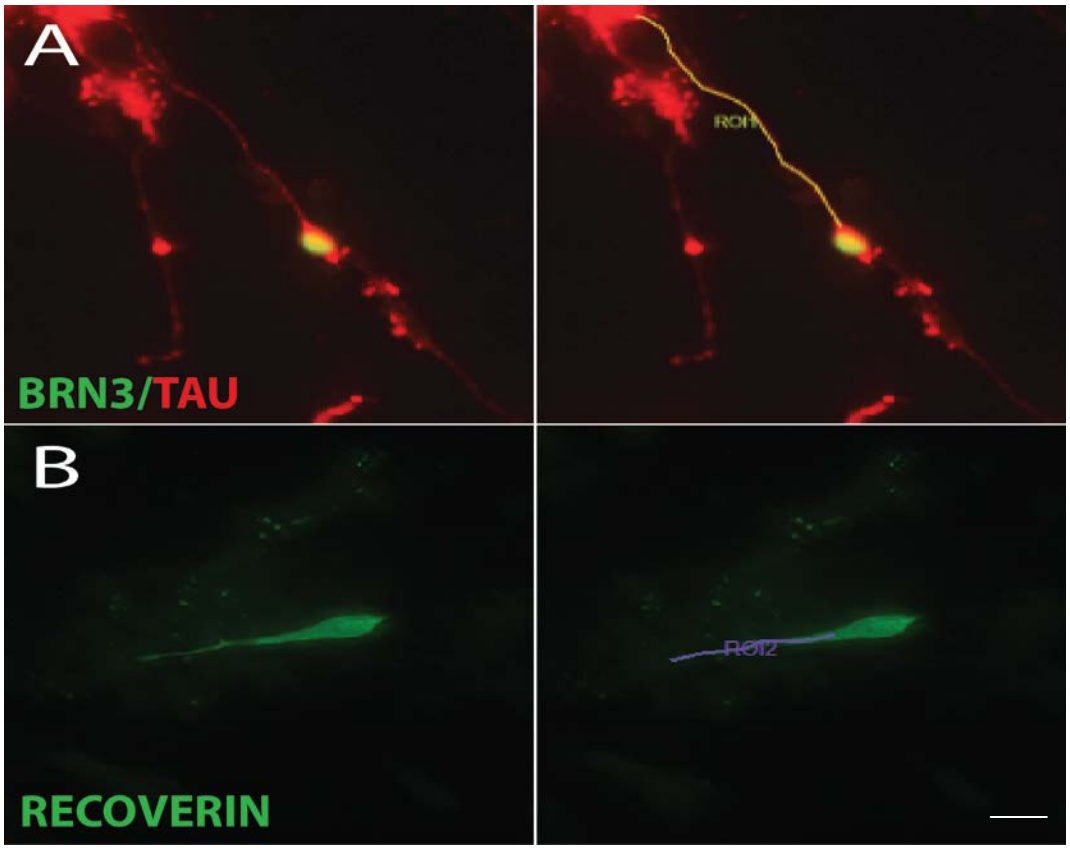

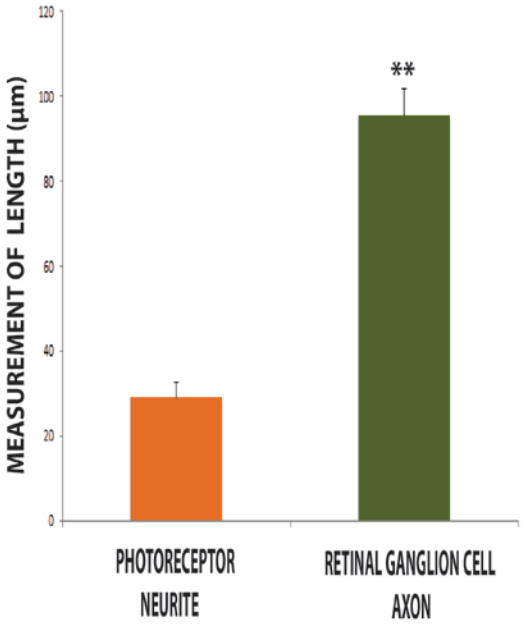

Figure 29: Quantification of RGCs and Photoreceptor neurite lengths. The difference in lengths between the human iPS-derived RGC axons and photoreceptor neurites was measured. RGC axons were identified by the co-expression of BRN3 and TAU (A) whereas photoreceptors were identified by their mature expression of the RECOVERIN protein (B). Measurement revealed a statistically significant difference with a mean length of 95.31 µm (S.E. of 6.28) for RGCs compared to 29.18 µm (S.E. of 3.67) for that of photoreceptors. ($p<0.05$). (Scale bars, 10 µm in panel A and 4.44 µm in panel B).

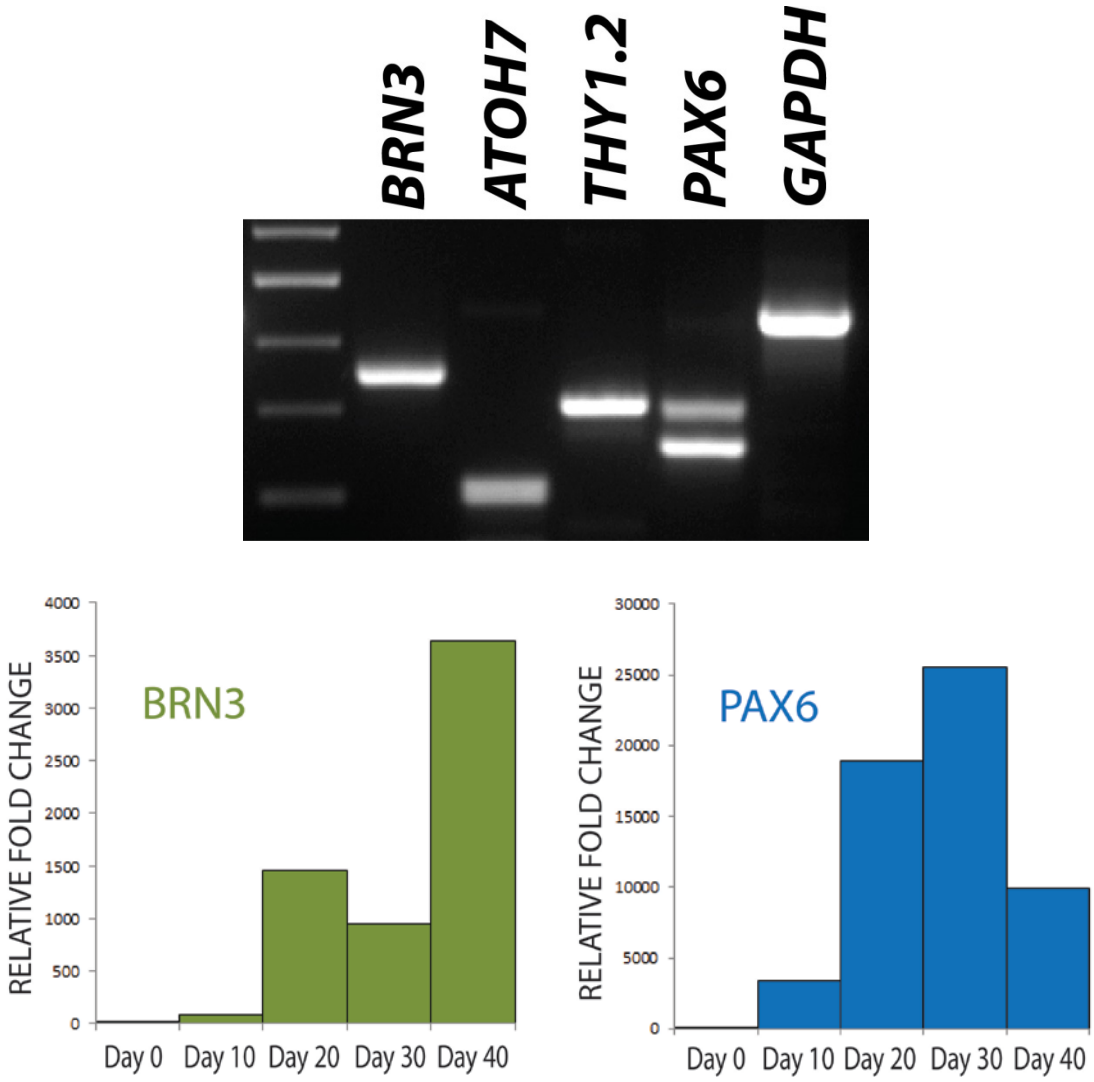

Figure 30: PCR analysis of RGCs specification. Gene expression analysis further confirmed the specification of RGCs from human iPS cells after 40 days of differentiation. RT-PCR revealed expression of RGC specific genes including *BRN3, ATOH7, THY1.2* and *PAX6.* qPCR analysis further demonstrated the progressive increase in BRN3 expression pattern from day 0 to day 40 in 10 day intervals. A similar trend was observed with *PAX6*, expected to peak earlier due to early neural specification from human iPS cells.

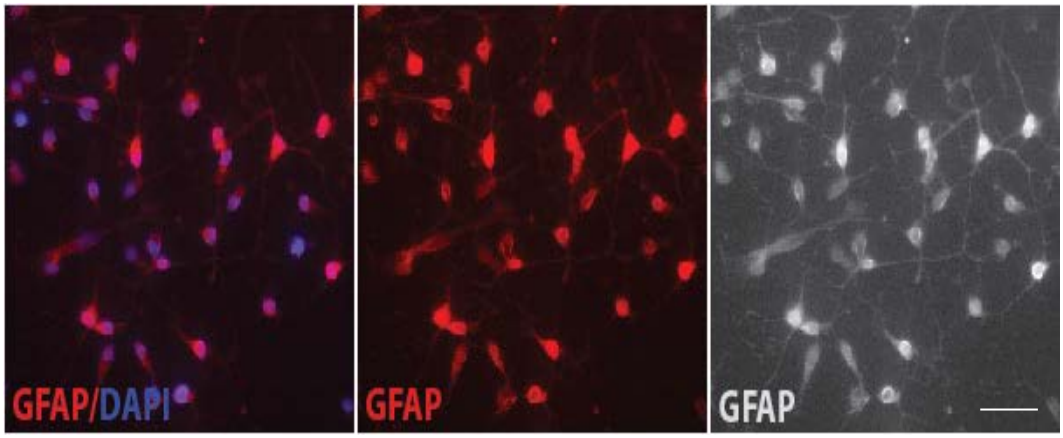

Figure 31: Differentiation of astrocytes at day 60. First signs of astroglial cells were observed in culture after 60 days of differentiation. Astrocytes appeared in their characteristic stellate type morphology and expressed the astrocyte specific cytoskeleton protein GFAP. ICC also revealed characteristic elongated processes generally associated with glial cell types. (Scale bars, 15 μm)

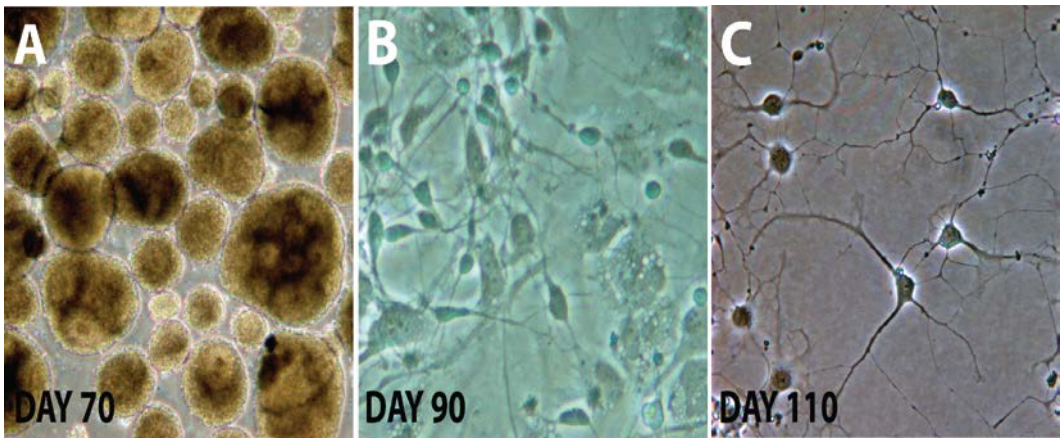

Figure 32: Brightfield timeline for *in vitro* astrocyte enrichment. *In vitro* culture and differentiation of the astrospheres (A) in suspension followed by passaging with accutase revealed a progressive increase in non-post-mitotic astrocyte numbers and specification (B-C) as identified under bright field microscopy over a period of 110 days of differentiation.

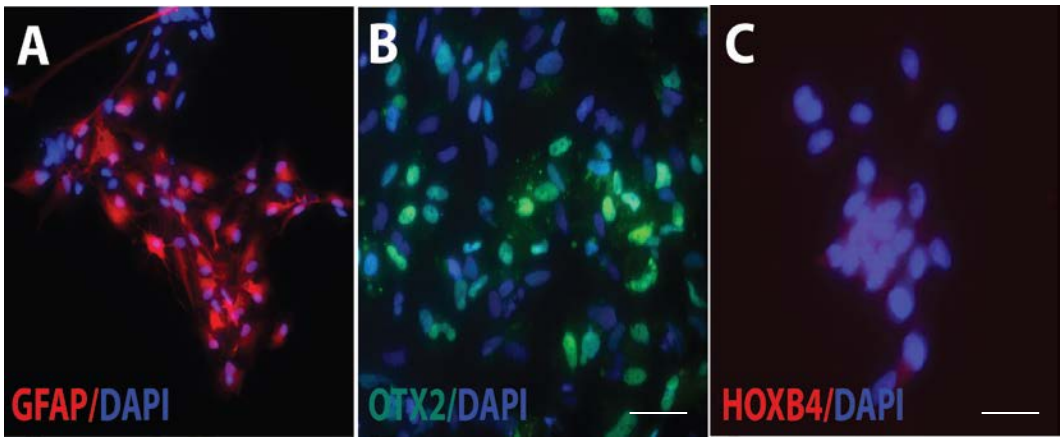

Figure 33: Anterior specification of astrocytes. After 125 days of differentiation, a qualitative increase in the expression of GFAP was observed (A). The astrocytes also expressed OTX2, a marker for anterior neural development (B), and were negative for the expression of HOXB4, a marker associated with spinal cord/ventral neural development (C). (Scale bars, 15 µm in panels A and B, 6.90 µm in panel C).

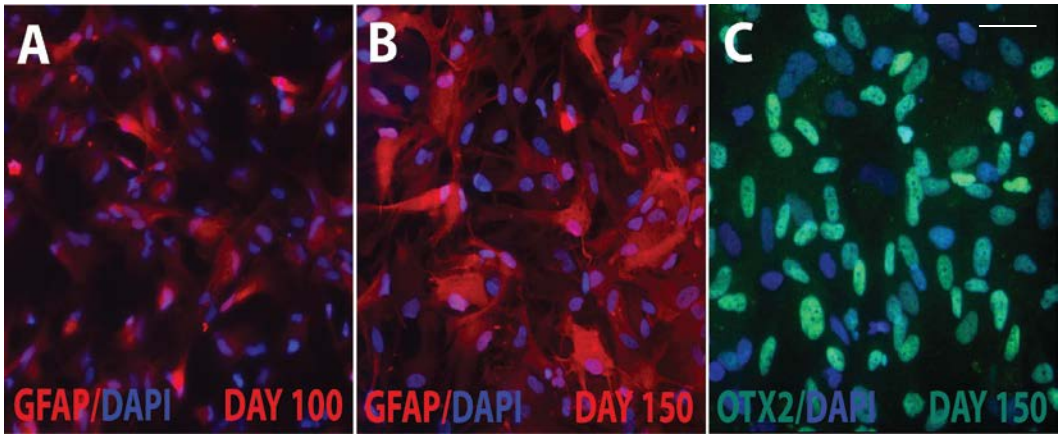

Figure 34: Long term differentiation of astrocytes. Prolonged differentiation of astrocytes in serum conditions revealed a higher amount of maturation of *in vitro* derived astrocytes identified by the qualitative increase in intensity and number and of cells expressing GFAP (A-B) and OTX2 (C) until 150 days of differentiation. (Scale bars, 15 µm in panels A-C).

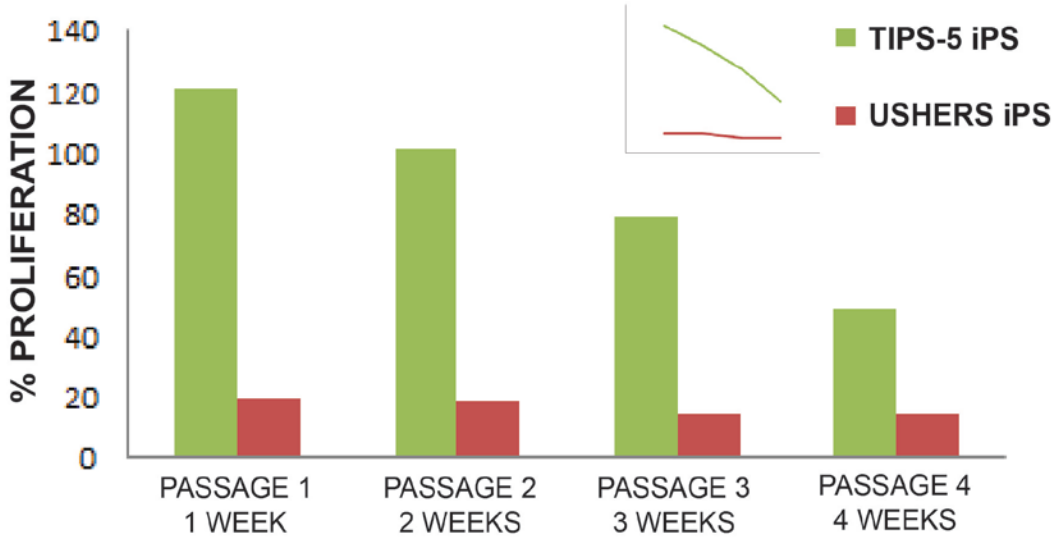

Figure 35: Measurement of astrocyte proliferation/ doubling rate. Rates of astrocyte proliferation were analyzed for both iPS cell lines. A general trend of decreasing ability to divide was observed from day 100 to day 130 for both. However, the TIPS-5 iPS cell line was more proliferative indicative of less doubling time between passages (1.48 days for passage 1 to 1.72, 2.13, and 3.17 for the next 3 passages) compared to that of the Usher iPS cell line, (5.96 days at passage 1 to 6.03, 6.86, and 6.93 for the next 3 passages).